REDEFINING CYCLIC ELECTRON FLOW AROUND PHOTOSYSTEM I (CEF1): THE INDUCTION, PATHWAY, AND ROLE OF CEF1 IN C3 PLANTS

BY

AARON KYLE LIVINGSTON

A dissertation submitted in partial fulfillment of the
requirements for the degree of

DOCTOR OF PHILOSOPHY

WASHINGTON STATE UNIVERSITY
School of Molecular Biosciences

May 2010

To the Faculty of Washington State University:

The members of the Committee appointed to examine the dissertation of Aaron Kyle Livingston find it satisfactory and recommend that it be accepted.

_____
David M. Kramer, Ph.D., Chair

_____
William B. Davis, Ph.D.

_____
Amit Dhingra, Ph.D.

_____
Gerald E. Edwards, Ph.D.

_____
Andris Kleinhofs, Ph.D.

REDEFINING CYCLIC ELECTRON FLOW AROUND PHOTOSYSTEM I (CEF1): THE INDUCTION, PATHWAY, AND ROLE OF CEF1 IN C3 PLANTS

Abstract

by Aaron Kyle Livingston, Ph.D.
Washington State University
May 2010

Chair: David M. Kramer

While traditional photosynthetic research has focused on the "linear" electron transfer pathway, alternative "cyclic" pathways have been proposed as a means to balance energy needs in plants. After decades of work, spanning a diverse field of techniques and ideas, controversy remains as to the pathway, role and regulation of cyclic electron flow around photosystem I (CEF1). CEF1 must be elucidated to understand how plants respond to and survive changing environmental stresses, such as drought, cold, heat and salt. We have isolated a new mutant phenotype where CEF1 is greatly increased with respect to normal photosynthesis or linear electron transfer. These high CEF1, or *hcef,* mutants provide a unique opportunity for answering key questions about the regulation, role, and pathway of CEF1. Through the utilization of map-based cloning, new spectroscopic techniques, and crossing with other known CEF1 mutants, we have determined

that CEF1 is a highly dynamic, regulated, and large capacity pathway in plants. CEF1 in C_3 plants appears to run through the thylakoid NAD(P)H dehydrogenase (NDH) complex and not the once favored antimycin A-sensitive ferredoxin-plastoquinone oxidoreductase (FQR), or PGR5 (proton gradient regulator 5) dependent pathway. Furthermore, hydrogen peroxide has been found to be both an inducer of the formation of the NDH complex and activator of NDH mediated CEF1.

TABLE OF CONTENTS

ABSTRACT iii

PREFACE 1

References 10

CHAPTER 1: An *Arabidopsis* mutant with high cyclic electron flow around photosystem I (*hcef*) involving the NADPH dehydrogenase complex 19

Abstract. 19

Introduction 20

Results 23

Discussion 31

Methods 38

Figures 47

References 54

Supplemental Figures 64

Supplemental References 71

CHAPTER 2: Regulation of Cyclic Electron Flow in C_3 Plants: Differential effects of limiting photosynthesis at Rubisco and Glyceraldehyde-3-phosphate Dehydrogenase 72

Abstract. 72

Introduction 73

Material and Methods 76

Results 78

Discussion 83

Table 89

Figures 90

References 94

CHAPTER 3: A mutation in glyceraldehyde-3-phosphate dehydrogenase subunit B induces cyclic electron flow around photosystem I 102

Abstract 102

Introduction 103

Material and Methods 105

Results 108

Discussion 114

Figures 118

References 123

CHAPTER 4: Regulation of Cyclic Electron Flow around Photosystem I *in vivo* by hydrogen peroxide. 130

Abstract 130

Introduction 131

Material and Methods 134

Results 137

Discussion 141

Conclusion 144

Figures 146

References 153

PREFACE

Through the process of photosynthesis, photonic energy from the sun is converted into stored energy, as both reducing equivalents (NADPH) (Ort & Yocum, 1996) and an electrochemical gradient or proton motive force (*pmf)* (Cruz, Sacksteder, Kanazawa & Kramer, 2001, Kramer, Cruz & Kanazawa, 2003) through a process known as linear electron flow (LEF). The *pmf* has two separate functions. First, *pmf* can be used to make a stable form of energy in the conversion of ADP to ATP (Allen, 2002). Secondly, the *pmf* regulates the photosynthetic process by slowing the electron flow through the cytochrome b_6f complex (Hope, Valente & Matthews, 1994, Takizawa, Cruz, Kanazawa & Kramer, 2007) and up-regulating a process to dissipate excess energy, q_E (energy dependent quenching) (Horton, Ruban & Walters, 1996). The *pmf* is built up by the translocation of protons into the thylakoid lumen during LEF. LEF uses light energy to transfer electrons through both photosystem II (PSII) and photosystem I (PSI) to ultimately produce NADPH. Since the electron and proton transfers are coupled together, LEF produces a fixed ratio of ATP to NADPH (1.3 ATP per NADPH) (Sacksteder, Kanazawa, Jacoby & Kramer, 2000, Seelert, Poetsch, Dencher, Engel, Stahlberg & Müller, 2000, Kramer, Avenson & Edwards, 2004).

However, the rate at which a plant is predicted to consume ATP to NADPH is expected to be significantly higher (1.45 ATP per NADPH) than that produced (Noctor & Foyer, 1998, Kramer *et al.*, 2004, Avenson, Kanazawa, Cruz, Takizawa, Ettinger & Kramer, 2005b). This short fall in the production of ATP must be corrected otherwise an over-abundance of reduced PSI electron acceptors would be created (Kramer *et al.*, 2004). An over-abundance of reduced PSI acceptors can lead to superoxide production (Scandalios, 1993) and singlet oxygen species

(Macpherson, Telfer, Barber & Truscott, 1993, Hideg, Spetea & Vass, 1994) which can cause damage or death to the plant.

Methods of balancing the ATP/NADPH ratio

A shortfall in ATP production can be augmented by one of three mechanisms: the water-water cycle (WWC), the malate shunt, and cyclic electron flow around photosystem I (CEF1). In the WWC, instead of electrons from LEF being used to make NADPH, the electrons are pushed onto oxygen to make superoxide. The superoxide is scavenged into hydrogen peroxide (Macheroux, Kleweg, Massey, Söderlind, Stenberg & Lindqvist, 1993) and, by consuming NADPH, is, ultimately, converted back into water (Asada, 2000). The WWC increases the amount of *pmf*, while consuming NADPH, helping to increase the ATP to NADPH ratio. Unfortunately, the actual contribution of the WWC in energy balancing is still largely unknown (Miyake & Yokota, 2000, Heber, 2002).

In the malate shunt, NADPH created by LEF is used inside the chloroplast to make malate. The malate is then transferred from the chloroplast to the mitochondria, where it is consumed to produce ATP (Scheibe, 2004). Essentially, the malate shunt functions as an exchange of NADPH for ATP. However, the shunt has a limited capacity (~1% of LEF) and probably has little effect on the actual ATP/NADPH ratio (Fridlyand, Backhausen & Scheibe, 1998).

During CEF1 the electrons, instead of being used to make NADPH, are transferred back into LEF between PSII and PSI (Heber & Walker, 1992). The electrons can then circle around PSI, while translocating additional protons into the thylakoid lumen. The translocation of additional protons increases the *pmf* without any net increase in NADPH (Kramer *et al.*, 2004,

Eberhard, Finazzi & Wollman, 2008). The increased *pmf* helps balance the ATP/NADPH ratio as well as regulating photosynthesis by enhancing photoprotection (q_E) and slowing LEF through the cytochrome b_6f complex (Heber & Walker, 1992, Kramer *et al.*, 2004, Livingston, Cruz, Kohzuma, Dhingra & Kramer, 2010a, Chapter 1).

Controversy around CEF1

While some research groups have found significant increases in CEF1 under environmental stress, e.g. drought (Jia, Oguchi, Hope, Barber & Chow, 2008, Kohzuma, Cruz, Akashi, Munekage, Yokota & Kramer, 2008), high light (Baker & Ort, 1992), or during the induction of photosynthesis from prolonged dark (Joët, Cournac, Peltier & Havaux, 2002, Joliot & Joliot, 2002), other groups found that CEF1 is only activated in very small amounts, particularly under steady-state conditions (Genty, Briantais & Baker, 1989, Harbinson, Genty & Baker, 1989, Avenson, Cruz, Kanazawa & Kramer, 2005a).

In C_4 plants (Kubicki, Funk, Westhoff & Steinmüller, 1996), cyanobacteria (Carpentier, Larue & Leblanc, 1984) and green algae (Finazzi, Rappaport, Furia, Fleischmann, Rochaix, Zito & Forti, 2002), the amount of CEF1 is constantly high due to the increased ATP demand. The extra ATP is necessary to drive the organism's CO_2 concentrating mechanisms. Since C_3 plants do not concentrate CO_2 there is no increased ATP demand, so under nonstressed conditions the plant probably only requires a small contribution by CEF1 (Kramer *et al.*, 2004, Avenson *et al.*, 2005a).

Until recently, the only way to study CEF1 was to use mutants that are CEF1 knockouts, either *pgr5* (Munekage, Hojo, Meurer, Endo, Tasaka & Shikanai, 2002) a mutant deficient in the antimycin A (AA)-sensitive ferredoxin-plastoquinone oxidoreductase (FQR) pathway (Bendall

& Manasse, 1995), or *crr2-2,* which is impared in the NAD(P)H dehydrogenase (NDH) complex (Endo, Shikanai, Sato & Asada, 1998, Shikanai, Endo, Hashimoto, Yamada, Asada & Yokota, 1998, Nixon, 2000). Currently there is a push towards finding and using mutants with consistently high amounts of CEF1, such as a chloroplast fructose-1,6-bisphosphatase mutant (*high cyclic electron flow* mutant 1 or *hcef1)* (Livingston *et al.*, 2010a, Chapter 1), a fructose-6-phosphate aldolase mutant (Gotoh, Matsumoto, Ogawa, Kobayashi & Tsyama, 2009) and mutants in glyceraldehydes-3-phosphate dehydrogenase (GAPDH), both an anti-sense tobacco mutant, gapR (Livingston, Kanazawa, Cruz & Kramer, 2010b) and a GAPDH subunit B *Arabidopsis* mutant (*hcef2)* (Chapter 3).

Activation of CEF1 by H_2O_2

The following theories have been proposed about what induces CEF1: (1) the ATP/ADP ratio (Joliot & Joliot, 2002); (2) the redox status of PSI electron acceptors (NAD(P)H, ferredoxin) (Breyton, Nandha, Johnson, Joliot & Finazzi, 2006); (3) Calvin-Benson cycle intermediates; (Fan, Nie, Hope, Hillier, Pogson & Chow); (Fan *et al.*) and (4) the reactive oxygen species, hydrogen peroxide (H_2O_2) (Lascano, Casano, Martin & Sabater, 2003, Gambarova, 2008). We compared these possibilities by constructing a large-scale metabolic analysis of mutants with both high levels of CEF1 and no CEF1 (see Chapter 3). In the high CEF1 mutants, *hcef1* (Livingston et al., 2010a, Chapter 1) and gapR (Livingston *et al.*, 2010b, Chapter 2), we found that the ATP/ADP levels were not significantly altered, however there was an increase in ATP/ADP level in the non-CEF1 mutant, an anti-sense Rubisco small subunit mutant (ssuR), suggesting that the ATP/ADP levels do not trigger CEF1.

Additionally, the metabolic comparison showed that only one Calvin-Benson Cycle intermediate, Rubisco 1,5-bisphosphate (RuBP), could possibly be the trigger of CEF1 (Livingston *et al.*, 2010b, Chapter 2). RuBP increased in ssuR, which showed no CEF1, and decreased in the high CEF1 mutants. This suggests that RuBP could be an inhibitor of CEF1. However, when plants were subject to drought conditions, where RuBP is expected to accumulate, there was an increase in CEF1 (Jia *et al.*, 2008, Kohzuma *et al.*, 2008). Overall this suggests that CEF1 is not directly induced by any Calvin-Benson Cycle intermediate.

Furthermore, a study on gapR showed no change in the $NADP^+$/NADPH ratio compared to wild-type (Ruuska, Andrews, Badger, Price & von Caemmerer, 2000), suggesting that NADPH is not the regulator of CEF1.

Overall, this suggests that CEF1 is activated by some other intracellular messenger, such as H_2O_2. Studies have found that varying H_2O_2 concentrations in C_3 plants can cause an array of overall physiological responses (reviewed in (Veal, Day & Morgan, 2007)), changes in the levels of protein transcription (Quinn, Findlay, Dawson, Jones, Morgan & Toone, 2002), and changes in the levels of enzyme activation (Casano, Martin & Sabater, 2001). Importantly, the high CEF1 mutant, *hcef1,* has very high levels of intercellular hydrogen peroxide (Chapter 4). To test the role of hydrogen peroxide on CEF1, wild-type plants where soaked in H_2O_2 for two hours, and an increase in CEF1 was observed (Chapter 4). Since hydrogen peroxide can cause many changes throughout the plant, mutants that have increased levels of hydrogen peroxide in the chloroplast only were also tested. These glycolate oxidase (GO) or GO mutants produce varying levels of additional H_2O_2 in the chloroplast. The GO mutants also showed varying levels of CEF1 activation which correlates to the concentration of hydrogen peroxide produced

(Chapter 4). Taken together these data suggest that hydrogen peroxide in the chloroplast plays a role in the induction of CEF1.

Previous work, suggests that the formation of a protein or protein complex is necessary to induce CEF1 (Chapter 1, 3 and 4). Following a time course, we found that if wild-type plants where subjected to H_2O_2 it took at least 60 minutes to start and 105 minutes to achieve full induction of CEF1. Furthermore, if a plant is subjected to H_2O_2 and lincomycin, which inhibits protein formation, CEF1 is never induced (Chapter 4). This suggests that H_2O_2 induces the formation of the CEF1 protein complex.

In fact under all conditions where elevated CEF1 is seen, cold (Apostol, Szalai, Sujbert, Popova & Janda, 2006), heat (Jin, Li, Hu & Wang, 2009), salt (Lu, Yang, He & Jiang, 2007), and drought (Kohzuma *et al.*, 2008), we also find elevated levels of H_2O_2 [cold (Dia, Huang, Zhou & Zhang, 2009), heat (Volkov, Panchuk, Mullineaux & Schöffl, 2006), salt (Xiong, Schumaker & Zhu, 2002, Mandhania, Madan & Sawhney, 2005), and drought (Xiong *et al.*, 2002)]. Pre-treatment of plants to H_2O_2 causes increased survival in all CEF1 inducing conditions: cold, heat, drought, and salt stress (Gong, Chen, Li & Guo, 2001).

Pathway of CEF1

Currently, there are two major pathways that CEF1 is proposed to run through: 1) the antimycin A (AA)-sensitive ferredoxin-PQ oxidoreductase (FQR) (Bendall & Manasse, 1995) which is inhibited in the *pgr5* mutant; and 2) through the NADPH dehydrogenase (NDH) complex (Endo *et al.*, 1998). Recent studies suggest that the NDH and PGR5 pathways are slow under non-stressed conditions, or that the two pathways can compensate for each other (Munekage *et al.*, 2002, Avenson *et al.*, 2005a).

Recent work with the high CEF1 mutants, *hcef1* (Livingston *et al.*, 2010a, Chapter 1) and *hcef2* (Chapter 3), show no change in CEF1 rates when crossed with a FQR knockout (*pgr5*). This suggests that the AA-sensitive FQR pathway of CEF1 is not active under these circumstances. Additionally, when the FQR knockout mutant, *pgr5*, was subjected to H_2O_2 CEF1 was induced to approximately the same level as at that induced in wild-type + H_2O_2 (Chapter 4). When protein content was looked at for the high CEF1 mutant, *hcef1* (Livingston *et al.*, 2010a, Chapter 1) the amount of PGR5 goes down, further suggesting that PGR5 does not have a role in CEF1.

When the high CEF1 mutants *hcef1* (Livingston *et al.*, 2010a, Chapter 1), *hcef2* (Chapter 3), and FBPaldolase (Gotoh *et al.*, 2009) where crossed with a knockout of NDH, *crr2-2,* there was an almost complete loss of CEF1 function. Additionally, the protein levels of *hcef1* (Livingston *et al.*, 2010a, Chapter 1), showed a dramatic (10X) increase in NDH compared to wild-type. When the NDH knockout mutant, *crr2-2,* was subjected to H_2O_2 there was no induction of CEF1 (Chapter 4). Furthermore when wild-type was subjected to the conditions that induce CEF1, i.e. cold (Lee, Henderson & Zhu, 2005, Hannah, Wiese, Freund, Fiehn, Heyer & Hincha, 2006), heat (Balasubramanian, Sureshkumar, Lempe & Weigel, 2006), drought (Abdeen, Schnell & Miki, 2010), and H_2O_2 (Vandenbroucke, Robbens, Vandepoele, Inzé, Van de Peer & Van Breusegem, 2008), microarray data shows an increase in the expression levels of NDH subunits in *Arabidopsis*. This suggest that NDH is a necessary component of CEF1. A further correlation has been seen between the amount of CEF1 in C_4 plants and the expression level of NDH, but not the expression level of PGR5 (Sazanov, Burrows & Nixon, 1996, Quiles, 2005).

Roles of CEF1: Importance of energy balancing

Cyclic electron flow is proposed to have two purposes: (1) CEF1 is proposed to increase the output ratio of ATP to NADPH (ATP/NADPH) (Allen, 2003) balancing the energy deficit. (2) In photoprotection, CEF1 increases *pmf* to increase excess energy dissipation (Heber & Walker, 1992) and decrease the flow of electrons through LEF (Miyake, Shinzaki, Miyata & Tomizawa, 2004). We know that the amount of CEF1 is highly regulated, as seen in the anti-sense GAPDH tobacco mutant (Chapter 2) and that a high level of flexibility is necessary to fix the energy balance without causing damage to the plant (Kramer *et al.*, 2004).

Like under changing CO_2 conditions (Kanazawa & Kramer, 2002), plants rapidly increase *pmf,* and thereby photoprotection, by simply altering the conductivity through the ATP synthase (g_{H^+}). This means that a plant can rapidly engage and disengage photoprotection by changing g_{H^+}, whereas CEF1 takes hours to induce. Since CEF1 requires the formation of an additional protein complex that takes hours to fully induce (Chapter 4), CEF1 cannot rapidly respond to changing environmental conditions like altering g_{H^+} can. However, if the CEF1 complex is already induced it can be rapidly activated, as seen when high CEF1 mutants were subject to changing levels of oxygen (Chapter 4). This means that if CEF1 does play a role in photoprotection it would likely be for long term photoprotection in response to repeated or constant stress conditions.

Additionally, in all the conditions we find elevated CEF1, i.e. drought, salt stress, heat stress and cold, we find increased ATP demand. Under drought conditions the amount of ATP decreases (Rezara, Mitchell, Driscoll & Lawlor, 1999, Flexas & Medrano, 2002) due to the loss of functioning ATP synthases (Lawlor & Tezara, 2009). Under cold stress, that ATP/ADP ratio decreases due to increased sucrose production (Savitch, Harney & Huner, 2003). Salt stress

induces the activation of a vacuolar ATPase proton/salt pumping mechanism which is necessary for the plant to survive the salt stress but costs additional ATP to run (Marlaux, Fischer-Schliebs, Lüttge & Ratajczak, 1997). High temperatures leads to leak of protons through the thylakoid membrane (Svintitskikh, Andrianov & Bulychev, 1985) or slip of protons through the ATP synthase (Groth & Junge, 1993). Leak and slip decreases in the amount of available *pmf* without effecting electron transfer, which causes a decrease in the amount of ATP produced per NADPH (Groth & Junge, 1993). Overall this suggests that CEF1 is likely induced to increase ATP production to balance the energy budget in C_3 plants, although CEF1 could be used for long term photoprotection under continuing stress conditions.

Conclusion

Overall this work suggests that CEF1 in C_3 plants is a finely tuned mechanism for balancing the energy budget, which is induced by H_2O_2 and runs through the NDH complex.

References

Abdeen A., Schnell J. & Miki B. (2010) Transcriptome analysis reveals absence of unintended effects in drought-tolerant transgenic plants overexpressing the transcription factor ABF3. *BMC Genomics*, **11**, 1-21.

Allen J.F. (2002) Photosynthesis of ATP- electrons, proton pumps, rotors, and poise. *Cell*, **110**, 273-276.

Allen J.F. (2003) Cyclic, pseudocyclic and noncyclic photophosphorylation: new links in the chain. *Trends in Plant Science*, **8**, 15-19.

Apostol S., Szalai G., Sujbert L., Popova L.P. & Janda T. (2006) Non-invasive monitoring of the light-induced cyclic photosynthetic electron flow during cold hardening in wheat leaves. *Z Naturforsch*, **61c**, 734-740.

Asada K. (2000) The water-water cycle as alternative photon and electron sinks. *Philosophical Transactions of the Royal Society B: Biological Sciences*, **355**, 1419-1431.

Avenson T.J., Cruz J.A., Kanazawa A. & Kramer D.M. (2005a) Regulating the proton budget of higher plant photosynthesis. *Proceedings of the National Academy of Sciences*, **102**, 9709–9713.

Avenson T.J., Kanazawa A., Cruz J.A., Takizawa K., Ettinger W.E. & Kramer D.M. (2005b) Integrating the proton circuit into photosynthesis: progress and challenges. *Plant, Cell and Environment*, **28**, 97-109.

Baker N.R. & Ort D.R. (1992) Light and crop photosynthetic performance. *In Crop Photosynthesis: Spatial and Temporal Determinants (eds N.R. Baker & H. Thomas)*, **Elsevier Science Publishers, Amsterdam, the Netherlands**, 289-312.

Balasubramanian S., Sureshkumar S., Lempe J. & Weigel D. (2006) Potent induction of Arabidopsis thaliana flowering by elevated growth temperature. *PLoS Genetics*, **2**, e106.

Bendall D.S. & Manasse R.S. (1995) Cyclic photophosphorylation and electron transport. *Biochemia Biophysica Acta*, **1229**, 23-38.

Breyton C., Nandha B., Johnson G., Joliot P. & Finazzi G. (2006) Redox modulation of cyclic electron flow around Photosystem I in C3 plants. *Biochemistry*, **45**, 13465-13475.

Carpentier R., Larue B. & Leblanc R.M. (1984) Photoacoustic spectroscopy of Anacystis nidulans : III. Detection of photosynthetic activities. *Archives of Biochemistry and Biophysics*, **228**, 534-543.

Casano L.M., Martin M. & Sabater B. (2001) Hydrogen peroxide mediates the induction of chloroplastic Ndh complex under photooxidative stress in barley. *Plant Physiology*, **125**, 1450-1458.

Cruz J.A., Sacksteder C.A., Kanazawa A. & Kramer D.M. (2001) Contribution of electric field ($\Delta\psi$) to steady-state transthylakoid proton motive force (*pmf*) *in vitro* and *in vivo*. Control of *pmf* parsing into $\Delta\psi$ and ΔpH by ionic strength. *Biochemistry*, **40**, 1226-1237.

Dia F., Huang Y., Zhou M. & Zhang G. (2009) The influence of cold acclimation on antioxidative enzymes and antioxidants in sensitive and tolerant barley cultivars. *Biologia Plantarum*, **53**, 257-262.

Eberhard S., Finazzi G. & Wollman F.-A. (2008) The Dynamics of Photosynthesis. *Annual Review of Genetics*, **42**, 463-515.

Endo T., Shikanai T., Sato F. & Asada K. (1998) NAD(P)H dehydrogenase dependet, antimycin A-sensitive electron donation to plastoquinone in tobacco chloroplasts. *Plant Cell Physiology*, **39**, 1226-1231.

Fan D.-Y., Nie Q., Hope A.B., Hillier W., Pogson B.J. & Chow W.S. (2007) Quantification of cyclic electron flow around Photosystem I in spinach leaves during photosynthetic induction. *Photosynthesis Research*, **94**, 347-357.

Finazzi G., Rappaport F., Furia A., Fleischmann M., Rochaix J.D., Zito F. & Forti G. (2002) Involvement of state transitions in the switch between linear and cyclic electron flow in *Chlamydomonas reinhardtii*. *European Molecular Biology Organization*, **3**, 280–285.

Flexas J. & Medrano H. (2002) Drought-inhibition of photosynthesis in C_3 plants: Stomatal and non-stomatal limitations revisted. *Annals of Botany*, **89**, 183-189.

Fridlyand L.E., Backhausen J.E. & Scheibe R. (1998) Flux control of the Malate Valve in leaf cells. *Archives of Biochemistry and Biophysics*, **349**, 290-298.

Gambarova N.G. (2008) Activity of photochemical reactions and accumulation of hydrogen peroxide in chloroplasts under stress conditions. *Russian Agricultural Sciences*, **34**, 149-151.

Genty B., Briantais J.M. & Baker N.R. (1989) The relationship between the quantum yield of photosynthetic electron transport and quenching of chlorophyll fluorescence. *Biochimica et Biophysica Acta*, **990**, 87-92.

Gong M., Chen B.O., Li Z.G. & Guo L.H. (2001) Heat-shock-induced cross adaption to heat, chilling, drought and salt stress in maize seedlings and involvement of H_2O_2. *Journal of Plant Physiology*, **158**, 1125-1130.

Gotoh E., Matsumoto M., Ogawa K., Kobayashi Y. & Tsyama M. (2009) A qualitative analysis of the regulation of cyclic electron flow around photosystem I form the post-illumination chlorophyll flyorescence transient in Arabidopsis: a new platform for th in vivo invesigation of the chloroplast redox state. *Photosynthesis Research*, **103**, 111-123.

Groth G. & Junge W. (1993) Proton slip of the chloroplast ATPase: Its nucleotide dependence, energetic threshold, and relation to an alternating site mechanism of catalysis. *Biochemistry*, **32**, 8103-8111.

Hannah M.A., Wiese D., Freund S., Fiehn O., Heyer A.G. & Hincha D. (2006) Natural Genetic Variation of Freezing Tolerance in Arabidopsis. *Plant Physiology*, **142**, 98-112.

Harbinson J., Genty B. & Baker N.R. (1989) Relationship between the Quantum Efficiencies of Photosystems I and II in Pea Leaves. *Plant Physiology*, **90**, 1029-1034.

Heber U. (2002) Irrungen, Wirrungen? The Mehler reaction in relation to cyclic electron transport in C3 plants. *Photosynthesis Research*, **73**, 23-231.

Heber U. & Walker D. (1992) Concerning a dual function of coupled cyclic electron transport in leaves. *Plant Physiology*, **100**, 1621-1626.

Hideg É., Spetea C. & Vass I. (1994) Singlet oxygen production in thylakoid membranes during photoinhibition as detected by EPR spectroscopy. *Photosynthesis Research*, **39**, 191-199.

Hope A.B., Valente P. & Matthews D.B. (1994) Effects of pH on the kinetics of redox reactions in and around the cytochrome *bf* complex in an isolated system. *Photosynthesis Research*, **42**, 111-120.

Horton P., Ruban A. & Walters R. (1996) Regulation of light harvesting in green plants. *Annual Review of Plant Physiology and Plant Molecular Biology*, **47**, 655-684.

Jia H., Oguchi R., Hope A.B., Barber J. & Chow W.S. (2008) Differential effects of severe water stress on linear and cyclic electron fluxes through Photosystem I in spinach leaf discs in CO_2-enriched air. *Planta*, **228**, 803-812.

Jin S.H., Li X.Q., Hu J.Y. & Wang J.G. (2009) Cyclic electron flow around photosystem I is required for adaption to high temperature in a subtropical forest tree, *Ficus concinna*. *Journal of Zhejiang University Science*, **10**, 784-790.

Joët T., Cournac L., Peltier G. & Havaux M. (2002) Cyclic electron flow around photosystem I in C3 plants. *In vivo* control by the redox state of chloroplasts and involvement of the NADH-dehydrogenase complex. *Plant Physiology*, **128**, 760–769.

Joliot P. & Joliot A. (2002) Cyclic electron transfer in plant leaf. *Proceedings of the National Academy of Sciences*, **99**, 10209–10214.

Kanazawa A. & Kramer D.M. (2002) *In vivo* modulation of nonphotochemical exciton quenching (NPQ) by regulation of the chloroplast ATP synthase. *Proceedings of the National Academy of Sciences*, **99**, 12789-12794.

Kohzuma K., Cruz J.A., Akashi K., Munekage Y., Yokota A. & Kramer D.M. (2008) The long-term responses of the photosynthetic proton circuit to drought. *Plant, Cell & Environment*, **32**, 209-219.

Kramer D.M., Avenson T.J. & Edwards G.E. (2004) Dynamic flexibility in the light reactions of photosynthesis governed by both electron and proton transfer reactions. *Trends in Plant Science*, **9**, 349-357.

Kramer D.M., Cruz J.A. & Kanazawa A. (2003) Balancing the central roles of the thylakoid proton gradient. *Trends in Plant Science*, **8**, 27-32.

Kubicki A., Funk E., Westhoff P. & Steinmüller K. (1996) Differential expression of plastome-encoded ndh genes in mesophyll and bundle-sheath chloroplasts of the C4 plant Sorghum bicolor indicates that the complex I-homologous NAD(P)H-plastoquinone oxidoreductase is involved in cyclic electron transport. *Planta*, **199**, 276-281.

Lascano H.R., Casano L.M., Martin M. & Sabater B. (2003) The activity of the chloroplastic Ndh complex is regulated by phosphorylation of the NDH-F subunit. *Plant Physiology*, **132**, 256-262.

Lawlor D.W. & Tezara W. (2009) Causes of decreased photosynthetic rate and metabolic capacity in water-deficient leaf cells: a critical evaluation of mechanisms and integration of processes. *Annals of Botany*, **103**, 561-579.

Lee B., Henderson D.A. & Zhu J.K. (2005) The Arabidopsis cold-responsive transcriptome and its regulation by ICE. *Plant Cell*, **17**, 3155-3157.

Livingston A.K., Cruz J.A., Kohzuma K., Dhingra A. & Kramer D.M. (2010a) An Arabidopsis mutant with high cyclic electron flow around photosystem I (*hcef*) involving the NDH complex. *Plant Cell*, **22**, 1-13.

Livingston A.K., Kanazawa A., Cruz J.A. & Kramer D.M. (2010b) Regulation of Cyclic Electron Flow in C3 Plants: Differential effects of limiting photosynthesis at Rubisco and Glyceraldehyde-3-phosphate Dehydrogenase. *Plant Cell and the Environment*.

Lu K.X., Yang Y., He Y. & Jiang D.A. (2007) Induction of cyclic electron flow around photosystem 1 and state transitions are correlated with salt tolerance in soybean. *Photosynthetica*, **46**, 10-16.

Macheroux P., Kleweg V., Massey V., Söderlind E., Stenberg K. & Lindqvist Y. (1993) Role of tyrosine 129 in the active site of spinach glycolate oxidase. *European Journal of Biochemistry*, **213**, 1047-1054.

Macpherson A.N., Telfer A., Barber J. & Truscott T.G. (1993) Direct detection of singlet oxygen from isolated Photosystem II reaction centres. *Biochimica et Biophysica Acta*, **1143**, 301-309.

Mandhania S., Madan S. & Sawhney V. (2005) Antioxidant defense mechanism under salt stress in wheat seedlings. *Biologia Plantarum*, **50**, 227-231.

Marlaux J., Fischer-Schliebs E., Lüttge U. & Ratajczak R. (1997) Dynamics of activity and structure of the tonoplast vacuolar-type H^+-ATPase in plants with differing CAM expression and in a C_3 plant under salt stress. *Protoplasma*, **196**, 181-189.

Miyake C., Shinzaki Y., Miyata M. & Tomizawa K.-i. (2004) Enhancement of Cyclic Electron Flow Around PSI at High Light and its Contribution to the Induction of Non-Photochemical Quenching of Chl Fluorescence in Intact Leaves of Tobacco Plants. *Plant and Cell Physiology*, **45**, 1426-1433.

Miyake C. & Yokota A. (2000) Determination of the Rate of Photoreduction of O2 in the Water-Water Cycle in Watermelon Leaves and Enhancement of the Rate by Limitation of Photosynthesis. *Plant Cell Physiol.*, **41**, 335-343.

Munekage Y., Hojo M., Meurer J., Endo T., Tasaka M. & Shikanai T. (2002) PGR5 is involved in cyclic electron flow around photosystem I and is essential for photoprotection in Arabidopsis. *Cell*, **110**, 361-371.

Nixon P.J. (2000) Chlororespiration. *Philosophical Transactions of the Royal Society B: Biological Sciences*, **355**, 1541-1547.

Noctor G. & Foyer C. (1998) A re-evaluation of the ATP:NADPH budger during C3 photosynthesis: a contribution form nitrate assimilation and its associated respiratory activity. *Journal of Experimental Botany*, **49**, 1895-1908.

Ort D.R. & Yocum C.F. (1996) Light reactions of oxygenic photosynthesis. In: *Oxygenic Photosynthesis: The Light Reactions* (ed C.F. Yocum), pp. 1-9. Kluwer Academic Publishers, The Netherlands.

Quiles M.J. (2005) Regulation of the expression of chloroplast *ndh* genes by light intensity applied during oat plant growth. *Plant Science*, **168**, 1561-1569.

Quinn J., Findlay V.J., Dawson K., Jones N., Morgan B.A. & Toone W.M. (2002) Distinct regulatory proteins control the adaptive and acute response to H_2O_2 in *Schizosaccharomyces pombe. Molecular Biology of the Cell*, **13**, 805-816.

Rezara W., Mitchell V.J., Driscoll S.D. & Lawlor D.W. (1999) Water stress inhibits plant photsynthesis by decreasing coupling factor and ATP. *Nature*, **401**, 914-917.

Ruuska S.A., Andrews T.J., Badger M.R., Price G.D. & von Caemmerer S. (2000) The role of chloroplast electron transport and metabolites in modulating rubisco activity in tobacco. Insights from transgenic plants with reduced amounts of cytochrome *b/f* complex or glyceraldehyde 3-phosphate dehydrogenase. *Plant Physiology*, **122**, 491–504.

Sacksteder C., Kanazawa A., Jacoby M.E. & Kramer D.M. (2000) The proton to electron stoichiometry of steady state photosynthesis in living plants: a proton-pumping Q-cycle is continuously engaged. *Proceedings of the National Academy of Sciences*, **97**, 14283-14288.

Savitch L.V., Harney T. & Huner N.P.A. (2003) Sucrose metabolism in spring and winter wheat in response to high irradiance, cold stress and cold acclimation. *Physiologia Plantarum*, **108**, 270-278.

Sazanov L.A., Burrows P.A. & Nixon P.J. (1996) Detection and characterization of a complex I-like NADH-specific dehydrogenase from pea thylakoids. *Biochemical Society Transactions*, **24**, 739-743.

Scandalios J.G. (1993) Oxygen Stress and Superoxide Dismutases. *Plant Physiology*, **101**, 7-12.

Scheibe R. (2004) Malate valves to balance cellular energy supply: Redox regulation: from molecular responses to environmental adaptation. *Physiologia Plantarum*, **120**, 21-26.

Seelert H., Poetsch A., Dencher N.A., Engel A., Stahlberg H. & Müller D.J. (2000) Structural biology. Proton-powered turbine of a plant motor. *Nature*, **405**, 418-419.

Shikanai T., Endo T., Hashimoto T., Yamada Y., Asada K. & Yokota A. (1998) Directed disruption of the tobacco ndhB gene impairs cyclic electron flow around photosystem I. *Proceedings of the National Academy of Sciences*, **95**, 9705-9709.

Svintitskikh V.A., Andrianov V.K. & Bulychev A.A. (1985) Photo-induced H^+ transport between chloroplast and the cytoplasm in a protoplasmic droplet of *Characeae*. *Journal of Experimental Botany*, **36**, 1414-1419.

Takizawa K., Cruz J.A., Kanazawa A. & Kramer D.M. (2007) The thylakoid proton motive force *in vivo*. Quantitative, non-invasive probes, energetics, and regulatory consequences of light-induced *pmf*. *Biochimica et Biophysica Acta*, **1767**, 1233-1244.

Vandenbroucke K., Robbens S., Vandepoele K., Inzé D., Van de Peer Y. & Van Breusegem F. (2008) Hydrogen Peroxide-Induced gene expression across kingdoms: A comparative analysis. *Molecular Biology and Evolution*, **25**, 507-516.

Veal E.A., Day A.M. & Morgan B.A. (2007) Hydrogen peroxide sensing and signaling. *Molecular Cell*, **26**, 1-14.

Volkov R.A., Panchuk I.I., Mullineaux P.M. & Schöffl F. (2006) Heat stress-induced H_2O_2 is required for effective expression of heat shock genes in *Arabidopsis*. *Plant Molecular Biology*, **61**, 733-746.

Xiong L., Schumaker K.S. & Zhu J.-K. (2002) Cell signaling during cold, drought, and salt stress. *The Plant Cell*, **14**, 165-183.

Chapter 1: An *Arabidopsis* mutant with high cyclic electron flow around photosystem I (*hcef*) involving the NADPH dehydrogenase complex

(As published in Plant Cell, Jan 2010)

Aaron K. Livingston, Jeffrey A. Cruz, Kaori Kohzuma, Amit Dhingra and David M. Kramer

Abstract

Cyclic electron flow (CEFI) has been proposed to balance the chloroplast energy budget, but the pathway, mechanism and physiological role remains unclear. We isolated a new class of mutant in *Arabidopsis thaliana*, *hcef* for high CEF1, which shows constitutively elevated CEF1. The first of these, *hcef1* was mapped to chloroplast fructose-1,6-bisphosphatase. Crossing *hcef1* with *pgr5*, which is deficient in the antimycin A-sensitive pathway for plastoquinone reduction, resulted in a double mutant which maintained the high CEF1 phenotype, implying that the PGR5-dependent pathway is not involved. By contrast, crossing *hcef1* with *crr2-2*, deficient in thylakoid NADPH dehydrogenase (NDH) complex, results in a double mutant which was highly light sensitive and lacked elevated CEF1, suggesting that NDH plays a direct role in catalyzing or regulating CEF1. Additionally, the NdhI component of the NDH complex was highly expressed in *hcef1* whereas other photosynthetic complexes, as well as PGR5 decreased. We propose that 1) NDH is specifically up-regulated in *hcef1*, allowing for increased CEF1; 2) the *hcef1* mutation imposes an elevated ATP demand that may trigger CEF1; and 3) alternative mechanisms for augmenting ATP cannot compensate for the loss of CEF1 through NDH.

Introduction

The majority of photosynthetic energy in green plants is stored by the chloroplast in a process termed linear electron flow (LEF). LEF involves light-stimulated electron transfer in two separate reaction centers, photosystem II (PS II) and photosystem I (PS I). Photoexcitation of PS II leads to the extraction of electrons from water, producing molecular oxygen, and the reduction of plastoquinone (PQ) to plastoquinol (PQH_2). Meanwhile, photoexcitation of PS I oxidizes plastocyanin and reduces ferredoxin (Fd). The redox reactions at the two photocenters are linked in series by the cytochrome b_6f complex, which transfers electrons from PQH_2 to plastocyanin. Ferredoxin reduces $NADP^+$ to NADPH via ferredoxin:$NADP^+$ oxidoreductase (FNR) (Ort & Yocum, 1996). The electron transfer reactions of LEF are coupled to the translocation of protons from the stroma into the lumen, leading to the establishment of an electrochemical gradient of protons, or proton motive force (*pmf*) (Mitchell, 1976, Cruz *et al.*, 2001).

The *pmf* generated by the light reactions drives the synthesis of ATP via the chloroplast CF_O CF_1-ATP synthase (ATP synthase) (Jagendorf & Uribe, 1966). The *pmf* also acts as a major regulator of photosynthesis, slowing electron transfer at the cytochrome b_6f complex (Hope *et al.*, 1994a, Takizawa *et al.*, 2007) and triggering photoprotective q_E 'quenching' of excitation energy (Crofts & Yerkes, 1994). The q_E response is activated by acidification of the lumen via the conversion of violaxanthin to zeaxanthin by violaxanthin de-epoxidase (VDE) (Gilmore, 1997) and protonation of the PsbS protein (Li, Bjorkman, Shih, Grossman, Rosenquist, Jansson & Niyogi, 2000).

The production of ATP and NADPH are tightly coupled in LEF, resulting in a fixed ATP/NADPH output ratio. This rigidity can lead to metabolic congestion and inhibition of

photosynthesis if the relative consumption rates of ATP and NADPH do not match their production rates (Edwards & Walker, 1983, Noctor & Foyer, 1998). Recent work on the mechanism of the ATP synthase suggests that 4.67 protons are required for the production of one molecule of ATP (Seelert et al., 2000) (but see (Berry & Rumberg, 1996, Turina, Samoray & Gräber, 2003)), resulting in an ATP/NADPH ratio of 1.29 for LEF. In contrast, the Calvin-Benson cycle requires a 1.5 ratio of ATP/NADPH, leading to a substantial shortfall in ATP/NADPH production. Even after considering the overall energy requirement in photorespiration and nitrate assimilation, the ATP/NADPH demand is estimated to be ~1.43 for C_3 plants (Edwards & Walker, 1983). This shortfall may be exacerbated under environmental stress, where additional ATP is needed to drive protein repair and transport. Without mechanisms to produce additional ATP/NADPH, the chloroplast would be unable to balance its energy budget (Kramer et al., 2004).

Three main mechanisms are proposed to account for balancing of the ATP/NADPH output ratio: 1) the water-water cycle, in which electrons from LEF reduce O_2 to H_2O in the chloroplast (Asada, 2000); 2) the malate shunt, in which electrons from LEF are shuttled to oxidative phosphorylation in the mitochondrion (Scheibe, 2204); and 3) cyclic electron flux around photosystem I (CEF1) (Allen, 2003). In this work, we focus on CEF1, a process in which electrons from the reducing side of PSI are shunted back into the PQ pool via a PQ reductase (PQR), forming PQH_2. The cycle is completed by oxidation of PQH_2 via the cytochrome b_6f complex and plastocyanin, which transfers electrons back to PSI. Proton translocation associated with CEF1 drives ATP synthesis without net reduction of NADPH, increasing the ATP/NADPH output ratio and initiating photoprotection by acidification of the lumen (Heber & Walker, 1992).

Some groups have reported substantial increases in CEF1 under environmental stress, e.g. drought (Jia *et al.*, 2008b, Kohzuma *et al.*, 2008a) or high light (Baker & Ort, 1992), or during the induction of photosynthesis from prolonged dark acclimation (Joët *et al.*, 2002, Joliot & Joliot, 2002). Others have found only small contributions of CEF1 to the photosynthetic energy budget, especially under steady-state conditions (Genty *et al.*, 1989, Harbinson *et al.*, 1989, Avenson *et al.*, 2005a). The confusion may partly be due to the difficulty in measuring cyclic processes such as CEF1 (Baker et al., 2007) or to real differences in CEF1 activity between species or conditions (Kramer et al., 2004). In C_4 plants (Kubicki et al., 1996) and green algae (Finazzi et al., 2002), CEF1 is required to generate the ATP necessary to drive the CO_2^- concentrating mechanisms. However, C_3 plants do not concentrate CO_2 and we estimated that balancing the ATP/NADPH budget in a C_3 plant would require proton flux from CEF1 of only about 14% of that from LEF (Kramer *et al.*, 2004, Avenson *et al.*, 2005a).

At least three different pathways have been proposed for the key step that completes the CEF1 cycle, the transfer of electrons from PSI into the PQ pool: 1) via an antimycin A (AA)-sensitive ferredoxin-PQ oxidoreductase (FQR) (Bendall & Manasse, 1995) which is inhibited in the *pgr5* mutant (Munekage et al., 2002); 2) via the Q_i site of the cytochrome b_6f complex (Bendall & Manasse, 1995); and 3) through ferredoxin-$NADP^+$ oxidoreductase and a thylakoid NADPH dehydrogenase (NDH) (Endo et al., 1998). Genetics and reverse-genetics approaches suggested that the NDH and PGR5 pathways may be relatively slow under non-stressed conditions, or that the loss of either process can be compensated by the other (Munekage *et al.*, 2002, Avenson *et al.*, 2005a).

The mechanism by which CEF1 is regulated is also unknown, but several plausible models have been proposed, including via stromal ADP or ATP levels (Joliot & Joliot, 2006), the

redox state of NADPH/$NADP^+$ (Munekage, Hashimoto, Miyake, Tomizawa, Endo, Tasaka & Shikanai, 2004) or the availability of PS I electron acceptors (Breyton et al., 2006). It is clear, though, that regulation of CEF1 is essential to fulfill its proposed role in balancing the ATP/NADPH output ratio; too much activity will result in depletion of ADP, while too little will result in over-reduction of the electron transfer chain (Kramer et al., 2004). One may thus expect random mutagenesis to produce strains both with lower than wild type CEF1 activity (e.g. *pgr5* (Munekage et al., 2002)) as well as those with high activity, as we report here.

Results

Genetic selection of *hcef* mutants

The first aim of this work was to select mutants that displayed high levels of CEF1 under permissive non-stress conditions. Approximately 20,000 EMS-mutagenized *Arabidopsis thaliana* plants (ecotype Columbia) were screened for high q_E phenotypes using chlorophyll fluorescence imaging (as described in Materials and Methods and see Supplemental data Figure 1 online), yielding approximately 300 stable lines. A secondary screen, using electrochromic shift (ECS) decay kinetics, was used to select mutants that had high levels of light-driven proton motive force (*pmf*) and relatively small changes in thylakoid proton conductivity (g_H^+) which would indicate increased proton translocation. The secondary screen yielded 12 stable lines.

Finally, we conducted a tertiary screen, comparing linear electron flow (LEF) and light-induced proton translocation reflected in the rate of ECS decay (Takizawa, Kanazawa & Kramer, 2008), as described below. The tertiary screen yielded only 5 lines with increased CEF1 rates, which we have designated *hcef* (high cyclic electron flow) mutants. Here, we describe the characterization of *hcef1*, the first of the *hcef* mutants to be extensively studied.

Growth of *hcef1*

The *hcef1* mutant grew photoautotrophically in soil, but with a diminished growth rate, reaching a rosette diameter at maturity approximately 25% of Col (Supplemental Figure 2 online). Bolting was delayed in *hcef1* (35-40 days) compared to Col (24-28 days).

Responses of photosynthetic electron transport and photoprotection.

The maximal photochemical efficiency of PSII in extensively dark-adapted leaves was unaffected by the *hcef1* mutation, with both Col and *hcef1* attaining values near 0.8. However, light-saturated LEF was about 4-fold lower in *hcef1* (Fig. 1A) compared to Col indicating a limitation in photosynthesis downstream of PSII. The light half-saturation point for LEF in *hcef1* (~50 μmol photons m^{-2} s^{-1}) was approximately one third that of Col (~150 μmol photons m^{-2} s^{-1}).

The photoprotective q_E response developed to a larger extent and at lower light intensities in *hcef1* than in Col. In *hcef1*, a q_E value of 0.5 was attained at ~70 μmol photons m^{-2} s^{-1} whereas Col this point was not reached until more than 300 μmol photons m^{-2} s^{-1} (Fig. 1B). The q_E half-saturation was reached at a ~3-fold lower light intensity in *hcef1* (~50 μmol photons m^{-2} s^{-1}) than for Col (~175 μmol photons m^{-2} s^{-1}). At saturating light, q_E reached a level of ~0.7 in Col, consistent with previous values for plants grown under these (relatively low light) conditions (Takizawa et al., 2008) but was substantially higher (~1.2) in *hcef1*. The difference in extent of q_E was particularly pronounced at ~150 μmol photons m^{-2} s^{-1} where the extent in *hcef1* was ~5 fold higher than in Col. In *hcef1*, the extent of q_E decreased between 300 to 500 μmol photons m^{-2} s^{-1} most likely reflecting the onset of increased photodamage, the slowly-reversible

form of excitation quenching associated with photodamage (Muller, Li & Niyogi, 2001). This was supported by the fact that *hcef1* showed a two fold increase in q_I when light intensity was increased from 110 to 480 μmol photons m^{-2} s^{-1}, whereas wild-type showed no significant change in q_I under these conditions (see Supplemental Figure 3 online).

Comparison of the photosynthetic electron and proton circuits in *hcef1* and Col.

We measured chlorophyll fluorescence yields and the kinetics of the thylakoid electrochromic shift (ECS) signal as probed by the electron and proton transfer reactions in leaves. The ECS techniques, reviewed in (Sacksteder & Kramer, 2000, Cruz, Avenson, Kanazawa, Takizawa, Edwards & Kramer, 2005), monitor changes in the thylakoid electric field, and can be used to estimate light-driven fluxes of protons through the photosynthetic apparatus. In a typical experiment, the kinetics of the ECS signal are measured during a brief dark interval punctuating steady-state actinic illumination, an experiment called DIRK for "dark-interval relaxation kinetics". The total amplitude of the DIRK signal, over a few hundred ms, gives a parameter termed ECS_t, that is used to estimate the light-driven *pmf* across the thylakoid (Sacksteder & Kramer, 2000, Cruz *et al.*, 2005). The initial rate of change in the ECS signal can be used to estimate the light-driven proton flux, v_H^+. The ECS decay lifetime yields an estimate of the conductivity of the thylakoid to proton efflux, g_H^+, attributed predominantly to the activity of the chloroplast ATP synthase (reviewed in (Kramer & Crofts, 1996, Cruz *et al.*, 2001).

Figure 1C shows that light-induced *pmf*, as estimated by the ECS_t parameter, was higher and more sensitive to increasing light in *hcef1* than in Col (Fig. 1C). The half-saturation point for *hcef1* was reached at ~75 μmol photons m^{-2} s^{-1} compared to over 150 μmol photons m^{-2} s^{-1} for

Col. Near the growth light intensity (50-150 μmol photons m^{-2} s^{-1}) light-driven *pmf* was 3-4-fold larger in *hcef1* than in Col.

Figure 1D shows that, for both Col and *hcef1*, the conductivity of the thylakoid to protons, g_H+, reflecting mainly the activity of the chloroplast ATP synthase, decreased with increasing light intensity. However, g_H^+ in *hcef1* remained consistently lower, about 60-70% of that in Col (Fig. 1D).

Analysis of photosynthetic parameters of *hcef1* and Col.

To reveal relationships among measured photosynthetic parameters, we have replotted data from Figs. 1A, 1B, and 1C to produce Figure 2. Fig. 2A shows that *hcef1* displayed an approximate 10-fold higher sensitivity of q_E to LEF than Col. However, as shown in Fig. 2B the extent of q_E (taken from Fig. 1B) to *pmf* (ECS_t, Fig. 1C) fall upon the same curve for *hcef1* and Col, i.e. the relationship between qE and ECS_t remained continuous. Figure 2C shows that *hcef1* produces ~5 fold higher light-driven *pmf* (ECS_t values from Fig. 1C) for a given LEF (from Fig. 1A).

Because the proton conductivity of the ATP synthase is ohmic (potential difference is equal to current times resistance) under steady-state conditions, the *pmf* produced by a given proton flux should be proportional to 1/ g_H^+ (Kanazawa & Kramer, 2002, Cruz *et al.*, 2005). Given a constant stoichiometry of proton translocation for LEF (Sacksteder et al., 2000), the relative *pmf* expected from LEF alone can be estimated given by the term pmf_{LEF} = LEF/ g_H^+ (Avenson et al., 2005a), and the relationship of pmf_{LEF} (the *pmf* expected from LEF alone) against ECS_t (a measure of total *pmf*) should be linear with a slope proportional to the proton-to-electron stoichiometry for LEF (Fig. 2d). Upwards deviations from this curve will indicate

proton transfer above that supported by LEF alone. Figure 2D shows that *hcef1* produced ~2-fold higher *pmf* than can be accounted for by LEF alone, i.e. the slope of *pmf* against pmf_{LEF} was 2-fold higher in *hcef1* than Col., consistent with the activation of CEF1in *hcef1* (see Discussion).

The *hcef1* mutant shows higher light-driven proton fluxes from CEF1.

Figure 3 shows the relationship between relative light-driven proton flux (v_H^+) and LEF. This plot is devised to test for contributions from CEF1, since v_H^+ should reflect proton flux generated by turnover of both CEF1 and LEF, while the chlorophyll fluorescence-derived LEF parameter only measures electron transfer from PS II. The *hcef1* mutant showed a ~2-fold higher υ_{H+} as a function of LEF (slopes of the linear regression of LEF versus v_H^+ (in units of $\Delta A/\mu mol\ e^-\ m^{-2}\ s^{-2}$) equal to 0.025) over Col (slope equal to 0.011) (analysis of covariance (ANCOVA) $P<0.05$), and suggesting that *hcef1* has higher light-driven proton fluxes than can be attributed to LEF alone. Upon infiltration of methyl viologen (MV) to inhibit CEF1, the slopes for *hcef1* (slope of 0.012) and Col (with (slope of 0.0095) and without MV) became statistically indistinguishable (ANCOVA $P>0.1$). The observed MV-sensitivity implicates CEF1 as the origin of the increased proton fluxes observed in *hcef1* (see Discussion).

Comparison of PSII photochemical efficiency, Φ_{II} with PSI redox state confirm increased CEF1 in *hcef1*.

Figure 4 plots estimated PSI quantum efficiency (ϕ_I), as determined by Klughammer and Schreiber (1993b) against ϕ_{II}, the photochemical efficiency of PSII measured by saturation-pulse chlorophyll fluorescence yields. (It should be noted that this assay probes the fraction of PS I centers in photochemically-active states, and not ϕ_I *per se*, but should provide good estimates of

ϕ_I as long as PSI antenna size and efficiency remains constant (Baker et al., 2007)). We observed a linear relationship, with a slope near unity, between estimated ϕ_I and ϕ_{II} for Col, implying that the rates of PS I and PSII electron were nearly identical, and that CEF1 was not substantially activated under these conditions in Col (slope of linear regression 1.006). This conclusion was supported by the fact that the slope of ϕ_I vs. ϕ_{II} was unchanged after inhibiting CEF1 by infiltration with MV (slope equal to 1.012) (Fig. 4, open squares). In contrast, *hcef1* showed a nearly 2-fold higher relationship between ϕ_I and ϕ_{II}, (slope of linear regression equal to 1.56)compared to Col (Fig. 4, closed triangles). The differences in slopes between *hcef1* and Col were statistically significant (ANCOVA $P<0.05$), and disappeared upon infiltration with MV (slope of 0.996), implying that CEF1 was responsible for the increased PS I activity.

Chloroplast metabolites

Figure 5 shows relative contents of major stromal metabolites from Col and *hcef1* in rapidly-frozen leaves exposed to continuous actinic light (500 μmol photons m^{-2} s^{-1}) obtained as described in Cruz et al. (2008). It should be noted that these profiles were not calibrated for changes in metabolite sensitivity (Cruz, Emery, Wüst, Kramer & Lange, 2008), and were only intended to give estimates of relative changes, not in absolute concentrations. Compared to Col, *hcef1* showed ~80% decrease in d ribulose 1,5-bisphosphate (RuBP), but a dramatic, 3-fold increase in fructose 1,6-bisphosphate (FBP), suggesting a lesion at FBPase. Despite this large change in stromal metabolic profiles, *hcef1* showed little change in relative ADP/ATP concentrations or 6 carbon single phosphate sugars (HEXP). Similar metabolic effects were seen in a transgenic potato line which had an antisense knockdown for the chloroplast form of fructose 1,6-bisphospatase (Kossmann, Sonnewald & Willmitzer, 1994).

Map-based cloning and complementation of *hcef1*

Using map-based cloning, the *hcef1* mutation was localized to At3g54050, the chloroplast targeted fructose-1,6-bisphosphatase (FBPase), consistent with our observation of large accumulation of FBP in this mutant (Fig. 5) and similar effects on photosynthetic performance (nonphotochemical quenching and q_E) seen in tobacco and potato antisense-FBPase mutants (Bilger, Fisahn, Brummet, Kossmann & Willmitzer, 1995, Fisahn, Kossmann, Matzke, Fuss, Bilger & Willmitzer, 1995). Upon sequencing the gene encoding FBPase, we found a G to A transition, resulting in substitution of lysine for arginine at amino acid 361 (Supplemental Figure 4 online). This residue is in the highly conserved substrate binding pocket of FBPase (Villeret, Huang, Zhang, Xue & Lipscomb, 1995).

The correct identification of the *hcef1* mutation was confirmed by complementation with a construct of the gene At3g54050 and screening using kanamycin resistance (Clough & Bent, 1998). Analysis of three independent *hcef1*-complemented lines showed a return to wild type growth and photosynthetic rates as well as a reversal of the additional proton flux, higher q_E responses, and extent of light-induced *pmf* seen in *hcef1* (Supplemental Figure 5 online). An independent allele of this mutation was provided by *Arabidopsis* seed stock from TAIR, CS836161, in which the FBPase gene (At3g54050) is interrupted with a T-DNA insertion in the promoter region, directly before the start of the gene between all promoter elements and the gene. The T-DNA line, which should have little to no FBPase activity, showed a phenotype similar to *hcef1*, i.e.slowed photosynthesis, and increased CEF1 and q_E (Supplemental Figure 6 online). It is noteworthy, that Serrato et al. (2009) recently described cpFBPaseII, a redox-independent isoform of FBPase, capable of dephosphorylating fructose-1,6-bisphosphate, thus

explaining the photosynthetic competence of the FBPase T-DNA insertion line and possibly *hcef1*.

Characterization of double mutants *hcef1 pgr5* and *hcef1 crr2-2*.

To test whether *hcef1* used the PGR5 dependent pathway for CEF1,the *hcef1* mutant was crossed with the PGR5 knockout line *pgr5* to obtain the *hcef1 pgr5* double mutant. Double homozygous lines were screened using mutation-specific PCR and confirmed by sequencing. Three independent crosses were found to be phenotypically and genotypically identical, and thus results from only one line are shown. The *hcef1 pgr5* line displays approximately 40% reduction in light-saturated LEF compared to *hcef1*. Notably, however, *hcef1 pgr5* retained the MV-sensitive increases in proton flux υ_{H+} as a function of LEF seen in *hcef1* (Fig. 6A), with a slope indistinguishable from that of *hcef1* (ANCOVA P>0.1). Infiltration with methyl viologen decreased the slope for the *hcef1 pgr5* double mutant to nearly match that of the wild type Col (ANCOVA P>0.1).

We also constructed the *hcef1 crr2-2* double mutant (with lesions in both FBPase and NDH) in order to test if *hcef1* used the NDH dependent pathway to run CEF1 . Three independent crosses (double homozygous *hcef1 crr2-2*, confirmed by genotype specific PCR and sequencing) were selected and were found to be phenotypically indistinguishable. The *hcef1 crr2-2* double mutant showed severe growth impairment and light sensitivity, requiring very low growth light (<50 μmol photon m^{-2} s^{-1}) to avoid photobleaching. When grown at 40 μmol photon m^{-2} s^{-1}., maximal LEF in *hcef1* was is about 17% while that in *hcef1 crr2-2* is about 9% of Col. Strikingly, *hcef1 crr2-2* showed a complete loss of elevated proton flux υ_{H+} relative to LEF (showing a slope similar to Col (ANCOVA P>0.1)), associated with increased CEF1 which

is characteristic of *hcef1* (Fig. 6B). Infiltration of MV did not significantly alter the relationship between υ_{H+} (Fig. 6B) (ANCOVA P>0.1), indicating that CEF1 was undetectable in *hcef1 crr2-2* under our conditions.

NDH but not other photosynthetic components are up-regulated in *hcef1*.

We determined relative changes in representative protein levels for key photosynthetic complexes using western blot analysis, applying equal amounts of total protein for *hcef1* and Col. Under our relative low light growth conditions (85-90 μmol photons $m^{-2}s^{-1}$), we observed no significant change between Col and *hcef1* in the PSII component OEC33 and the cytochrome b_6f complex subunit PetD (Fig. 7A). We measured small decreases in the β- and ε- subunits of the ATP synthase (Fig. 7A), consistent with the decreases in ATP synthase activity observed *in vivo* by ECS decay (Fig. 1D). In Fig. 7A, we also observed a small (~50%) decrease in PGR5, associated with the AA-sensitive CEF1 pathway (Munekage et al., 2002).

Under our growth conditions (low light conditions required to maintain *hcef1*) we were unable to detect NDH expression in Col even when loading 75 μg protein per lane whereas we still saw a clear band with *hcef1* diluted to 5 μg protein (Fig. 7B). This means that *hcef1* has at least a 15-fold increase in the accumulation of the NDH-I component of the NDH complex compared to Col.

Discussion

Mutants with high CEF1: implications for the role of CEF1.

CEF1 is proposed to balance the chloroplast ATP/NADPH output, and thus must be finely regulated, probably via metabolic signals (Kramer et al., 2004). Therefore, we expected

to find mutants not only with low CEF1, as have already been reported (Munekage et al., 2002), but also those with higher than normal, or even excessive, CEF1. Our results show that high CEF1 mutants can be isolated via a straightforward process. Presented here is the characterization of the first of these mutants, *hcef1*.

Proton translocation, in addition to that attributable to LEF, increases `$q_E$ sensitivity` in *hcef1* .

Figure 2A shows the *hcef1* mutant displayed a higher sensitivity of q_E to LEF than Col. This would be expected for a mutant with excess CEF1, since additional proton translocation by CEF1 should acidify the lumen. However, an elevated q_E sensitivity can also result from an increase in sensitivity of the q_E response (activation of VDE or protonation of PsbS) to lumen pH, an increase in the fraction of *pmf* stored as ΔpH, or a decrease in the conductivity of the thylakoid membrane to proton efflux (g_H^+) (Kanazawa & Kramer, 2002, Avenson, Cruz & Kramer, 2004, Avenson *et al.*, 2005b). However, Fig. 2B shows that the responses of q_E to estimated light-induced *pmf* were nearly identical in *hcef1* and Col, implying that neither changes in partitioning of *pmf* towards ΔpH nor q_E responses to lumen pH played large roles in changing the overall q_E response in *hcef1*.

Strikingly, *hcef1* produced much higher *pmf* for a given LEF than Col (Fig. 2C), indicating either a decrease in proton conductivity through the ATP synthase or an increase in proton pumping via CEF1 (Kanazawa & Kramer, 2002). The conductivity for proton efflux, g_H^+ was, indeed, decreased in *hcef1* by about 40% with respect to that seen in Col (Fig. 1D), but this difference could not by itself explain the observed 3-5-fold increase in *pmf* and q_E in the mutant (Fig. 1C and 1B).

After eliminating other plausible explanations for increased q_E and *pmf* in *hcef1*, we used three complementary approaches to test directly for increased CEF1. First, we compared estimates of light-driven *pmf* with that expected by LEF alone (with no CEF1) (reviewed in (Baker et al., 2007), determined by pmf_{LEF}. (The term pmf_{LEF} is equal to LEF divided by conductivity of protons through the ATP synthase (g_{H^+}); it is an estimate of the *pmf* generated by LEF-coupled proton influx taking into account the control of proton efflux by g_{H^+}.) Additional proton pumping through CEF1 should cause an engagement of ECS, resulting in an increase of *pmf* above that expected from LEF alone, and thus a steeper slope in the relationship between ECS_t and pmf_{LEF} (Avenson et al., 2005a). We observed a ~2-fold larger *pmf* than could be explained by LEF (Fig 2D) suggesting a substantial increase in CEF1.

As an alternative measure of CEF1, we analyzed dark-interval relaxation kinetics (DIRK) of the ECS signal, using the initial rate of decay of ECS was used as an indicator of the total light-driven flux of protons (v_{H^+}) (Takizawa et al., 2008). We observed ~2-fold higher v_{H^+} as a function of LEF in *hcef1* compared to Col (Fig. 3), indicating a higher proton flux in *hcef1* than can be explained by LEF alone. Importantly, infiltration of MV, which blocks CEF1 by shunting PSI electrons away from the PQ pool to O_2, completely abolished the 'excess' proton translocation in *hcef1*, but had no detectable effects on Col (Fig. 3). Comparison of the slope of v_{H^+} against LEF in the control leaves (with both CEF1 and LEF) and those infiltrated with MV (with LEF only), was used to estimate of the extent of proton translocation contributed by CEF1 (see dashed lines in Fig 3). From this analysis, we conclude that CEF1 was minimally engaged in Col, contributing less that 10% of proton flux, consistent with previous results (Avenson et al., 2005a). In *hcef1*, by contrast, the absolute rate of CEF1 was greatly enhanced, and contributed about the same extent to proton translocation as LEF.

As a third test for increased CEF1 in *hcef1*, we measured the PSI redox state using dark-interval and saturation-pulse-induced absorbance changes in the near infrared, which are often used to obtain estimates of CEF1 (Klughammer & Schreiber, 1993b). Provided that the effective size and efficiency of the PSI-associated antenna remain constant, the fraction of PSI centers in photochemically open states, (i.e. with reduced P_{700} and oxidized FeS centers), will give an estimate of PSI photochemical efficiency (Φ_I). Under steady state photosynthetic conditions with LEF only, Φ_I and Φ_{II} should be equal since electron flux through the two photosystems is balanced. Engagement of CEF1 requires PSI to turn over faster than PSII, increasing Φ_I over Φ_{II}. Thus, CEF1 should register as an increase in Φ_I versus Φ_{II}. This is observed in Fig. 4 as the increase in slope of estimated Φ_I against Φ_{II}. Overall, three complementary approaches qualitatively confirmed a substantial increase in CEF1 in *hcef1*.

Interestingly, the three different spectroscopic approaches to measuring CEF1 suggested different energetic contributions from CEF1. Those based on the proton circuit (v_H^+ vs. LEF, Fig. 3, and pmf_{LEF} vs. ECS_t, Fig. 2D) suggested that in *hcef1* proton flux from CEF1 is about equal to that from LEF. The ϕ_I vs. ϕ_{II} assay (Fig. 4) suggested that about electron transfer through CEF1 was about 50% that through LEF. At this point, we cannot tell whether these differences are due to inaccuracies in any of the methods, or to an elevated proton pumping capacity for CEF1.

hcef1 is a metabolic mutant in fructose 1,6-bisphosphatase.

Map-based cloning and subsequent sequencing, together with complementation studies and known alleles (see See Supplemental Figures 5 and 6 online), demonstrated that the *hcef1* mutation resides in the gene for chloroplast FBPase. This assignment also explains the

observation that *hcef1* accumulated large levels of fructose 1,6-bisphosphate, while being depleted of many other stromal intermediates (Fig. 5).

The reduction of FBPase activity limits the overall photosynthesis, presumably at the Calvin-Benson cycle. However, previous work on *Arabidopsis* showed that decreasing assimilation by itself, e.g. by lowering CO_2 levels, does not substantially activate CEF1 (Avenson et al., 2005a). Rather, we propose that hindering the Calvin-Benson cycle at FBPase resulted in a higher demand for ATP or the accumulation of specific metabolites that activate CEF1.

The *hcef1* and *crr2-2* mutants show photosynthetic growth under the "normal" light conditions used here (90 μmol photons m^{-2} s^{-1}), whereas the *hcef1 crr2-2* double mutant is severely compromised and cannot survive at this intensity. These results suggest that the simplest model is one where 1) *hcef1* has a requirement for extra ATP, but CEF1 is able to meet that need; 2) the *crr2-2* mutant is deficient in NDH, but since the normal demand for ATP is nearly met by LEF, other processes may compensate for the loss of CEF1; and 3) the *hcef1 crr2-2* double mutant has an increased requirement for ATP, but cannot meet this demand via CEF1, probably because it is deficient in NDH activity.

One plausible model suggested by the metabolite profiling data (Fig. 5) involves the feedback-induced disruption of regulation of glyceraldehyde-3-phosphate dehydrogenase (GAPDH), resulting in the depletion of PGA and the accumulation of 1,3-bisphosphoglycerate (BPG). Since BPG is unstable, it will be hydrolyzed back to 3PGA. In fact, mutants with decreased GAPDH function showed a large decrease in PGA (Ruuska *et al.*, 2000, Cruz *et al.*, 2008). This futile cycle would consume ATP without NADPH, requiring an additional ATP source to maintain photosynthesis.

We observed no major changes in the whole leaf ATP/ADP ratios in *hcef1* (Fig. 5), suggesting that the supplementation of ATP, e.g. by increased CEF1, was able to compensate for any extra ATP demand, or that changes in ATP levels in the stroma were compensated by those in the cytosol. These results suggest that the ATP/ADP ratio itself might not be the regulatory trigger that activated CEF1, in contrast to earlier suggestions (Joliot & Joliot, 2006). It is also possible that an ATP deficit induces changes in the redox state of the PSI acceptor pool, leading to redox-induced up-regulation of CEF1, as previously suggested (Breyton et al., 2006). Additionally, a lack of oxidized electron acceptors at the reducing side of PSI could lead to an increase in the formation of reactive oxygen species, such as H_2O_2 which has been show to modulate NDH expression and activity (Lascano, Casano, Martin & Sabater, 2003a). More detailed analysis of the metabolic intermediates in *hcef1* may allow us to directly assess these questions.

Elevated CEF1 in *hcef1* involves NDH, but not the PGR5 pathway

Past work has identified several CEF1 pathways, leading from the reducing side of PSI back into the PQ pool, namely the FQR pathway mediated by PGR5 and the NDH mediated pathway. Upon crossing *hcef1* with the FQR impaired mutant *pgr5*, we found no decrease in the elevated CEF1 (Fig. 6A). These results suggest that additional CEF1 induced by *hcef1* does not involve PGR5. In contrast, crossing with a knockout of chloroplast NDH, *crr2-2,* resulted in double mutants that lost the increased CEF1 observed in *hcef1* (Fig. 6B), implying that NDH is an important component of increased CEF1. This is strongly supported by western blot analyses, which show that *hcef1* has, on a total protein level, decreased PGR5 (Fig. 7A), but strongly upregulated (>15x) NdhI, a component of NDH (Fig. 7B).

We conclude that expression of NDH is specifically up-regulated in *hcef1*, allowing for higher CEF1 capacity under specific conditions. This conclusion is consistent with the reported strong correlation between the expression levels of NDH, but not PGR5, and the extent of CEF1 in C_4 plants (Takabayashi, Kishine, Asada, Endo & Sato, 2005, Darie, De Pascalis, Mutschler & Haehnel, 2006). Our results may also explain the apparent discrepancy between the apparent function of NDH, as a NAD(P)H:plastoquinone oxidoreductase, and its very low expression levels under permissive conditions (Sazanov *et al.*, 1996, Quiles, 2005) where the need for CEF1 is minimal (Kramer et al., 2004), but strongly upregulated under stress where ATP demand may be high (Sazanov *et al.*, 1998, Nixon, 2000, Quiles, 2006), requiring the activation of CEF1 or chlororespiration. Our results do not rule out the participation of PGR5 in CEF1 under other conditions, but because we observe high CEF1 and q_E responses in *hcef1 pgr5*, this protein does not appear to be essential either for CEF1 or for induction of photoprotection (Munekage et al., 2002).

CEF1 involving NDH appears to be critical for maintaining the energy budget of C_3 photosynthesis in *hcef1*.

Our results (Fig. 3) showed that CEF1 was minimally engaged in Col under permissive conditions, in line with previous observations (Harbinson & Foyer, 1991, Kramer *et al.*, 2004, Avenson *et al.*, 2005a). These results are consistent with the ability of *crr2-2* in *Arabidopsis* and the NdhI mutant of tobacco to grow well photosynthetically under permissive conditions, but poorly under stress (Endo *et al.*, 1998, Shikanai *et al.*, 1998, Nixon, 2000). In contrast, introducing the *crr2-2* mutation into *hcef1* (*hcef1 crr2-2*, Fig. 6B) resulted in severely hindered photosynthesis suggesting that *hcef1* imposes a requirement for additional ATP that is fulfilled

via CEF1 that involves NDH. Similar increases in CEF1, presumably reflecting increased chloroplast ATP demand, have been reported upon imposing environmental stresses, such as drought (Jia *et al.*, 2008b, Kohzuma *et al.*, 2008a). At least in the case of *hcef1*, alternative ATP/NADPH balancing mechanisms, e.g. water-water cycle (Asada, 2000), the malate shunt (Scheibe, 2004b) were apparently unable to compensate for the loss of CEF1 upon mutation of NDH. Our results thus support the proposal (Allen, 2003, Kramer *et al.*, 2004, Joliot & Joliot, 2006, Baker *et al.*, 2007) that CEF1 is critical for maintaining the energy budget of C_3 photosynthesis under varying ATP demands.

Methods

Plant Material and Growth Conditions.

Wild-type *Arabidopsis thaliana* (Columbia ecotype) and derived mutants were grown on soil under 16 h:8 h light:dark photoperiod at 85-90 μmol photons $m^{-2}s^{-1}$ at 23°C. Double mutants *pgr5 hcef1* and *crr2-2 hcef1*, along with *hcef1* and wild-type for comparison, were grown under 16:8 photoperiod at 35-40 μmol photons m^{-2} s^{-1} at 23°C. The *pgr5* and *crr2-2* mutants were provided by Dr. T. Shikanai (Kyoto University, Japan).

EMS mutagenesis of *Arabidopsis* and screening of mutants.

Wild-type Columbia (Colell, Green & Ricci) was mutagenized by EMS (ethylmethanesulfonate) as previously described (Kim, Schumaker & Zhu, 2006) and those with high CEF1 were selected through a three-stage screening process. In the first stage of screening, EMS mutants with high q_E responses were selected via chlorophyll fluorescence imaging screening using an approach similar to that employed earlier (Lokstein, Hrtel, Hoffmann &

Renger, 1993, Niyogi, Grossman & Björkman, 1998). The fluorescence imager was constructed in-house using a Sony monochrome camera (Minato, Tokyo, Japan) filtered with a 750 nm interference filter (750FS40-25, Andover, Salem, New Hampshire, USA). Both saturating (~5000 μmol photons $m^{-2}s^{-1}$) and background actinic light (~100 μmol photons $m^{-2}s^{-1}$) were provided by four banks of 9 red (626nm) light emitting diodes (Red Luxeon STAR/O, LXHL-ND94, Phillips Lumiled Lighting Company, San Jose, California, USA). To achieve a higher dynamic range, the electronic shutter speed of the video camera was varied electronically, using a longer shutter opening during weak or steady-state illumination and a shorter shutter speed during saturation pulses.

Trays of intact, mutagenized plants, approximately 12 days after planting, were placed into the darkened chamber of the video imager and given weak and saturating pulses (as above). Fluorescence images were recorded during these light treatments to estimate minimal (F_0) and maximal fluorescence yields (Lokstein et al., 1993). The plants were then illuminated with actinic light (~100 μmol photons $m^{-2}s^{-1}$) for 20 minutes, with saturating pulses every 4 minutes, during which fluorescence images were recorded to estimate steady-state photosynthetic conditions (Krall & Edwards, 1992) and pulse-induced (F_M') fluorescence yields. After 20 minutes, the actinic light was switched off and fluorescence images were recorded during a series of 10 saturating pulses at one minute intervals to probe the relaxation of NPQ, estimating the F_M'' parameter (Genty et al., 1989). The F_M' and F_M'' images were used to calculate false-color representations of the q_E responses as described previously (Niyogi et al., 1998).

In the second stage of screening, high q_E plants were tested for the buildup of elevated light-driven *pmf* using our ECS probes, as described in (Sacksteder & Kramer, 2000, Cruz *et al.*, 2005) and in detail in the following section In the third screening stage, mutants were selected in

which the proton flux, estimated by the v_H^+ parameter, exceeded that expected by LEF alone (Takizawa et al., 2008), as described in the following section.

***In Vivo* Spectroscopic Assays.**

Fully-expanded leaves between 24 and 28 days old at 23°C were placed in the leaf chamber of an in-house constructed non-focusing optics spectrophotometer/fluorometer (NoFOSpec) (Sacksteder & Kramer, 2000, Kanazawa & Kramer, 2002), modified to allow continuously-flowing humidified air. Saturation-pulse chlorophyll fluorescence yield changes were used to calculate q_E and the photochemical yield of photosystem II (ϕ_{II}) (Genty *et al.*, 1989, Kanazawa & Kramer, 2002, Avenson *et al.*, 2005a). Chlorophyll fluorescence was excited with 30 μs pulses of green (525 nm) light from an LED (Hewlett-Packard HLMP-CMR) and detected with a photodiode protected from actinic light by an infrared (RG730, Schott) filter. The pulsed fluorescence signal was filtered electronically and measured by an analog-to-digital converter (Kramer and Crofts, 1996). An Ulbricht integrating sphere was used (Knapp & Carter, 1998) to estimate the relative absortivities of Col and mutant *hcef1* at 0.5 and 0.4 respectively allowing us to calculate rates of LEF from ϕ_{II} (Ziyu, Maurice & Edwards, 2004a).

LEF was measured after approximately 15 minutes of actinic illumination, to establish steady-state photosynthetic conditions. The extent of q_E was estimated as described previously (Genty *et al.*, 1989, Kramer & Crofts, 1996, Kanazawa & Kramer, 2002) taking F_M' just before switching off the actinic light and F_M'' after 10 minutes of dark relaxation. F_V/F_M and q_I measurements were taken from plants that were dark adapted for 12 hours.

Steady-state, light-induced *pmf* was estimated from dark-interval relaxation kinetics (DIRK) changes in absorbance associated with the electrochromic shift (ECS) at around 520 nm

as described previously (Sacksteder & Kramer, 2000, Cruz *et al.*, 2005). The maximal extent of the ECS signal over a ~300 ms dark interval, termed ECS_t, is proportional to the light-induced *pmf*. The conductivity of the thylakoid membrane to protons (g_H^+), attributable to the activity of the ATP synthase, was estimated from the inverse of the time constant of ECS decay (τ_{ECS}) (Kramer & Crofts, 1996, Kanazawa & Kramer, 2002, Cruz *et al.*, 2005). The amplitude of *pmf* contributed by LEF, termed pmf_{LEF}, was estimated by dividing LEF by g_H^+ (Avenson et al., 2005a). The relative value of steady state proton flux across the thylakoid membrane (v_H^+) was estimated from the initial slope of the ECS decay (Takizawa et al., 2008). To account for variations in leaf thickness and pigmentation, ECS measurements were normalized either to the extent of the rapid rise in ECS induced by a saturating, single-turnover flash (Kramer and Crofts, 1989) or to leaf chlorophyll content (Porra et al., 1989), resulting in very similar corrections, with *hcef1* showing ECS responses relative to Col of 54% and 56%, respectively (Supplemental Table 1 online).

The redox state of PSI was measured using the technique of (Klughammer & Schreiber, 1993b) using a probe beam provided by an 810 nm LED (ELD-810-525 Roithner, Vienna, Austria). Light reaching the detector was filtered using an infrared-transmitting filter (RT-830, Edmund Optics, Barrington, NJ). Data were collected and calculated as described in (Peterson, 1991, Klughammer & Schreiber, 1993b). Key experiments were repeated using the two-wavelength deconvolutions described in (Oja et al., 2004) (ΔA(820-940 nm)) with similar results indicating that absorbance changes from plastocyanin or other components did not substantially affect the measurements.

Introduction of methyl viologen into leaves.

Where indicated, plants were infused by placing them between two Kimwipes (Kimberly-Clark, Mississauga, Ontario) saturated either with distilled water or a solution of 100 μM methyl viologen, and incubated under dim light (~5 μmol photon m^{-2} s^{-1}) for 1 hour. After infiltration, leaves were gently blotted to remove excess liquid prior to experimentation.

Map-based cloning.

The *hcef1* mutant was mapped using molecular markers based on single nucleotide polymorphisms (Drenkard, Richter, Rozen, Stutius, Angell, Mindrinos, Cho, Oefner, Davis & Ausubel, 2000) and cleaved amplified polymorphic sequences (Baumbusch, Sundal, Hughes, Galau & Jakobsen, 2001, Jander, Norris, Rounsley, Bush, Levin & Last, 2002). F2 plants were derived from breeding homozygous *hcef1* (Columbia background) and wild-type (Landsberg *erecta* background). The *hcef1* mutation was found to be recessive. Genomic DNA was isolated from homozygous F2 plants (*hcef1 hcef1*) which expressed a high q_E response using chlorophyll fluorescence imaging (Niyogi et al., 1998). At3g54050 was PCR amplified from Columbia wild-type and *hcef1* genomic DNA, using Amplitaq Gold PCR Master Mix (Applied Biosystems, Branchburg, New Jersey, USA). The PCR products were sequenced using Big Dye Reagent and were run on an ABI Prism 377 (reagent and machine from AME Bioscience, Toroed, Norway) at the Washington State University Molecular Biology Core Laboratory, Pullman, Washington.

Metabolic profiling.

Metabolic profiling of the Calvin-Benson Cycle intermediates was accomplished as previously described (Cruz et al., 2008), except that 1g of fresh weight *Arabidopsis* plants was used in place of tobacco leaf disks. Plants were dark adapted for 24 hours and place for 20

minutes under 500 μmol photon m^{-2} s^{-1}. The 1g of fresh weight *Arabidopsis* was rapidly flash-frozen in liquid nitrogen and ground using a liquid nitrogen chilled mortar. Extraction and LCMS assays were completed as described by Cruz et al. (2008), yielding relative changes of metabolites (but not absolute concentrations, since no spike-recovery assays were performed).

Measurement of ATP and ADP content

ATP and ADP levels in leaf tissue extracts were determined using the luciferase assay as described previously (Lundin & Thore, 1975) with the following modifications. Extracts were incubated for 30 minutes at room temperature in buffer containing 50 mM Tris-HCl, pH 8.0, 5 mM $MgCl_2$, 4 mM KCl, 50 μM phosphoenol pyruvate in the presence or absence of 4 units of pyruvate kinase (PK) (Sigma-Aldrich, St. Louis, Missouri) in a total volume of 450 microliters. Fifty microliters of Enliten® Luciferase reagent (Promega Corp., Madison, Wisconsin) was added and luminescence was measured immediately using an LKB 1250 Luminometer, linked to computer via a USB-1608FS (Measurement Computing, Norton, Massachussettes). The amplitude of the luminescent signal in the PK(-) samples was proportional ATP content. To obtain relative ADP content the amplitudes from samples without PK were subtracted from the corresponding samples with PK.

Complementation of *hcef1*.

The *hcef1* mutation was complemented with the wild-type Columbia coding sequence of the gene At3g54050, the chloroplast targeted fructose 1,6-bisphosphatase (FBPase). The coding sequence was created using the Thermoscript RT-PCR system (Invitrogen, Carlsbad, California), primers 5'CAGAAACCATGGCAGCAACCGCCGCAAC3' and

5'TTAGTATCTAGATCAAGCCAAGTACTTCTCC3', with RNA isolated from wild-type Columbia (RNA was isolated using RNeasy Plant Mini Kit, Qiagen, Valencia, California). The PCR product was verified by sequencing and subcloned into pAVA 121 to add a tobacco etch virus translational enhancer, a double 35S promoter regions, and the the nopaline synthase terminator (tNOS) to the construct. The resulting construct was then subcloned into the pCAMBIA 2300 plasmid (www.cambia.org) and transferred to *Agrobacterium tumefaciens* GV3101 (pMP90) strain. *A. tumefaciens* cells were suspended at OD_{600}=0.85 then used to transform homozygous *hcef1* plants using the floral dip method as described by Clough and Bent (1998). The transformed plants were then selected for using 50 μg/ml Kanamycin with 0.43 % Murashige and Skoog salts and 1.0% sucrose (Clough & Bent, 1998).

***hcef1* crosses.**

Crosses of *pgr5 hcef1* and *crr2-2 hcef1* were screened by genetic analysis for the presence of each mutation in the double cross. The following primers were used: *pgr5*- forward 5'CCTTTGGGAACGAATGCTTTA3', reverse 5'AAACCCGCAACATGAGAAAC3', specific 5'GACCTAAGCAAGGAAACC3'; *hcef1*- forward 5'GCTGCCGTCTCTACTGGTTC3'; reverse 5'AGACCACCAATGCAACATCC; specific 5'GCAAAGAGCAAAAATGGAAAACTTAG3'; *crr2-2*- forward 5'GCAAAGAACGGGAAAGCTT3', reverse 5'AGGACACAACATCCCGGTC3', specific 5'CGTTCCCTTTAACTAAGTAT3'. The presence of both mutations in the double mutants was confirmed by PCR and sequencing. Both double mutant varieties were grown at ~40 μmol photon m^{-2} s^{-1}.

Protein extraction and western blot analyses

For immunoblot analyses, leaf total protein was extracted by grinding full fresh *Arabidopsis* leaves under liquid nitrogen and extracted with 100mM Tricine-KOH, pH 7.5, 2mM $MgCl_2$, 10mM NaCl, 1mM ethylenediaminetetraacetic acid, 1mM phenylmethylsulfonyl fluoride and 10mM β- mercaptoethanol. The suspension was microcentrifuged for 5 min at 13000 r.p.m., and the resulting pellet containing the leaf insoluble proteins was dissolved in sample buffer [50 mm Tris-HCl, pH 6.8, 2% sodium dodecyl sulphate, 10 mmβ-mercaptoethanol, 10% glycerol and 0.04% bromophenol blue (BPB)]. Proteins were separated by 12% sodium dodecyl sulphate–polyacrylamide gel electrophoresis and then blotted onto polyvinylidene difluoride membranes (Invitrogen, Carlsbad, California). The amount of protein loaded was revealed by Ponceau S staining (Sigma-Aldrich, St Louis, Missouri).

The membranes were then probed with the following antibodies: NdhI (from Peter Nixon and Mako Boehm, Imperial College London), PetD (from Alice Barkan University of Oregon), OEC33 and CF_1-β (from Dr. Akiho Yokota Nara Institute of Science and Technology) and the CF_1-ε (from Dr. T. Shikanai Kyoto University). Using a conjugated anti-rabbit secondary antibody, immunoblots were cast onto x-ray films (Kodak, Rochester, New York) by an ECL^+ chemiluminescence kit (Amersham Biosciences Co., Piscataway, New Jersey)

The amount of total protein introduced into each lane, determined by the Lowry assay (Lowry, Rosebrough, Farr & Randell, 1951), was optimized to give the best signals for each target protein. For detection of CF_1- β and CF_1- ε, we introduced 5 μg protein, whereas with NdhI, OEC33 and the Rieske iron-sulfur protein (PetD) we loaded, 10 μg proteins.

Accession Numbers

Sequence data from this article can be found in the EMBL/GenBank data libraries under the following accession number(s): chloroplast targeted fructose-1,6-bisphosphatase (FBPase), AY039934 (At3g54050); proton gradient regulator 5 (PGR5), BX821933 (At2g05620); and chlororespiratory reduction 2-2, AK226825 (At3g46790). The T-DNA insertion line in this gene was obtained from TAIR as stock number CS836161, The *pgr5* and *crr2-2* mutants were provided by Dr. T. Shikanai (Kyoto University, Japan).

Acknowledgements:

The authors would like to thank Drs. Jeremy Harbinson, Thomas Sharkey, Murray Badger, Atsuko Kanazawa and Susanne von Caemmerer for interesting discussions. We are grateful to Drs. Peter Nixon and Marko Boehm (Imperial College London) for the NdhI antibody, Dr. Alice Barkan (University of Oregon) for the PetD, OEC33 and CF_1-β antibodies, Dr. Akiho Yokota (Nara Institute of Science and Technology) for the CF_1-ε antibodies and Dr. T. Shikanai (Kyoto University) for the PGR5 antibodies and the *pgr5* and *crr2-2* mutants. We would also like to thank Dr. Mark Lange (Washington State University) for his assistance, guidance, and use of equipment during the metabolomic studies. We also acknowledge the expert assistance of Mr. Craig Whitney for plant growth management and Heather Enlow and Kara Blizzard for their technical assistance. This work was supported by U.S. DOE grant DE-FG02-04ERl5559 to DMK.

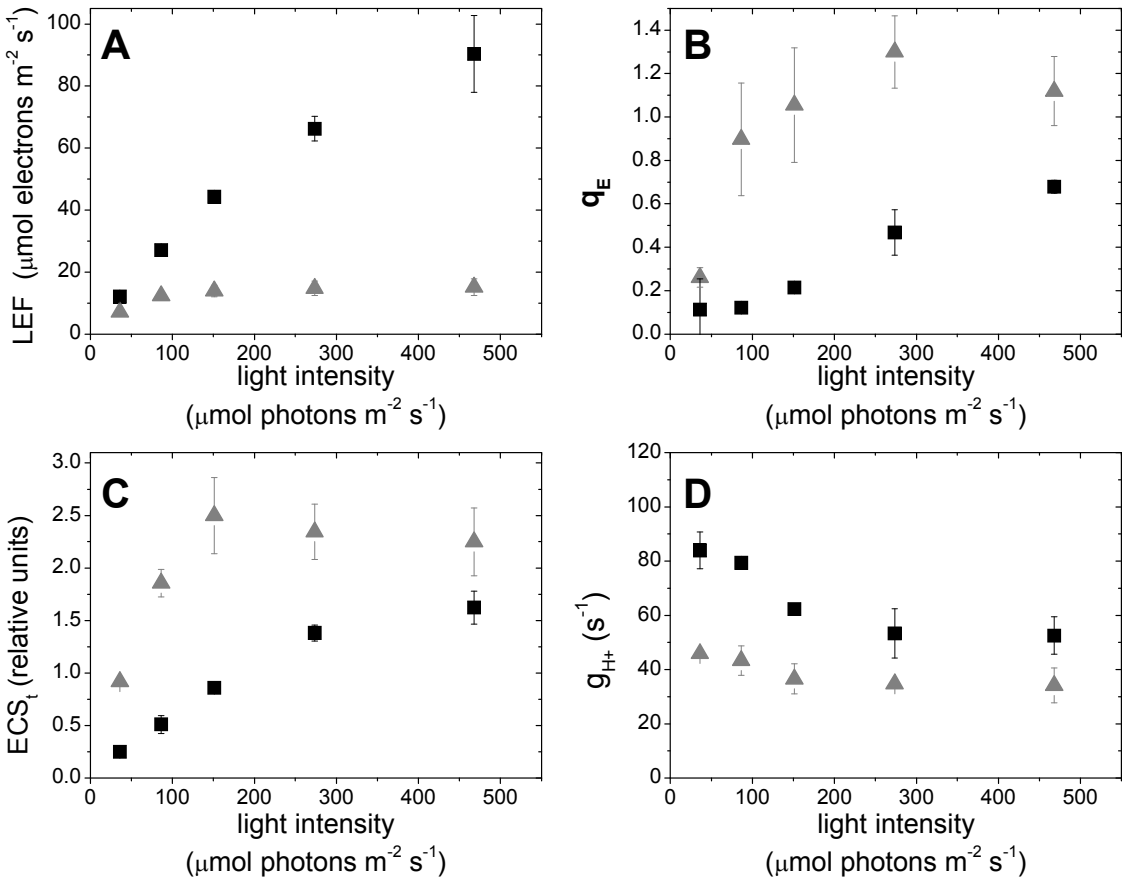

Figure 1. Comparison of photosynthetic properties of Col and *hcef1*. (A-D) Columbia (■) and *hcef1* (▲) are compared for differences in LEF **(A)**, q_E **(B)**, ECS_t **(C)** and g_H^+ **(D)** versus light intensity. Error bars equal standard deviation, *n*=4 individual plants.

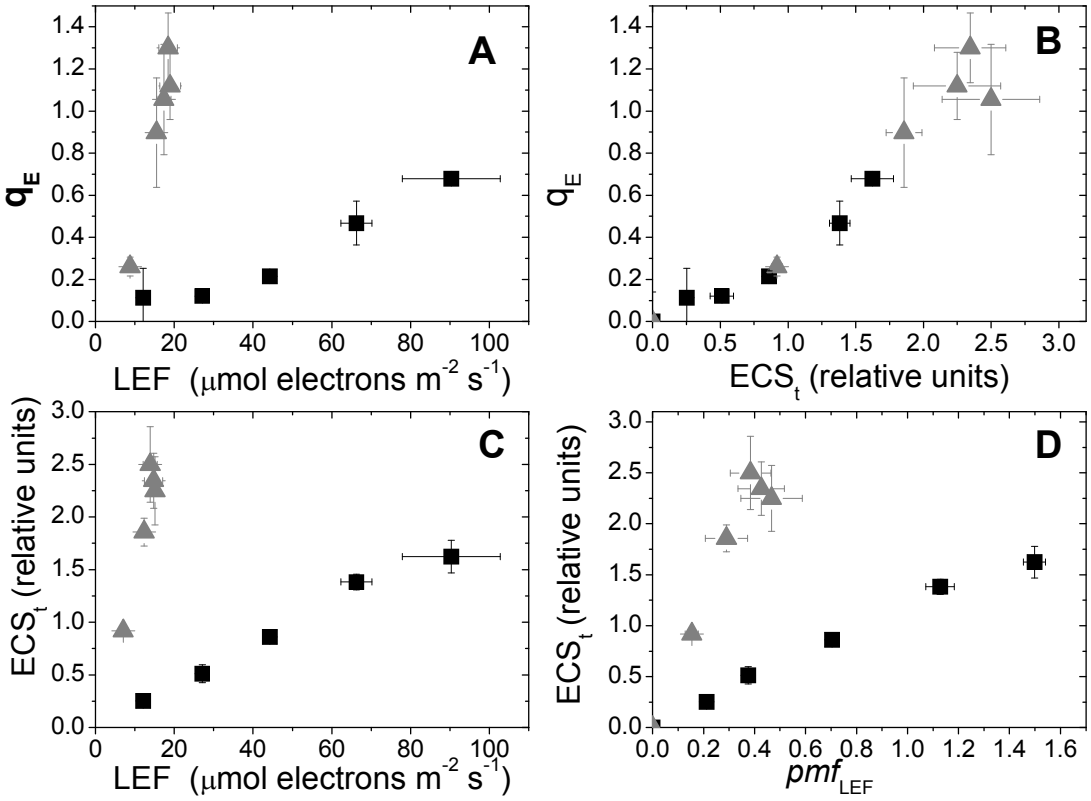

Figure 2. Analysis of photosynthetic regulation in Col and *hcef1*. Data from Columbia (■) and *hcef1* (▲) were replotted to show the following relationships:

(A) q_E vs. LEF.

(B) q_E vs. light-driven *pmf* (ECS_t,),

(C) light driven *pmf* (ECS_t) and LEF.

(D) light-driven *pmf* and the *pmf* expected from LEF alone (pmf_{LEF}).

All data represent averages of *n*=4 individual plants +/- standard deviation.

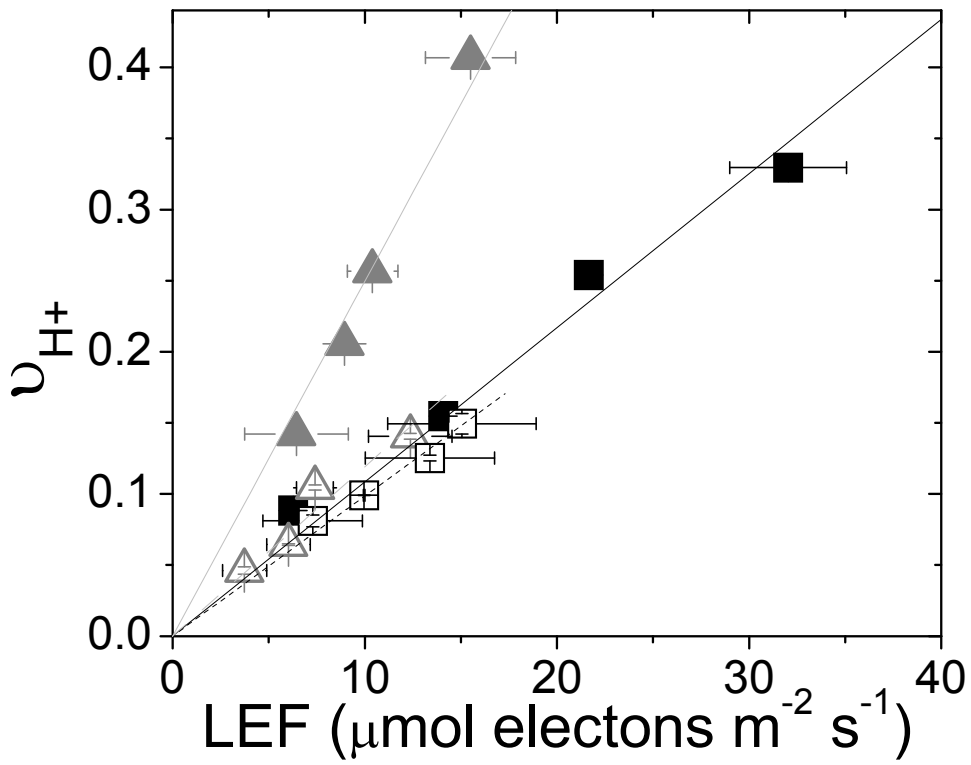

Figure 3. Evidence for elevated CEF1 in *hcef1:* The relationship between light-driven proton translocation across the thylakoid (v_H^+) and linear electron flow (LEF). Columbia (,■,□) and *hcef1* (▲,△) leaves were infused with either water (closed symbols) or methyl viologen (open symbols). To avoid photodamage, particularly in the methyl viologen treated leaves, data were taken at light intensities below the light saturation point for LEF in Col, i.e. between 0 and ~ 120 μmol photons m^{-2} s^{-1}. Only *hcef1* infused with water was significantly different. Error bars represent standard deviation *n*=3 individual plants.

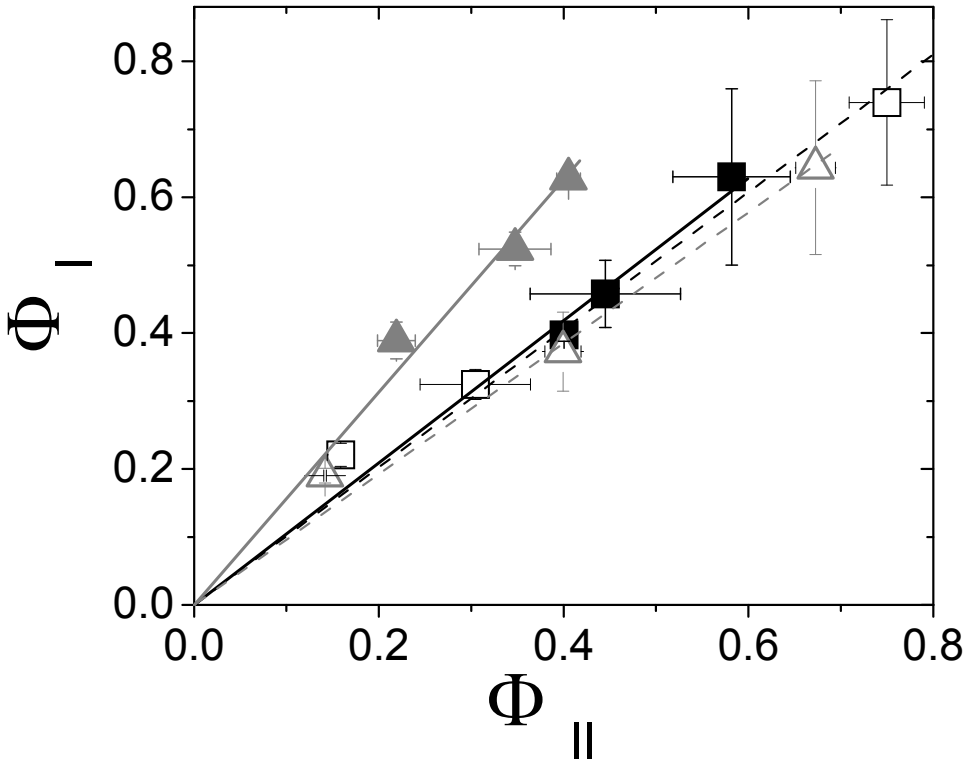

Figure 4. Comparison of PSII photochemical efficiency, Φ_{II} with PSI redox state: The relationship between estimated photochemical efficiencies of PS I (ϕ_I) and PS II (ϕ_{II}). Columbia (■,□) and *hcef1* (▲,△) leaves were infused with either water (closed symbols) or methyl viologen (open symbols). To avoid photodamage, data were taken at light intensities below the light saturation point for LEF in Col, i.e. between 0 and ~ 120 μmol photons m^{-2} s^{-1}. Estimates of photochemical efficiencies of PS I (ϕ_I) and PS II (ϕ_{II}) were made spectroscopically as described in Materials and Methods. Only *hcef1* infused with water was significantly different. Error bars represent standard deviation *n*=3 individual plants.

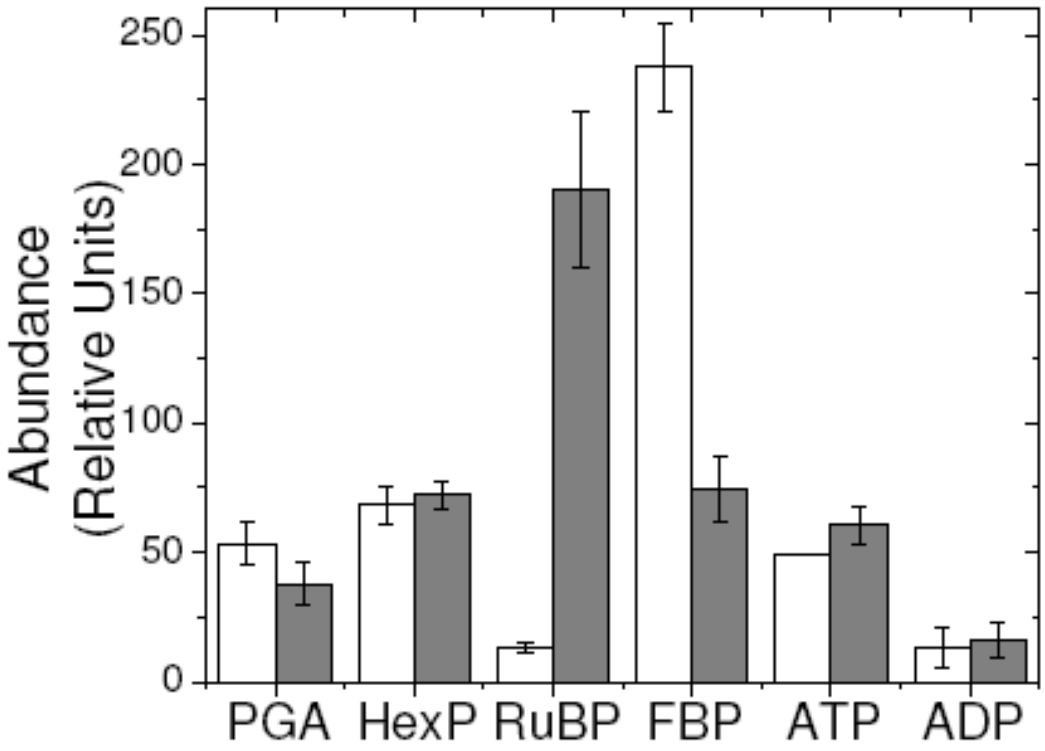

Figure 5. Metabolic profiling of illuminated *hcef*1 and Col leaves. The grey bars represent Col and the white bars represent *hcef*1. *Arabidopsis* plants were dark adapted for 24 hours, then illuminated with 500 μmol photons m^{-2} s^{-1} for 20 minutes. Leaves (one gram of fresh weight) were rapidly flash-frozen in liquid nitrogen. Metabolite levels were measured as described in Methods.

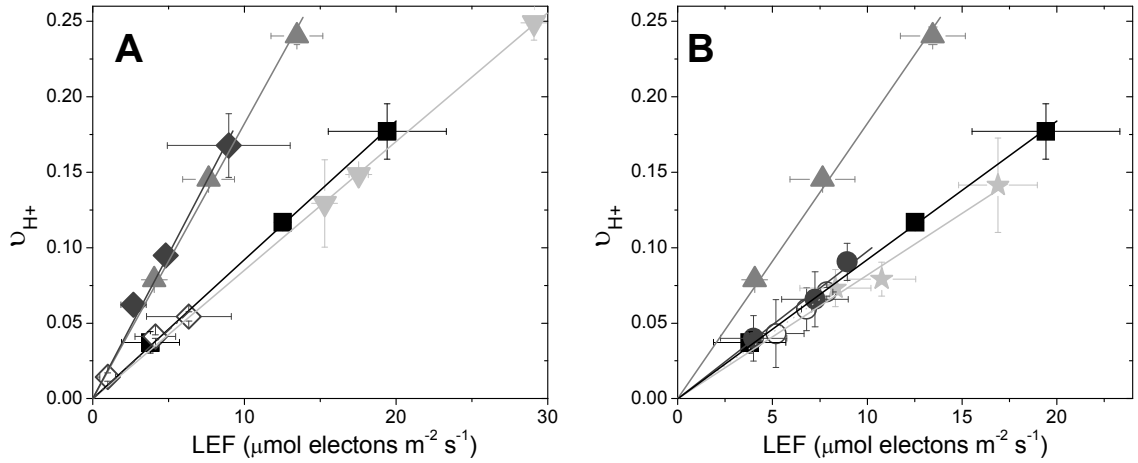

Figure 6. Effects of double mutations on elevated CEF1. The relationships between light-driven proton translocation across the thylakoid (v_H^+) and linear electron flow (LEF) were assessed in leaves of Col (■), *hcef1* (▲), *pgr5* (▼), *crr2-2* (★), the *hcef1 pgr5* double mutant (◆◇) and the *hcef1 crr2-2* double mutant (●◯). All data indicated by the filled symbols were obtained on leaves infiltrated with distilled water. The double mutants were also treated with methyl viologen, as described in Fig. 3, as indicated by the open symbols. The data for Col and *hcef1* is reproduced in both **(A)** and **(B)** for comparison with the other mutants.

(A) The *hcef1 pgr5* double mutant compared to Col, *pgr*5 and *hcef1*.

(B) The *crr2-2* mutant and the *hcef1 crr2-2* double mutant show no increases in CEF1. For all linear fits $P < 0.05$. Error bars represent standard deviation, with *n*=3 individual plants.

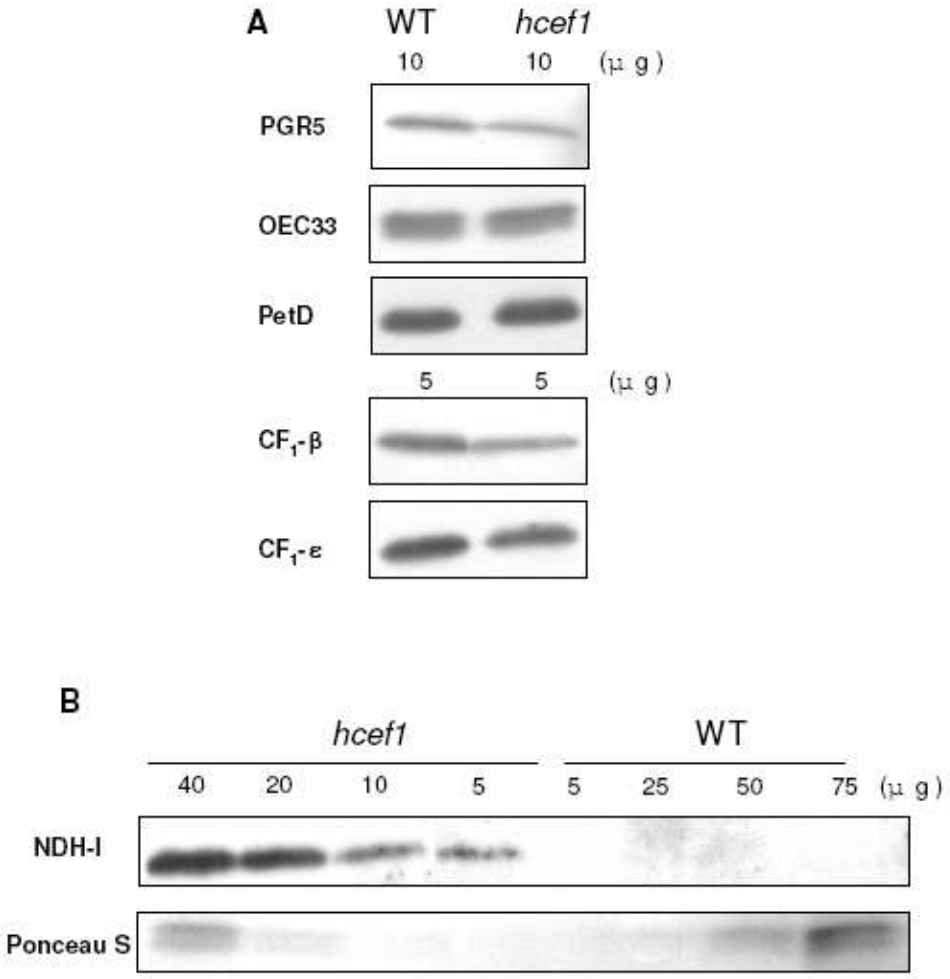

Figure 7. Changes in the protein levels of representative photosynthetic components of Col and *hcef1*.

(A) Lanes were loaded with either 5 μg (CF_1- β,ε) or 10 μg (PGR5, OEC33 and PetD) total proteins and blotted with primary and secondary antibodies as described in Methods.

(B) Titrations for NDH-I expression (top) were accomplished using a range of total protein content as indicated above each blot for both *hcef1* and wild-type. Protein loading was confirmed by Ponceau S staining (bottom), representative bands of ~10 kDa are shown.

References

Allen, J.F. (2003). Cyclic, pseudocyclic and noncyclic photophosphorylation: new links in the chain. *Trends in Plant Sciences,* **8,** 15-19.

Asada, K. (2000). The water-water cycle as alternative photon and electron sinks. *Philosophical Transactions of the Royal Society B: Biological Sciences,* **355**, 1419-1431.

Avenson, T.J., Cruz, J.A., and Kramer, D.M. (2004). Modulation of energy dependent quenching of excitons (q_E) in antenna of higher plants. *Proceeding of the National Academy of Science,* **101**, 5530-5535.

Avenson, T.J., Cruz, J.A., Kanazawa, A., and Kramer, D.M. (2005a). Regulating the proton budget of higher plant photosynthesis. *Proceeding of the National Academy of Science,* **102**, 9709–9713.

Avenson, T.J., Kanazawa, A., Cruz, J.A., Takizawa, K., Ettinger, W.E., and Kramer, D.M. (2005b). Integrating the proton circuit into photosynthesis: Progress and challenges. *Plant Cell and Environment.* **28**, 97-109.

Baker N.R. & Ort D.R. (1992) Light and crop photosynthetic performance. *In Crop Photosynthesis: Spatial and Temporal Determinants (eds N.R. Baker & H. Thomas)*, **Elsevier Science Publishers, Amsterdam, the Netherlands**, 289-312.

Baumbusch, L.O., Sundal, I.K., Hughes, D.W., Galau, G.A., and Jakobsen, K.S. (2001). Efficient protocols for CAPS-based mapping in Arabidopsis. *Plant Molecular Biology Reporter,* **19**, 137-149.

Bendall, D.S., and Manasse, R.S. (1995). Cyclic photophosphorylation and electron transport. *Biochimica et Biophysica Acta,* **1229**, 23-38.

Berry, S., and Rumberg, B. (1996). H^+/ATP coupling ratio at the unmodulated CF_0CF_1-ATP synthase determined by proton flux measurements. *Biochimica et Biophysica Acta,* **1276**, 51-56.

Bilger, W., Fisahn, J., Brummet, W., Kossmann, J., and Willmitzer, L. (1995). Violaxanthin Cycle Pigment Contents in Potato and Tobacco Plants with Genetically Reduced Photosynthetic Capacity. *Plant Physiol*ogy, **108**, 1479-1486.

Breyton, C., Nandha, B., Johnson, G., Joliot, P., and Finazzi, G. (2006). Redox modulation of cyclic electron flow around Photosystem I in C_3 plants. *Biochemistry* 45, 13465-13475.

Clough, S.J., and Bent, A.F. (1998). Floral dip: a simplified method for Agrobacterium-mediated transformation of *Arabidopsis thaliana*. *Plant Journal,* **16**, 735-743.

Crofts, A.R., and Yerkes, C.T. (1994). A molecular mechanism for q_E-quenching. *FEBS Letters,* **352**, 265-270.

Cruz, J.A., Sacksteder, C.A., Kanazawa, A., and Kramer, D.M. (2001). Contribution of electric field ($\Delta\psi$) to steady-state transthylakoid proton motive force (*pmf*) in vitro and in vivo. Control of *pmf* parsing into $\Delta\psi$ and ΔpH by ionic strength. *Biochemistry,* **40**, 1226-1237.

Cruz, J.A., Emery, C., Wüst, M., Kramer, D.M., and Lange, B.M. (2008). Metabolite profiling of Calvin cycle intermediates by HPLC-MS using mixed-mode stationary phases. *Plant Journal,* **55**, 1047-1060.

Cruz, J.A., Avenson, T.J., Kanazawa, A., Takizawa, K., Edwards, G.E., and Kramer, D.M. (2005). Plasticity in light reactions of photosynthesis for energy production and photoprotection. *Journal of Experimental Botany*, **56**, 395-406.

Darie, C.C., De Pascalis, L., Mutschler, B., and Haehnel, W. (2006). Studies of the Ndh complex and photosystem II from mesophyll and bundle sheath chloroplasts of the C-4-type plant *Zea mays*. *Journal of Plant Physiology*, **163**, 800-808.

Drenkard, E., Richter, B.G., Rozen, S., Stutius, L.M., Angell, N.A., Mindrinos, M., Cho, R.J., Oefner, P.J., Davis, R.W., and Ausubel, F.M. (2000). A simple procedure for the analysis of single nucleotide polymorphisms facilitates map-based cloning in Arabidopsis. *Plant Physiology,* **124**, 1483-1492.

Edwards G.E. & Walker D.A. (1983) C_3, C_4:Mechanisms, and Cellular and Environmental Regulation of Photosynthesis. *Textbook on C3, C4 Photosynthesis*, **Blackwell Scientific**.

Endo, T., Shikanai, T., Sato, F., and Asada, K. (1998). NAD(P)H dehydrogenase dependent, antimycin A-sensitive electron donation to plastoquinone in tobacco chloroplasts. *Plant and Cell Physiology,* **39**, 1226-1231.

Finazzi, G., Rappaport, F., Furia, A., Fleischmann, M., Rochaix, J.-D., Zito, F., and Forti, G. (2002). Involvement of state transitions in the switch between linear and cyclic electron flow in *Chlamydomonas reinhardtii*. *EMBO Journal,* **3**, 280–285.

Fisahn, J., Kossmann, J., Matzke, G., Fuss, H., Bilger, W., and Willmitzer, L. (1995). Chlorophyll fluorescence quenching and violaxanthin deepoxidation of FBPase antisense plants at low light intensities and low temperatures. *Physiologia Plantarum,* **95**, 1-10.

Genty, B., Briantais, J.M., and Baker, N.R. (1989). The relationship between the quantum yield of photosynthetic electron transport and quenching of chlorophyll fluorescence. *Biochimica et Biophysica Acta,* **990**, 87-92.

Gilmore, A.M. (1997). Mechanistic aspects of xanthophyll cycle-dependent photoprotection in higher plant chloroplasts and leaves. *Physiologia Plantarum,* **99**, 197-209.

Harbinson, J., and Foyer, C.H. (1991). Relationships between the efficiencies of Photosystems I and II and stromal redox state in CO_2-free air : Evidence for cyclic electron flow *in vivo*. *Plant Physiology,* **97**, 41-49.

Harbinson, J., Genty, B., and Baker, N.R. (1989). Relationship between the Quantum Efficiencies of Photosystems I and II in Pea Leaves. *Plant Physiology,* **90**, 1029-1034.

Heber, U., and Walker, D. (1992). Concerning a dual function of coupled cyclic electron transport in leaves. *Plant Physiology,* **100**, 1621-1626.

Hope, A.B., Valente, P., and Matthews, D.B. (1994). Effects of pH on the kinetics of redox reactions in and around the cytochrome *bf* complex in an isolated system *Photosynthesis Research,* **42**, 111-120.

Jagendorf, A.T., and Uribe, E. (1966). ATP formation caused by acid-base transition of spinach chloroplasts. *Proceedings of the National Academy of Sciences,* **55**, 170-177.

Jander, G., Norris, S.R., Rounsley, S.D., Bush, D.F., Levin, I.M., and Last, R.L. (2002). Arabidopsis map-based cloning in the post-genome era. *Plant Physiology,* **129**, 440-450.

Jia, H., Oguchi, R., Hope, A.B., Barber, J., and Chow, W.S. (2008). Differential effects of severe water stress on linear and cyclic electron fluxes through Photosystem I in spinach leaf discs in CO_2-enriched air. *Planta*, **228**, 803-812.

Joët, T., Cournac, L., Peltier, G., and Havaux, M. (2002). Cyclic electron flow around photosystem I in C_3 plants. In vivo control by the redox state of chloroplasts and involvement of the NADH-dehydrogenase complex. *Plant Physiology,* **128**, 760–769.

Joliot, P., and Joliot, A. (2002). Cyclic electron transfer in plant leaf. *Proceedings of the National Academy of Sciences,* **99**, 10209–10214.

Joliot, P., and Joliot, A. (2006). Cyclic Electron flow in C3 plants. *Biochimica et Biophysica Acta, **1757***, 362-368.

Kanazawa, A., and Kramer, D.M. (2002). In vivo modulation of nonphotochemical exciton quenching (NPQ) by regulation of the chloroplast ATP synthase. *Proceedings of the National Academy of Sciences,* **99**, 12789-12794.

Kim, Y., Schumaker, K.S., and Zhu, J.-K. (2006). EMS Mutagenesis of Arabidopsis. *Methods in Molecular Biology,* **323**, 101-103.

Klughammer, C., and Schreiber, U. (1993). An improved method, using saturating light pulses, for the determination of photosystem I quantum yield via $P700^{+}$-absorbance changes at 830 nm. *Planta*, **192**, 261-268.

Knapp, A.K., and Carter, G.A. (1998). Variability in leaf optical properties amoung 26 species from a broad range of habitats. *American Journal of Botany,* **85**, 940-946.

Kohzuma, K., Cruz, J.A., Akashi, K., Munekage, Y., Yokota, A., and Kramer, D.M. (2008). The long-term responses of the photosynthetic proton circuit to drought. *Plant Cell and the Environment,* **32**, 209-219.

Kossmann, J., Sonnewald, U., and Willmitzer, L. (1994). Reduction of the chloroplastic fructose-1,6-bisphosphatase in transgenic potato plants impairs photosynthesis and plant growth. *Plant Journal,* **6**, 637-650.

Krall, J.P., and Edwards, G.E. (1992). Relationship between photosystem II activity and CO_2 fixation in leaves. *Physiologia Plantarum,* **86**, 180-187.

Kramer, D., and Crofts, A. (1989). Activation of the chloroplast ATPase measured by the electrochromic change in leaves of intact plants. *Biochimica et Biophysica Acta,* **976**, 28-41.

Kramer D.M. & Crofts A.R. (1996) Control of photosynthesis and measurement of photosynthetic reactions in intact plants. In: *Photosynthesis and the Environment* . *Advances in Photosynthesis* (ed N. Baker), pp. 25-66. Kluwer Academic Press, Dordrecht, The Netherlands.

Kramer, D.M., Avenson, T.J., and Edwards, G.E. (2004). Dynamic flexibility in the light reactions of photosynthesis governed by both electron and proton transfer reactions. *Trends in Plant Sciences*, **9**, 349-357.

Kubicki, A., Funk, E., Westhoff, P., and Steinmüller, K. (1996). Differential expression of plastome-encoded *ndh* genes in mesophyll and bundle-sheath chloroplasts of the C_4 plant *Sorghum bicolor* indicates that the complex I-homologous NAD(P)H-plastoquinone oxidoreductase is involved in cyclic electron transport. *Planta*, **199**, 276-281.

Lascano, H.R., Casano, L.M., Martin, M., and Sabater, B. (2003). The Activity of the Chloroplastic Ndh Complex Is Regulated by Phosphorylation of the NDH-F Subunit. *Plant Physiology,* **132**, 256-262.

Li, X., Bjorkman, O., Shih, C., Grossman, A.R., Rosenquist, M., Jansson, S., and Niyogi, K.K. (2000). A pigment-binding protein essential for regulation of photosynthetic light harvesting. *Nature,* **403**, 391-395.

Lokstein, H., Härtel, H., Hoffmann, P., and Renger, G. (1993). Comparison of chlorophyll fluorescence quenching in leaves of wild-type with a chlorophyll-b-less mutant of barley (*Hordeum vulgare L.*). *Journal of Photochemistry and Photobiology B: Biology,* **19**, 217-225.

Lowry, O.H., Rosebrough, N.J., Farr, A.L., and Randell, R.J. (1951). Protein measurement with the folin phenol reagent. *Journal of Biological Chemistry,* **193**, 265-275.

Lundin, A., and Thore, A. (1975). Comparison of methods for extraction of bacterial adenine nucleotides determined by firefly assay. *Applied Microbiology,* **30**, 713-721.

Mitchell, P. (1976). Possible molecular mechanisms of the protonmotive function of cytochrome systems. *Journal of Theoretical Biology,* **62**, 327-367.

Müller, P., Li, X., and Niyogi, K.K. (2001). Non-photochemical quenching. A response to excess light energy. *Plant Physiology,* **125**, 1558-1566.

Munekage, Y., Hojo, M., Meurer, J., Endo, T., Tasaka, M., and Shikanai, T. (2002). PGR5 is involved in cyclic electron flow around photosystem I and is essential for photoprotection in Arabidopsis. *Cell,* **110**, 361-371.

Munekage, Y., Hashimoto, M., Miyake, C., Tomizawa, K., Endo, T., Tasaka, M., and Shikanai, T. (2004). Cyclic electron flow around photosystem I is essential for photosynthesis. *Nature,* **429**, 579-582.

Nixon, P.J. (2000). Chlororespiration. *Philosophical Transactions of the Royal Society B: Biological Sciences,* **355**, 1541-1547.

Niyogi, K.K., Grossman, A.R., and Björkman, O. (1998). Arabidopsis mutants define a central role for the xanthophyll cycle in the regulation of photosynthetic energy conversion. *Plant Cell,* **10**, 1121-1134.

Noctor, G., and Foyer, C. (1998). A re-evaluation of the ATP:NADPH budget during C_3 photosynthesis: a contribution form nitrate assimilation and its associated respiratory activity. *Journal of Experimental Botany,* **49**, 1895-1908.

Oja, V., Bichele, I., Hüve, K., Rasulov, B., and Laisk, A. (2004). Reductive titration of photosystem I and differential extinction coefficient of P700+ at 810-950 nm in leaves. *Biochimica et Biophysica Acta,* **1658**, 225-234.

Ort D.R. & Yocum C.F. (1996) Light reactions of oxygenic photosynthesis. In: *Oxygenic Photosynthesis: The Light Reactions* (ed C.F. Yocum), pp. 1-9. Kluwer Academic Publishers, The Netherlands.

Peterson, R.B. (1991). Effects of O_2 and CO_2 concentrations on quantum yields of photosystems I and II in tobacco leaf tissue. *Plant Physiology,* **97**, 1388-1394.

Porra, R.J., Thompson, W.A., and Kriedemann, P.E. (1989). Determination of accurate extinction coefficients and simultaneous equations for assaying chlorophylls a and b extracted with four different solvents: verification of the concentration of chlorophyll standards by atomic absorption spectroscopy. *Biochimica et Biophysica Acta,* **975**, 384-394.

Quiles, M.J. (2005). Regulation of the expression of chloroplast *ndh* genes by light intensity applied during oat plant growth. *Plant Science,* **168**, 1561-1569.

Quiles, M.J. (2006). Stimulation of chlororespiration by heat and high light intensity in oat plants. *Plant Cell and the Environment,* **29**, 1463-1470.

Ruuska, S.A., Andrews, T.J., Badger, M.R., Price, G.D., and von Caemmerer, S. (2000). The role of chloroplast electron transport and metabolites in modulating rubisco activity in tobacco. Insights from transgenic plants with reduced amounts of cytochrome b_6f complex or glyceraldehyde 3-phosphate dehydrogenase. *Plant Physiology,* **122**, 491–504.

Sacksteder, C., and Kramer, D.M. (2000). Dark-interval relaxation kinetics (DIRK) of absorbance changes as a quantitative probe of steady-state electron transfer. *Photosynthesis Research,* **66**, 145-158.

Sacksteder, C., Kanazawa, A., Jacoby, M.E., and Kramer, D.M. (2000). The proton to electron stoichiometry of steady state photosynthesis in living plants: a proton-pumping Q-cycle is

continuously engaged. *Proceedings of the National Academy of Sciences,* **97**, 14283-14288.

Sazanov, L.A., Burrows, P.A., and Nixon, P.J. (1996). Detection and characterization of a complex I-like NADH-specific dehydrogenase from pea thylakoids. *Biochemical Society Transactions,* **24**, 739-743.

Sazanov, L.A., Burrows, P.A., and Nixon, P.J. (1998). The chloroplast Ndh complex mediates the dark reduction of the plastoquinone pool in response to heat stress in tobacco leaves. *FEBS Letters,* **429**, 115-118.

Scheibe, R. (2004). Malate valves to balance cellular energy supply: Redox regulation: from molecular responses to environmental adaptation. *Physiologia Plantarum,* **120**, 21-26.

Seelert, H., Poetsch, A., Dencher, N.A., Engel, A., Stahlberg, H., and Müller, D.J. (2000). Structural biology: Proton-powered turbine of a plant motor. *Nature,* **405**, 418-419.

Serrato, A.J., Yubero-Serrano, E.M., Sandalio, L.M., Munoz-Blanco, J., Chueca, A., Caballero, J.L., and Sahrawy, M. (2009). cpFBPaseII, a novel redox-independent chloroplastic isoform of fructose-1,6-bisphosphatase. *Plant Cell and the Environment,* **32**, 811-827.

Shikanai, T., Endo, T., Hashimoto, T., Yamada, Y., Asada, K., and Yokota, A. (1998). Directed disruption of the tobacco *ndhB* gene impairs cyclic electron flow around photosystem I. *Proceedings of the National Academy of Sciences,* **95**, 9705-9709.

Takabayashi, A., Kishine, M., Asada, K., Endo, T., and Sato, F. (2005). Differential use of two cyclic electron flows around photosystem I for driving CO_2-concentration mechanism in C_4 photosynthesis. *Proceedings of the National Academy of Sciences,* **102**, 16898-16903.

Takizawa, K., Kanazawa, A., and Kramer, D.M. (2008). Depletion of stromal P_i induces high 'energy-dependent' antenna exciton quenching (q_E) by decreasing proton conductivity at CF_O-CF_1 ATP synthase. *Plant Cell and the Environment,* **31**, 235-243.

Takizawa, K., Cruz, J.A., Kanazawa, A., and Kramer, D.M. (2007). The thylakoid proton motive force *in vivo*. Quantitative, non-invasive probes, energetics, and regulatory consequences of light-induced *pmf*. *Biochimica et Biophysica Acta,* **1767**, 1233-1244.

Turina, P., Samoray, D., and Gräber, P. (2003). H^+/ATP ratio of proton transport-coupled ATP synthesis and hydrolysis catalysed by CF_0F_1–liposomes. *EMBO Journal,* **22**, 418-426.

Villeret, V., Huang, S., Zhang, Y., Xue, Y., and Lipscomb, W.N. (1995). Crystal structure of spinach chloroplast fructose-1,6-bisphosphatase at 2.8 A resolution. *Biochemistry,* **34**, 4299-4306.

Ziyu, D., Maurice, S.B.K., and Edwards, G.E. (2004). Oxygen sensitivity of photosynthesis and photorespiration in different photosynthetic types in the genus *Flaveria*. *Planta,* **198**, 563-571.

Supplemental data. Livingston et al. (2010) An *Arabidopsis* mutant with high cyclic electron flow around photosystem I (*hcef*) involving the NADPH dehydrogenase complex.

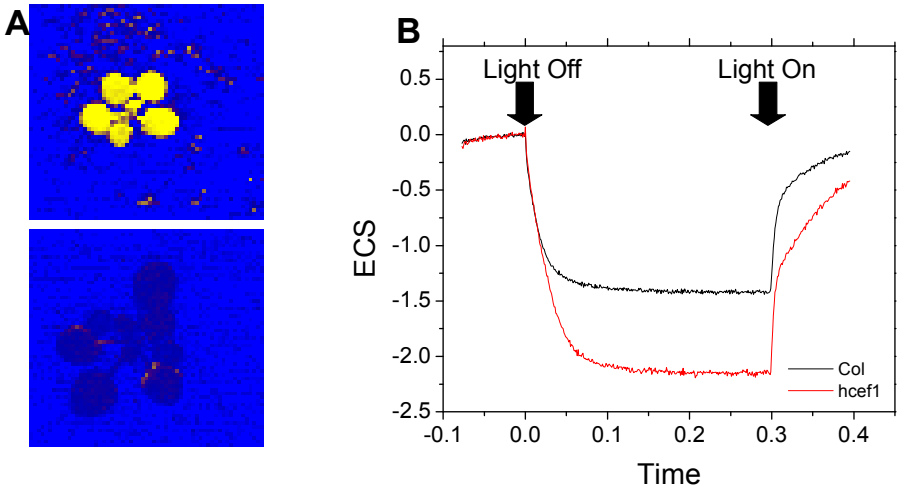

Supplemental Figure 1. Selection of *hcef1*. **(A)** False color representation of qE from the chlorophyll fluorescence imaging above is *hcef1* and below is Columbia wild-type; color scale is set so relative values of q_E are represented as follows: blue 0-0.2, red 0.2-0.8 and yellow 0.8 -1.1. **(B)** ECS responses of Col versus *hcef1* at 273 μmol photon m^{-2} s^{-1}.

Supplemental Figure 2. Growth of *hcef1*. Photographs of Columbia Wild-type (left) at maturity (29 days) and *hcef1* at maturity (41 days). The white arrow denotes 1 cm.

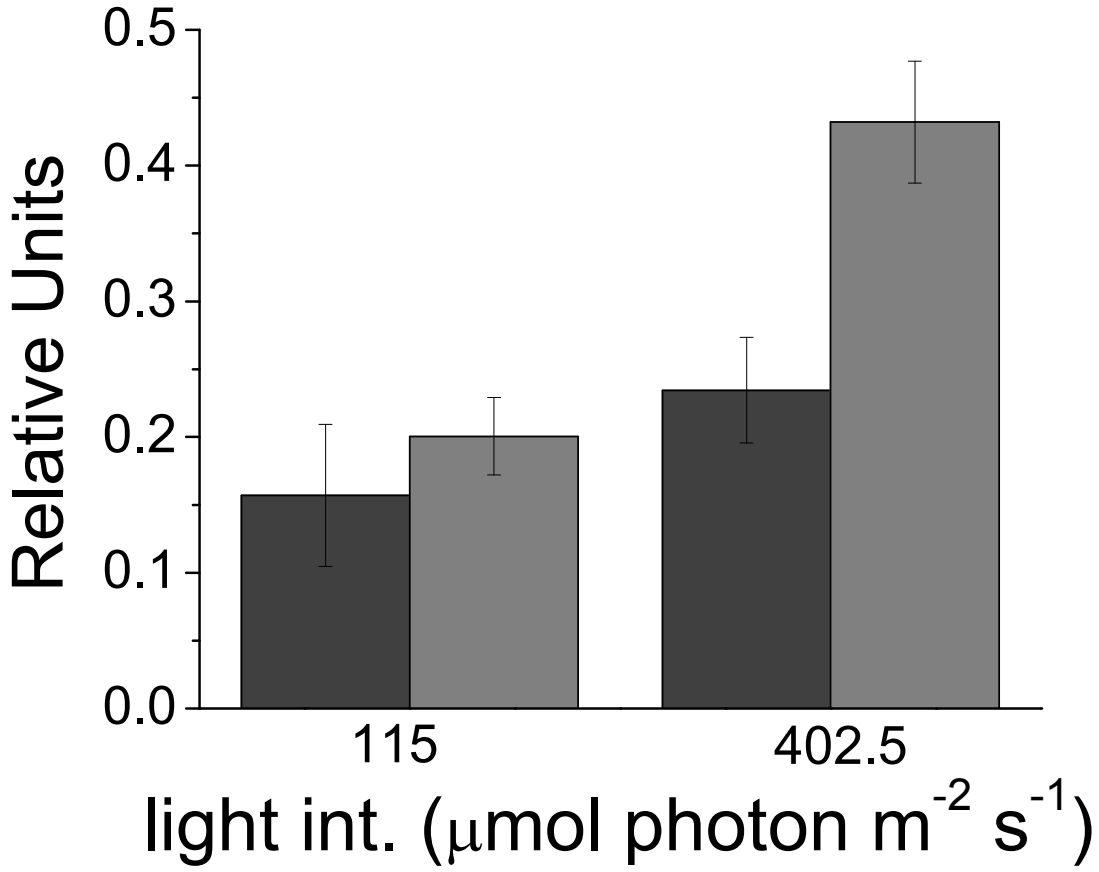

Supplemental Figure 3. qI in *hcef1*. Relative changes in qI amount under two different light conditions for col (dark grey bars) and *hcef1* (light grey bars). In *hcef1*, there was a noticeable decrease in q_E decreased when the light intensity increased from 300 to 500 μmol photons m^{-2} s^{-1}. This decrease is likely due to an increased in photodamage (q_I), measured as described in (Muller *et al.*, 2001). Error bars represent standard deviation, n=3 individual plants.

A

Sus scrofa	IFMYPANKKSPK**GKLRLLYEC**NPMAYVMEKAGG
Homo Sapien	IFLYPANKKSPN**GKLRLLYEC**NPMAYVMEKAGG
Oryctolagus cuniculus	IFLYPANKKSPD**GKLRLLYEC**NPMAFIMEKAGG
Spinacia oleracea	IYGYPRDAKSKN**GKLRLLYEC**APMSFIVEQAGG
Arabidopsis thaliana	IYGYPRDAKSKN**GKLRLLYEC**APMSFIVEQAGG

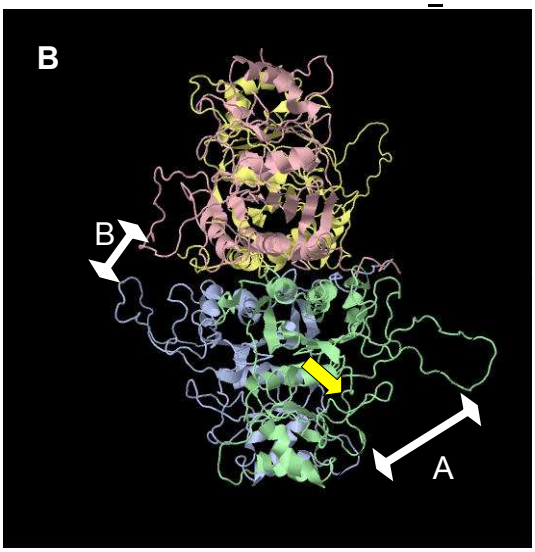

Supplemental Figure 4. *hcef1* mutation in chloroplast FBPase. (A) Comparison of Amino Acid sequences of Fructose 1,6-Bisphosphatase across several different species. The bold letters represent a nine amino acid run that is constitutively conserved across all species. The underlined letter represents the point of mutation in *hcef1,* in which this arginine was mutated to lysine. **(B)** Structure of Fructose 1,6-Bisphosphatase, from *Spinacia oleracea*. (A) represents the substrate binding pocket, (B) is the metal binding pocket. The yellow arrow points to Arginine 361 the point of mutation in *hcef1*. Figure from the RCSB Protein Data Bank, structure 1spi(Villeret et al., 1995).

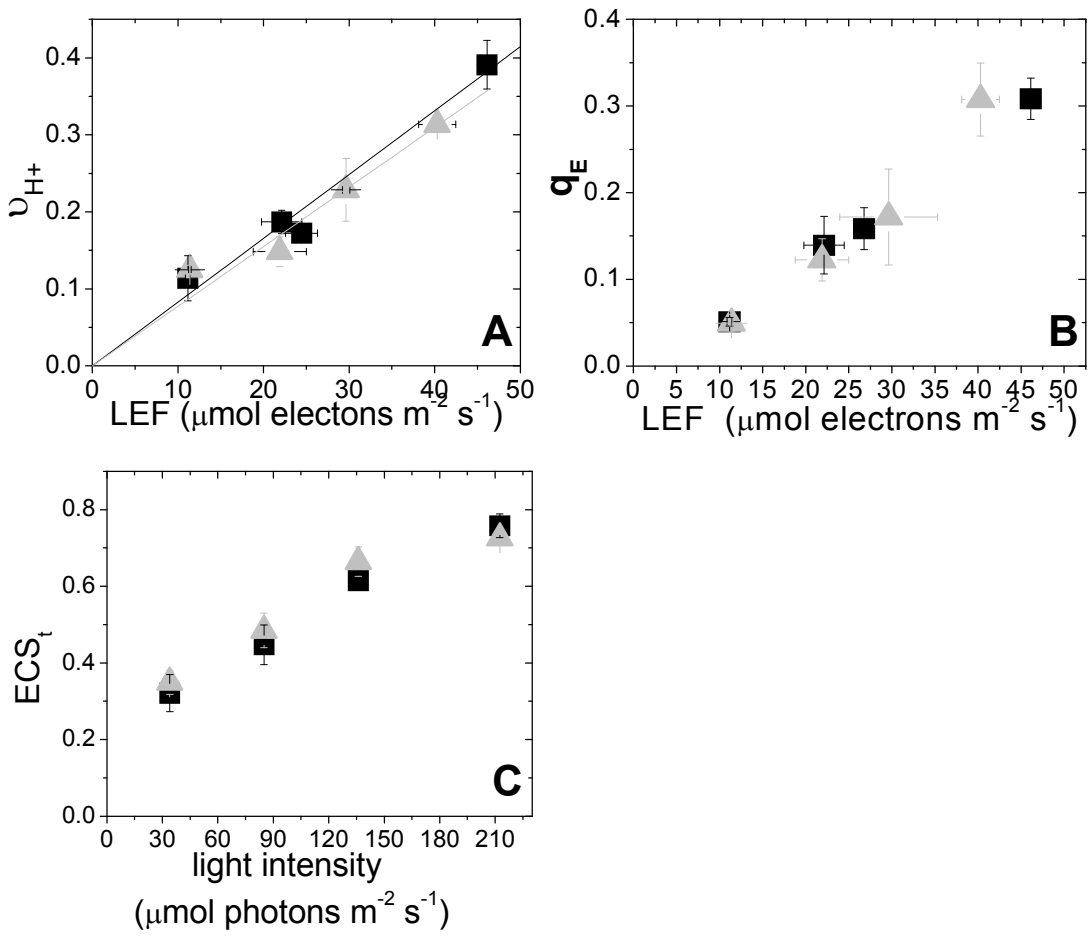

Supplemental Figure 5. Complementation of *hcef1*. Columbia wild-type (■) and *hcef1* complemented with the FBPase gene AT3G54050.1 (▲). After complementation three separate lines of transformed plants were evaluated. All the individuals showed chlorophyll content, growth rates and sizes throughout development that were indistinguishable from Col. **(A)** LEF versus v_H^+ (Col slope =0.00828 P=0.002 and *hcef1*complemented slope =0.00774 P=0.01 which are statistically indistinguishable (ANCOVA P>0.05)). **(B)** LEF versus qE. **(C)** ECSt versus light intensity. Error bars equal standard deviation *n*=3 (one individual plant from three separate transformed lines).

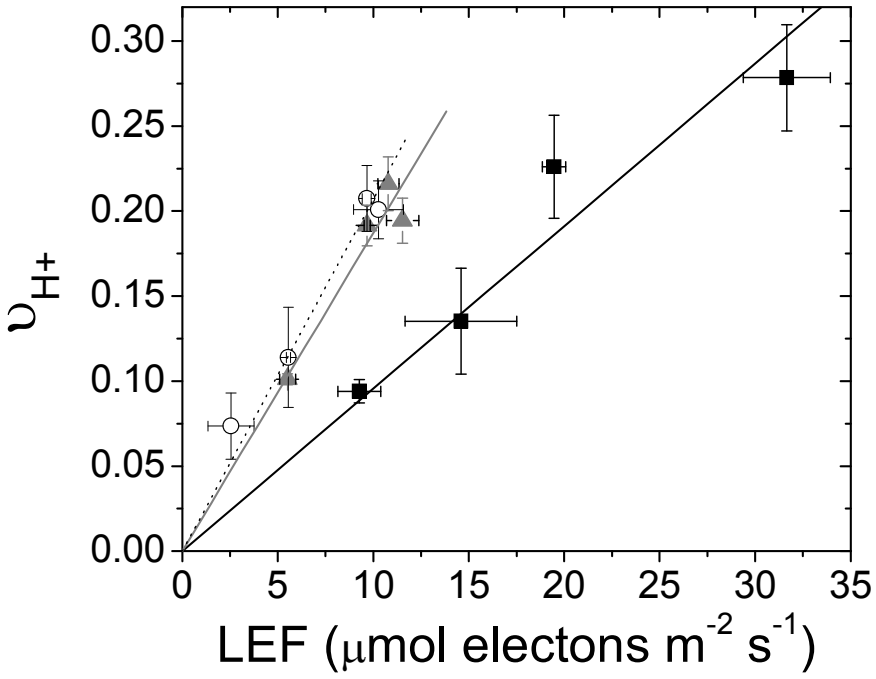

Supplemental Figure 6. Comparison of proton pumping as a function of LEF for *hcef1*, Col, and known FBPase knockout (CS836161). The mutants *hcef1* (▲) and CS836161 (O) have a higher proton pumping amount compared to Columbia (■). The slopes for *hcef1* (grey solid line; slope =0.01869) and CS836161 (dashed black line; slope = 0.02069) were statistically indiscernible (ANCOVA $P>0.05$). The slope for Col (solid black line; slope = 0.00956) was approximately half that of either mutant. For all slope fittings $P < 0.02$. Error bars equal standard deviation n=3 individual plants.

Supplemental Table 1. Phenotypic comparison of photosynthetic traits of Columbia, *hcef1, hcef1 crr2-2,* and *hcef1 pgr5.*

	Columbia Wild-type	*hcef1*	*hcef1 crr2-2*	*hcef1 pgr5*
Chlorophyll Content (mg chlorophyll/ mL)	7.47 ± 0.110	4.15 ± 0.187	4.08 ± 0.234	4.35 ± 0.136
signal turn over flash (relative units)	3.68 ± 0.179	1.979 ± 0.157	2.003 ± 0.40	2.22 ± 0.160
maximal photochemical efficiency of PSII	0.770 ± 0.0150	0.761 ± 0.00421	0.741 ± 0.0280	0.741 ± 0.00842

Supplemental References

.

Müller, P., Li, X., and Niyogi, K.K. (2001). Non-photochemical quenching. A response to excess light energy. *Plant Physiology,* **125**, 1558-1566.

Villeret, V., Huang, S., Zhang, Y., Xue, Y., and Lipscomb, W.N. (1995). Crystal structure of spinach chloroplast fructose-1,6-bisphosphatase at 2.8 A resolution. *Biochemistry,* **34**, 4299-4306.

Chapter 2: Regulation of Cyclic Electron Flow in C_3 Plants: Differential effects of limiting photosynthesis at Rubisco and Glyceraldehyde-3-phosphate Dehydrogenase.

(As submitted to Plant Cell and the Environment)

Aaron K. Livingston, Atsuko Kanazawa, Jeffrey A. Cruz, and David M. Kramer

Abstract

Cyclic electron flow around photosystem I (CEF1) is thought to augment ATP production of the light reactions of photosynthesis, balancing the ATP/NADPH output ratio to meet metabolic needs. Very little is known about the induction and regulation of CEF1. We investigated the effects on CEF1 of antisense suppression of the Calvin-Benson enzymes glyceraldehydes-3-phosphate dehydrogenase (GAPDH), gapR mutants, and ribulose-1,5-bisphosphate carboxylase/oxygenase (Rubisco) small subunit (SSU), ssuR mutants, in tobacco (*Nicotiana tabacum* cv. Wisconsin 38). We found that gapR, but not ssuR mutants showed substantial increases in CEF1. These results demonstrate that specific intermediates, rather than an overall slowing of assimilation are responsible for inducing CEF1. Despite the large differential effects on CEF1, both types of mutant showed increases in steady-state transthylakoid proton motive force (*pmf*) and subsequent activation of the photoprotective q_E response. With gapR, the increased *pmf* was caused both by up-regulation of CEF1 and down-regulation of the ATP synthase. In ssuR, the increased *pmf* could be attributed entirely to a decrease in ATP synthase activity, as previously seen in wild type plants when CO_2 levels were decreased. Comparison of major stromal metabolites in gapR, ssuR and *hcef1*, a mutant with decreased fructose 1,6-bisphosphatase activity, showed that neither the ATP/ADP ratio, nor major Calvin-Benson cycle intermediates can directly account for the activation of CEF1. This leaves the chloroplast redox status or reactive oxygen species as likely regulatory candidates.

Introduction

The light reactions of photosynthesis must be finely regulated to match the needs of downstream chloroplast metabolism and to prevent the generation of toxic side products (Edwards & Walker, 1983, Nixon & Mullineaux, 2001, Avenson, Cruz, Kanazawa & Kramer, 2005a). Light capture and electron transfer are regulated mainly via the formation of the proton motive force or *pmf* (reviewed in (Cruz, Sacksteder, Kanazawa & Kramer, 2001)).

Beyond driving the synthesis of ATP via the chloroplast ATP synthase (Allen, 2002), the *pmf* causes acidification of the lumen, which regulates the rate of electron transfer through the cytochrome b_6f complex (Hope, Valente & Matthews, 1994, Takizawa, Cruz, Kanazawa & Kramer, 2007) and activates photoprotective 'quenching' of excitation energy via the q_E mechanism (Horton, Ruban & Walters, 1996). These processes act in concert to prevent the buildup of reduced and strongly-reducing photosystem I (PSI) electron acceptors, which can produce superoxide, (reviewed in (Scandalios, 1993)), and preventing charge recombination within photosystem II (PSII) which can produce singlet oxygen (Macpherson, Telfer, Barber & Truscott, 1993, Hideg, Spetea & Vass, 1994).

The chloroplast must also balance its output of ATP and NADPH to precisely match the needs of downstream metabolism (See reviews in (Edwards & Walker, 1983, Noctor & Foyer, 1998, Livingston, Cruz, Kohzuma, Dhingra & Kramer, 2010)). Because the proton and electron transfer reactions of photosynthesis are tightly coupled, linear electron flow (LEF) produces a fixed ratio of ATP to NADPH of ~2.6 (Sacksteder, Kanazawa, Jacoby & Kramer, 2000, Seelert, Poetsch, Dencher, Engel, Stahlberg & Müller, 2000, Kramer, Avenson & Edwards, 2004), which may not meet biochemical needs.

The Calvin-Benson Cycle uses 3 ATP/ 2 NADPH. Even after factoring nitrate assimilation and photorespiration, the ATP/NADPH consumption ratio is ~2.9, i.e. above that supplied by LEF alone; moreover, this ATP/NADPH deficit is likely to be dynamic, changing rapidly and dramatically under various physiological stresses (reviewed in (Noctor & Foyer, 1998, Kramer *et al.*, 2004, Avenson, Kanazawa, Cruz, Takizawa, Ettinger & Kramer, 2005b)).

Three major mechanisms have been proposed to account for how ATP/NADPH balance is achieved, the water-water cycle (Asada, 2000), the malate shunt (Scheibe, 2004) and cyclic electron flux around photosystem I (CEF1) (Heber & Walker, 1992). In the malate shunt, NADPH reduced by LEF is used to reduce oxaloacetate to make malate, which is exported from the chloroplast to mitochondria where it is oxidized by the oxidative phosphorylation system, producing ATP. The malate shunt is thought to have very low capacity (1-2% of expected linear electron flow in the chloroplast) (Fridlyand, Backhausen & Scheibe, 1998), and thus may have limited impact on the ATP/NADPH budget.

In the water-water cycle (WWC, also called the Mehler-peroxidase reaction) involves transfer of electron from PSII, through the linear electron transfer chain to the acceptor side of PSI, where they are transferred to O_2, forming superoxide which is detoxified by superoxide dismutase and ascorbate peroxidase. The transfer of electrons through LEF results in proton translocation, powering ATP synthesis, while the reduction of dehydroascorbate consumes NADPH, potentially balancing ATP/NADPH deficits. On the other hand, the extent of activation of the WWC is controversial, partly because it is very difficult to measure (Miyake & Yokota, 2000, Heber, 2002).

In this work, we focus on the CEF1, in which electrons from the reducing side of PSI are transferred into the plastoquinone (PQ) pool, forming plastoquinol (PQH_2). PQH_2 is then

oxidized by the cytochrome b_6f complex, transferring electrons via plastocyanin back to the oxidizing side of PSI. The reduction of PQ on the stromal side of the thylakoid, and the subsequent oxidation of PQH_2 on the lumenal side, results in translocation of protons, which are used at the chloroplast ATP synthase. In this way, CEF1 produces no net formation NADPH, but drives ATP synthesis (reviewed in (Kramer *et al.*, 2004, Eberhard, Finazzi & Wollman, 2008)). In addition, the *pmf* generated by CEF1 can enhance photoprotection by acidifying the lumen (Heber & Walker, 1992, Johnson, 2005).

CEF1 has been found to be highly active in C_4 plants (Kubicki, Funk, Westhoff & Steinmüller, 1996), green algae (Finazzi, Rappaport, Furia, Fleischmann, Rochaix, Zito & Forti, 2002) and cyanobacteria (Carpentier, Larue & Leblanc, 1984), where 'extra' ATP is presumably needed, especially to run CO_2 concentrating mechanisms. On the other hand, C_3 plants do not concentrate CO_2 and LEF alone should nearly meet their ATP demands, and under non-stressed conditions; if all ATP/NADPH balancing was accomplished by CEF1, it would have to run at only about 14% the rate of LEF (Avenson *et al.*, 2005a). On the other hand, meeting additional ATP demands incurred by environmental stresses or developmental processes could substantially increase the need for CEF1. Consistent with this view, CEF1 has been reported to contribute little to overall photosynthetic energy production in C_3 plants under non-stressed steady-state conditions (Harbinson & Foyer, 1991, Avenson *et al.*, 2005a), but substantial increase in C_3 CEF1 was seen under stress conditions, such as drought (Jia, Oguchi, Hope, Barber & Chow, 2008, Kohzuma, Cruz, Akashi, Munekage, Yokota & Kramer, 2008), high light (Baker & Ort, 1992) or photosynthetic induction (Joët, Cournac, Peltier & Havaux, 2002, Joliot & Joliot, 2002).

There are several major open questions about CEF1. What is the specific pathway for electrons from PSI into the PQ pool? What is the maximal rate of CEF1 in C3 plant? What

could regulate CEF1 so precisely that it provides the correct amount of ATP without "over-charging" the thylakoid membrane?

Recently, we proposed that mutants with highly-elevated CEF1, i.e. the so-called *hcef* mutants, could address some of these questions. We showed that *hcef1*, an Arabidopsis mutant with highly elevated CEF1, was a mutant in the Calvin-Benson Cycle enzyme fructose-1,6-bisphosphatase (Livingston *et al.*, 2010). These results led us to ask whether CEF1 was induced by inhibition of assimilation in general, or by blockage of specific processes which could lead to imbalances in ATP/NADPH demands or accumulation of CEF1 activating metabolites. To answer this question, we compare the CEF1 phenotypes of plants with antisense-suppression of either the small subunit (SSU) of ribulose-1,5-bisphosphate carboxylase/oxygenase (Rubisco) and stromal glyceraldehydes-3-phosphate dehydrogenase (GAPDH). Chloroplast metabolism in these mutants have been well-characterized (Quick, Schurr, Scheibe, Schulze, Rodermel, Bogorad & Stitt, 1991, Hudson, Evans, von Caemmerer, Arvidsson & Andrews, 1992, Ruuska, Andrews, Badger, Price & von Caemmerer, 2000, Cruz, Emery, Wüst, Kramer & Lange, 2008), allowing us to compare results we obtain with *in vivo* spectroscopy with metabolite and CO_2 assimilation data.

Materials and Methods

Plant Material and Growth Conditions.

Tobacco (*Nicotiana tabacum* cv. Wisconsin 38), wild-type (W38), Rubisco small subunit antisense mutant (ssuR) (Hudson *et al.*, 1992) and GAPDH antisense mutant (gapR) (Price, Evans, von Caemmerer, Yu & Badger, 1995), were obtained from Professor Susanne von Caemmerer (Plant Environmental Biology, Research School of Biological Sciences, Australian

National University), and were grown on soil under greenhouse conditions, 16:8 photoperiod, ~850 μmol m^{-2} sec^{-1} light intensity, and 27°C/21°C (day/night) cycle.

In vivo Spectroscopic Assays.

Light-induced absorbance and chlorophyll fluorescence changes were performed on intact, mature tobacco leaves using a non-focusing optics spectrophotometer/fluorimeter (NoFOSpec) with continuously-flowing humidified air, as described in (Livingston *et al.*, 2010). The parameters q_E and photochemical yield of photosystem II (ϕ_{II}) were calculated by saturation-pulse chlorophyll fluorescence yield changes as described previously (Genty, Briantais & Baker, 1989, Sacksteder & Kramer, 2000, Kanazawa & Kramer, 2002, Avenson *et al.*, 2005b).

After 15 minutes of actinic illumination chlorophyll *a* fluorescence yield was measured under steady state photosynthetic conditions (F_s) and light saturated levels ($F_{M'}$) (Kanazawa & Kramer, 2002, Avenson, Cruz & Kramer, 2004), from which ϕ_{II} and LEF were calculated (Genty *et al.*, 1989). The parameter q_E was determined as described in (Genty *et al.*, 1989) by collecting F_M" after 10 minutes of dark relaxation and taking F_M' at the end of actinic light activation. Light-induced, steady-state *pmf* was estimated from dark-interval relaxation kinetics (DIRK) of absorbance at 520 nm, attributable to electrochromic shift (ECS) and proportional to changes in transthylakoid electric field (Sacksteder & Kramer, 2000, Cruz, Avenson, Kanazawa, Takizawa, Edwards & Kramer, 2005). The total amplitude of the ECS signal measured over a 300 ms dark interval, ECS_t, was taken to be proportional to the extent of light-induced *pmf,* while inverse of the time constant for the ECS decay (τ_{ECS}) is proportional to the conductivity of the thylakoid membrane to proton flux, g_H^+ (Kramer & Crofts, 1996, Sacksteder & Kramer, 2000, Cruz *et al.*, 2005). Steady state proton flux across the thylakoid membrane (v_H^+) was calculated from the

initial slope of ECS decay as described in (Avenson *et al.*, 2005a, Takizawa, Kanazawa & Kramer, 2008). To account for variations in leaf thickness and pigmentation, ECS measurements were normalized to the extent of the rapid rise single-turnover flash induced ECS (Avenson *et al.*, 2005b) and chlorophyll content; measured as described in (Porra, Thompson & Kriedemann, 1989). The two normalization procedures gave similar results.

Infiltration of methyl viologen into leaves.

Where indicated, 1 inch diameter leaf disks were wrapped with a layer of tissue paper (Kimwipe, Kimberly-Clark, Mississauga, Ontario) saturated with either distilled water or a solution of 100 μM methyl viologen, and incubated for 60 minutes at low light (5~10 μmol photon m^{-2} s^{-1}) (Livingston *et al.*, 2010). Before experimentation, leaf material was gently blotted with a fresh Kimwipe to remove excess liquid.

Results

Responses of the photosynthetic electron circuit of gapR and ssuR.

The photosynthetic phenotypes of both the gapR and ssuR antisense mutants varied substantially from plant to plant, depending on the expression levels of GAPDH or SSU, as previously reported (Hudson *et al.*, 1992, Ruuska *et al.*, 2000). Importantly, the maximal extent of linear electron flow (LEF) under saturating light was shown to be strongly correlated with GAPDH and SSU expression levels (Hudson *et al.*, 1992, Ruuska *et al.*, 2000). We thus used this property to pre-screen plants for various levels of GAPDH and Rubisco activity.

In the first set of experiments, we used gapR and ssuR antisense plants pre-screened for maximal LEF rates of approximately 35% that of W38, and we refer to these plants as $gapR_{35}$

and $ssuR_{35,}$ respectively. These plants both grew to about ~50-60% the height of wild-type. The dependence of maximal LEF on expression levels reported by (Hudson *et al.*, 1992, Ruuska *et al.*, 2000) indicates that $gapR_{35}$ and $ssuR_{35}$ express roughly 10% (*c.f.* Figure 1B in (Ruuska *et al.*, 2000)) and 18% (*c.f.* Fig. 2A in (Hudson *et al.*, 1992)) of GAPDH and SSU respectively.

At less than 200 μmol photons m^{-2} s^{-1} actinic light, $gapR_{35}$, $ssuR_{35}$, and W38 showed approximately the same LEF rates indicating a similar maximal quantum yield for photosynthesis (Fig.1A). However, the antisense plants reached saturation at ~470 μmol photons m^{-2} s^{-1} compared to ~900 μmol photons m^{-2} s^{-1} for the wild type. The light-saturation curves for $gapR_{35}$, $ssuR_{35}$ were super-imposable, implying similar effects of suppression of GAPDH and SSU on the rate of assimilation, leading to similar limitations in the light reactions.

Strikingly, the q_E responses of both $ssuR_{35}$ and $gapR_{35}$ were far more sensitive to light intensity than that seen in W38 (Fig. 1B). At the highest light intensity used, W38 displayed a q_E value of ~0.4, whereas $gapR_{35}$ and $ssuR_{35}$ achieved values of 1.7 and 0.9 respectively.

The light intensity-dependence of the q_E response in $gapR_{35}$ and $ssuR_{35}$ were also distinct. The q_E response in $ssuR_{35}$ reached half-saturation between 100 and 150 μmol photons m^{-2} s^{-1} in $ssuR_{35.}$ In contrast, the q_E response of $gapR_{35}$ continued to increase linearly, without signs of saturation, even at the highest light intensity used, 470 μmol photons m^{-2} s^{-1} (Fig. 1B), well above the saturation of LEF (Fig. 1A).

Responses of the photosynthetic proton circuit of gapR and ssuR.

In $gapR_{35}$, q_E increased with increasing light, even above the saturation point for LEF (Fig. 1A, 1B). This behavior might be attributed to contributions at high light from CEF1, a high-light-induced change in the response of q_E to *pmf*, or deactivation of the chloroplast ATP

synthase (Avenson *et al.*, 2005b). To distinguish among these possibilities, we probed the light-driven proton circuit using *in vivo* spectroscopic techniques based on analysis of the absorption changes around 520 nm, termed the electrochromic shift (ECS), which reflect changes in the transthylakoid electric field (Junge & Witt, 1968). The decay of the ECS signal during short, dark intervals that punctuate steady-state illumination, can be analyzed to give estimates of the light-driven *pmf*, a measurement termed ECS_t, (Kanazawa & Kramer, 2002), proton flux through the thylakoid, a measurement termed v_H^+ (Avenson *et al.*, 2005a), and the conductivity of the thylakoid membrane to protons, a measurement termed g_{H+}, reflecting ATP synthase activity (Kanazawa & Kramer, 2002).

The data in Fig. 1C shows light-induced transthylakoid *pmf*, estimated from the ECS_t parameter as a function of actinic light intensity, for W38 and the two antisense mutants. Both W38 and $ssuR_{35}$ showed similar light-saturation curves for ECS, reaching a half-saturation point of between 100-150 μmol photons m^{-2} $s^{-1,}$ at approximately the same point where LEF half-saturated (Fig. 1A). However, $ssuR_{35}$ generated light-driven *pmf* about 2-times that of W38 (Fig. 1C). The response of *pmf* to light was distinct in $gapR_{35}$, and did not saturate with light as did the W38 and $ssuR_{35}$, reaching a value ~3.5 times larger than W38 at the highest light intensity used.

The dependences of q_E on light-induced *pmf* (ECS_t) (Fig. 1C insert) were essentially identical for W38, $ssuR_{35}$, and $gapR_{35}$, indicating that the q_E response to *pmf* was unchanged. Therefore, we conclude that differences in the extents of q_E could be completely explained by alterations in the extent of light-driven *pmf*.

The extent of light-driven *pmf* is affected by both the rate of light-driven proton translocation (the sum of proton flux from LEF and CEF) and the conductivity of the thylakoid

membrane for proton efflux (g_H^+), which is determined by the activity of the ATP synthase. In W38, g_H^+ was nearly constant over the entire light intensity range (Fig. 1D). In $ssuR_{35}$, g_H^+ remained roughly about 15% that of W38, throughout the range of light intensities (Fig. 1D). This result indicates that the increased *pmf* in $ssuR_{35}$ compared to W38 was likely due to decreased ATP synthase activity, which decreases g_H^+, leading to a buildup of *pmf* even at diminished proton fluxes. Very similar results were obtained in tobacco when Rubisco catalytic rates were varied by decreasing CO_2 levels (Kanazawa & Kramer, 2002).

In contrast, $gapR_{35}$ displayed a more strongly light-dependent g_H^+ response, with values close to W38 at low light, but gradually decreasing with increasing light intensity. Importantly, though, g_H^+ in $gapR_{35}$ remained considerably higher than that seen in $ssuR_{35}$ at all light intensities. Thus, the higher *pmf* and q_E in $gapR_{35}$ compared to $ssuR_{35}$ cannot be completely explained by decreased ATP synthase activity. Instead, the most likely explanation for the increased proton translocation is that CEF1 is more engaged in $gapR_{35}$ than $ssuR_{35}$. To test for this, we compared light-induced thylakoid proton flux (v_H^+), determined using the ECS probe (Sacksteder & Kramer, 2000, Takizawa *et al.*, 2008), with LEF in W38, $gapR_{35}$ and $ssuR_{35}$, between 0 and ~400 μmol photon m^{-2} s^{-1}. The slope of this relationship should be proportional to the number of protons translocated into the lumen per electron transferred through PSII (Sacksteder & Kramer, 2000, Baker, Harbinson & Kramer, 2007). For LEF, H^+/e^- stoichiometry is set at 3 by the Z-scheme and Q-cycle (Sacksteder *et al.*, 2000), resulting in a linear relationship between v_H^+ and LEF. Activation of CEF1 should increase the slope, since it contributes to proton translocation without involvement of PSII (Kramer *et al.*, 2004, Avenson *et al.*, 2005a).

W38 and $ssuR_{35}$ showed similar relationships between v_H^+ and LEF (Fig. 2), indicating no changes in CEF contributions to protons flux. Addition of methyl viologen (MV, open

symbols, Fig. 2), which blocks CEF1 by diverting electrons from PSI to O_2 (Avenson *et al.*, 2005a) did not significantly change these relationships, indicating that CEF1 contributions were small in both W38 and $ssuR_{35}$. In contrast, the $gapR_{35}$ mutant showed a 40% increase in v_H^+ vs. LEF compared with W38 of $ssuR_{35}$ (Fig. 2), indicating an increase in proton translocation above that supported by LEF alone. Addition of MV completely eliminated the increased proton flux (Fig. 2), allowing us to conclude that CEF1 contributed substantial proton flux in $gapR_{35}$ (about 40% of that contributed by LEF). A substantial increase in CEF1/LEF in $gapR_{35}$ were confirmed (data not shown) using an independent measure of CEF1, comparing LEF with electron flow through PSI, using saturation pulse-induced changes in P_{700} redox state, as described in (Klughammer & Schreiber, 1993).

Effects of progressive suppression of GAPDH and Rubisco small subunit

We next selected a range of ssuR and gapR mutants that displayed varying maximal LEF, previously showed to correlate strongly with the expression levels of SSU (Hudson *et al.*, 1992) and GAPDH (Ruuska *et al.*, 2000). Figure 3 shows the relationship between the ratio of CEF1:LEF at saturating light intensities (~900 μmol photon m^{-2} s^{-2}), estimated using the relationship between v_H^+ and LEF (as in Fig. 2) plotted against the maximal LEF (an indicator of the extent of suppression of SSU or GAPDH). Small changes in maximal LEF, did not have any discernible effects on CEF1:LEF. With increasing suppression of enzyme expression (as reflected in decreased maximal LEF), gapR plants showed a striking increase in CEF1:LEF. A small change in LEF at saturating light produced only small effects on CEF1. However, below light-saturated LEF values of 50 μmol e^- m^{-2} s^{-2}, gapR showed a steep increase in CEF1:LEF,

reaching ~1:1 at maximal LEF of 10 μmol e^- m^{-2} s^{-2}. In contrast, suppression of ssuR to similar extents did not result in measurable increases in CEF.

Discussion

Suppressing specific metabolic processes, but not overall photosynthesis, triggers CEF1.

The most striking results of this work are the large differences in CEF1 activation when photosynthesis is limited at different points in assimilation. Lowering CO_2 levels (Kanazawa & Kramer, 2002, Avenson *et al.*, 2005a) or suppressing Rubisco levels (Fig. 2, 3) did not substantially increase CEF1 activity. In contrast, suppressing GAPDH caused a large increase in CEF1/LEF (Figs. 2,3). Clearly, diminishing overall assimilation by itself is not sufficient to induce CEF1. Instead, activation of CEF1 depends strongly on which step in the process is inhibited. This conclusion is supported by our recent studies on *hcef1* (Livingston *et al.*, 2010), a mutation in chloroplast fructose 1,6-bisphosphatase, which increases CEF1/LEF to an extent similar to that seen here with $gapR_{35}$.

The steady-state capacity of CEF1 in C_3 plants can be highly variable

We found large differences in the rate of CEF1, ranging from near zero (essentially below the noise of our measurements) in W38 and $ssuR_{35}$, to nearly equal to LEF in the more severely suppressed gapR mutants (Fig. 3). This demonstrates very large flexibility in the CEF1 activation and capacity, in line with previous observations during photosynthetic induction (Joliot & Joliot, 2002). We observed no evidence for increased proton leakage across the thylakoid in the mutants, as judged by the slow decay of the ECS after weak flashes in dark-adapted leaves (data not shown) implying that the ATP synthase probably remained the major

route of proton efflux from the lumen (Kramer & Crofts, 1989). We thus conclude that increased CEF1 in gapR was used to drive increased ATP synthesis, and consequently the photosynthetic ATP/NADPH output ratio was substantially higher in gapR.

It thus seems clear that the ATP/NADPH output ratio of the light reactions in C_3 plants can be varied to meet a wide range of demands. With LEF alone, we expect ~2.6 ATP/2 NADPH, but with CEF and LEF contributing equal proton flux, as in the more severe gapR mutants, we expect ~5.2 ATP/2 NADPH, well in excess of that needed to drive the Calvin-Benson cycle, 3 ATP/2 NADPH (Edwards & Walker, 1983).

There are two obvious hypotheses to explain the increased ATP synthesis in gapR: 1) CEF1 is up-regulated in gapR to meet increased demands for ATP/NADPH; 2) there is no increased ATP demand in gapR, but CEF1 is 'inappropriately' up-regulated, producing excess ATP. The first hypothesis implies that ATP/ADP levels would decrease or, if CEF1 fully compensates for increased demand, stay constant. The second hypothesis suggests that ATP/NADPH output would exceed that needed for metabolism, leading to an increase in ATP/ADP levels.

Previous work on the gapR mutants by (Ruuska *et al.*, 2000) and us (Cruz *et al.*, 2008) showed no measurable changes in total cell ATP/ADP ratios compared to wild type under steady state illumination, supporting the first hypothesis, that gapR induces an increase in ATP demand that is met by increased CEF1.

We propose here a possible mechanism for the putative increased ATP demand. In the Calvin-Benson Cycle, ATP is consumed in the conversion of 3-phosphoglycerate (PGA) to 1,3-bisphosphoglycerate (1,3-BPG) by phosphoglycerate kinase. In turn, GAPDH converts 1,3-BPG to glyceraldehyde 3-phosphate (GAP) and inorganic phosphate, using NADPH as the reductant.

One might expect chloroplasts with impaired GAPDH to accumulate 1,3-BPG, but the acyl phosphate bond of 1,3-bisphophoglycerate is unstable (Cruz *et al.*, 2008) and 1,3-BPG is rapidly degraded. As illustrated in Fig. 4, we propose that the stromal 2,3-bisphosphoglycerate mutase degrades 1,3-BPG back to PGA, similar to the Rapoport-Luebering glycolytic bypass (Rapoport, Berger, Elsner & Rapoport, 1977, Kauffman, Pajerowski, Jamshidi, Palsson & Edwards, 2002, Cho, King, Qian, Harwood & Shears, 2008). In the Rapoport-Luebering glycolytic bypass, 1,3-BPG is converted to 2,3-BPG, and dephosphorylated back to PGA by a single enzyme 2,3-bisphosphoglycerate mutase. This bypass has an energetic cost as it skips the ATP producing phosphoglycerate kinase in glycolysis (Cho *et al.*, 2008). Since 2,3-bisphosphoglycerate mutase is found to be active in the chloroplast (Hou, Xu, Du, Lin, Duan & Guo, 2009), it is feasible that in concurrence with phosphoglycerate kinase of the Calvin-Benson Cycle an ATP-consuming futile cycle could be activated by suppressing GAPDH . Suppressing Rubisco, on the other hand, should prevent the buildup of 1,3-BPG and inhibit this futile cycle.

The normal role of bisphosphoglycerate mutase in the stroma is unclear. We speculate that mutation of GAPDH may induce accumulation of 1,3-BPG and/or in the up-regulation of bisphosphoglycerate mutase, resulting in the consumption of ATP. This consumption could act as a 'release valve' to prevent the accumulation of excess ATP, and subsequent thermodynamic backpressure on the thylakoid *pmf*.

What is the link between metabolism and induction of CEF1?

From the above discussion, it is clear that CEF1 is likely to be tightly regulated to provide just the amount of ATP needed to balance the chloroplast energy budget (Edwards & Walker, 1983, Noctor & Foyer, 1998, Kramer *et al.*, 2004, Livingston *et al.*, 2010). Several

possible CEF1 activators have been proposed, including the ATP/ADP ratio (Joliot & Joliot, 2002), the redox status of PSI electron acceptors (NAD(P)H, ferredoxin) (Breyton, Nandha, Johnson, Joliot & Finazzi, 2006), Calvin-Benson cycle intermediates, or the reactive oxygen species H_2O_2 (Lascano, Casano, Martin & Sabater, 2003, Gambarova, 2008). We took advantage of the large differences in CEF1 in ssuR and gapR to partially test some of these regulatory models. Table 1 is a compilation of metabolite data taken from von Caemmerer, Badger, and coworkers (Price *et al.*, 1995, Ruuska *et al.*, 2000) and our previous work on $gapR_{35}$ and $ssuR_{35}$ (Cruz *et al.*, 2008), a similar Rubisco SSU antisense line from Quick et al. (1991), and *hcef1* (Livingston *et al.*, 2010). If a particular metabolite is a regulator (activator or inhibitor) of CEF1, we would expect its level to change differentially between wild type or mutants with no change in CEF1 (ssuR) and mutants that show elevated CEF1 (gapR, *hcef1*). No single metabolite in Table 1 appears to follow this pattern except Rubisco 1,5-bisphosphaste (RuBP), arguing against fructose 6-phosphate, dihydroxyacetone phosphate, fructose 1,6-bisphosphate, phosphoglycerate, ribulose 5-phosphate, glucose 6-phosphate, or phosphoenyolpyruvate as CEF1 signals. By contrast, RuBP decreased in the high CEF1 mutants, and increased in ssuR compared to wild-type. In principle this could mean that RuBP is an inhibitor of CEF1 (more RuBP, less CEF1). However, CEF1 has also been observed to increase under drought stress (Jia *et al.*, 2008, Kohzuma *et al.*, 2008) where RuBP is expected to accumulate. Our results thus argue against Calvin-Benson cycle intermediates as direct regulators of CEF1.

Whole leaf ATP/ADP ratios were nearly constant in the wild-type and all the mutants, despite the large differences in CEF1. Quick *et al*. also reported that Rubisco antisense mutants had a small (approximately 2-fold) change in ATP/ADP ratio (1991), where we saw no induction

of CEF1 even when photosynthetic efficiency was ~40% of wild-type. Therefore, it seems unlikely that the ATP/ADP ratio regulates CEF1, although we cannot rule out the possibilities that stromal and cytosolic ATP/ADP ratios changed in opposite directions, or that very small changes in this ratio can control CEF1.

Additionally, it was previously reported that NADPH malate dehydrogenase activity was not different between wild type and gapR, suggesting that $NADP^+$/NADPH ratio was not altered (Ruuska *et al.*, 2000). This data argues against NADPH as the regulator of CEF1.

Overall, this analysis showed no support for ATP/ADP, NADPH, or specific Calvin-Benson cycle intermediates in controlling CEF1. We suggest that the regulator of CEF1 is further 'upstream' in photosynthesis, reflecting the redox status of PSI or ferredoxin, or the generation of reactive oxygen species, e. g. H_2O_2 (see above).

Implications for the proposed dual roles of CEF1

Two roles have been proposed for the *pmf* generated by CEF1 (reviewed in (Kramer *et al.*, 2004)): balancing ATP/NADPH output with demand; or initiating feedback regulation of the light reactions. Compared to W38, both $ssuR_{35}$ and $gapR_{35}$ showed dramatic increases in *pmf* and q_E (Fig. 1B, C). The $ssuR_{35}$ mutant appeared to increase *pmf* exclusively by slowing proton efflux at the ATP synthase (as reflected in decreased g_H^+) (Fig. 1D), as also seen in wild type plants when CO_2 levels are decreased (Kanazawa & Kramer, 2002, Kramer *et al.*, 2004, Avenson *et al.*, 2005b). The decreased g_H^+ slows efflux of protons from the lumen, resulting in a buildup of *pmf*, acidification of the lumen and subsequent down-regulation of the antenna and cytochrome b_6f complex. The $gapR_{35}$ mutant also showed decreased g_{H+} with respect to W38, but only about half of that seen in $ssuR_{35}$. Instead, $gapR_{35}$ appeared to achieve high *pmf* by activating CEF1and decreasing g_H^+. We thus conclude that the two proposed roles for CEF1 are

not mutually exclusive, but can complement each other. The key difference is the relative output of ATP/NADPH; changing g_{H^+} does not alter ATP/NADPH whereas CEF1 does (Kramer *et al.*, 2004). We conclude that CEF1 probably serves primarily to balance the chloroplast energy budget rather than initiate q_E, but that it does contribute to down-regulation.

Acknowledgements

This work was supported by U.S. DOE grant DE-FG02-04ERl5559 to DMK. The authors thank Prof. Susanne von Caemmerer (Australian National University) for the tobacco antisense lines. We also thank the expert assistance of Mr. Craig Whitney and Mrs. Julia Gothard-Szamosfalvi for plant growth management.

TABLE 1. Comparison of changes in metabolites in wild type and CEF1 and non-CEF1 inducing mutants.

Metabolite	Direction change **↑, increase; ↑↑, strong increase (more than 3-fold); ↓, decrease; ↓↓, strong decrease, red=decrease compared to wild-type, grey=no change compared to wild-type, and green=increase compared to wild-type**		
	ssuR$_{35}$	gapR$_{35}$	*hcef1*
ATP/ADP	~[b], ↑[d]	~[b],~[c]	~[e]
NADPH-malate dehydrogenase (possibly reflecting NADPH/NADP$^+$)	X	~[b],~[c]	X
Fructose-6-phosphate (F6P)	↓[b], ↓[d]	↓[b]	X
Dihydroxyacetone phosphate (DHAP)	~[b]	~[b]	X
Fructose bisphosphate (FBP)	~[b]	↓↓[b]	↑↑[e]
Phosphoglycerate (PGA)	↓↓[b], ↓↓[d]	↓↓[a] ↓[b]	↓↓[e]
Ribulose-bisphosphate (RuBP)	↑[b], ↑[d]	↓↓[a] ↓↓[b]	↓↓[e]
Ribulose-5-phosphate (R5P)	↓↓[b]	↓[b]	X
Glucose-6-phosphate (G6P)	~[b], ~[d]	~[b]	X
Phosphoenylpyruvate (PEP)	↓↓[b]	↓[b]	X
Cyclic Electron Flux around PSI	~	↑↑	↑↑[e]

a= (Price *et al*., 1995); b= (Cruz *et al*., 2008); c= (Ruuska *et al*., 2000); d= (Quick *et al*., 1991); e = (Livingston *et al*., 2010)

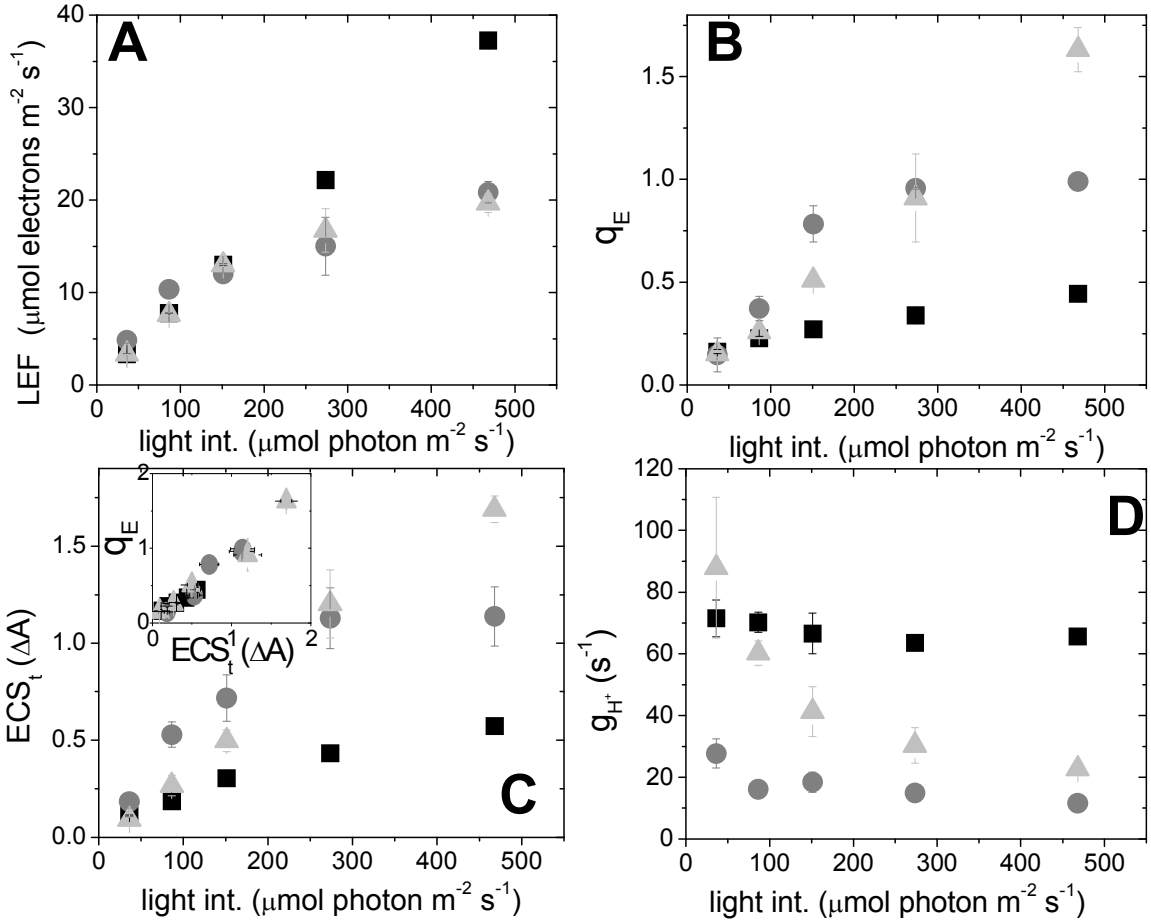

Figure 1. Comparison of photosynthetic traits of tobacco in wild-type (W38) Rubisco Small Subunit antisense mutant (ssuR$_{35}$), and the GAPDH antisense mutant (gapR$_{35}$). The two mutants where selected to represent individuals with ~35% the light-saturated LEF seen in W38. (A-D) W38 (■), ssuR$_{35}$ (●) and gapR$_{35}$ (▲) were compared for differences in LEF (A), q_E (B), ECS_t (C) and g_{H^+} (D) versus light intensity. The inset in C represents qE versus ECS_t. Error bars equal standard error n=3.

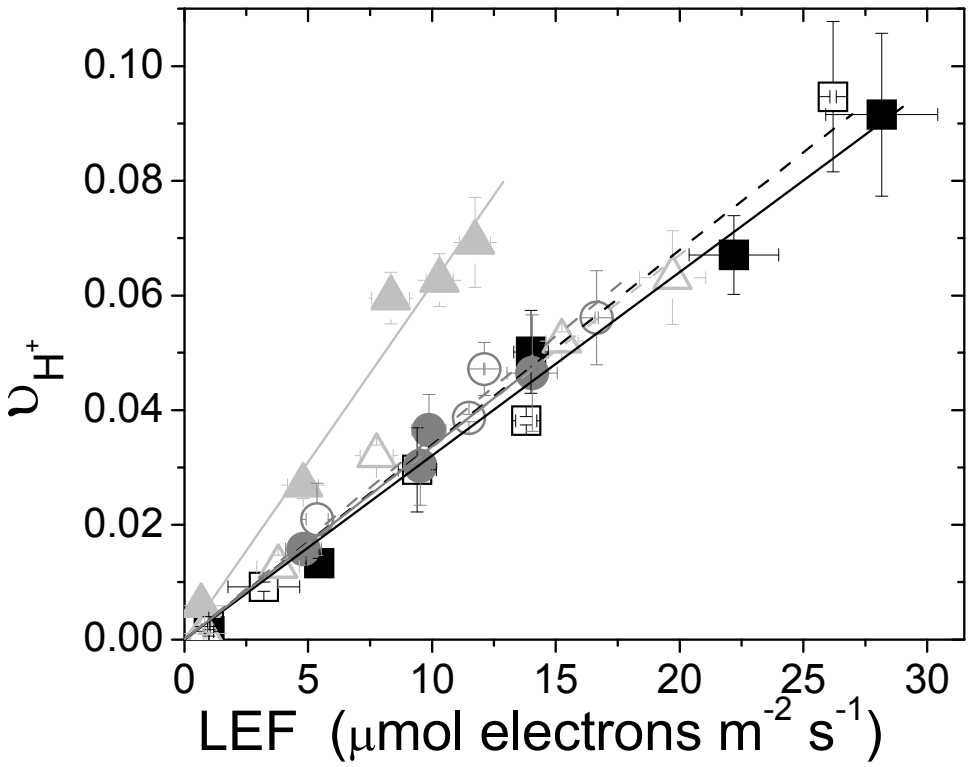

Figure 2. Comparison of CEF1 rates in tobacco wild-type and mutants. W38 (■,□) and mutants expressing a maximum LEF ~35% of that achieved by W38, $ssuR_{35}$ (●,○) and $gapR_{35}$ (▲,△). The plants where either infused with water, closed symbols or methyl viologen (MV), open symbols. W38 and ssuR had similar slopes (0.0032 ΔA/μmol e^- m^{-2} s^{-2} and 0.0035 ΔA/μmol e^- m^{-2} s^{-2} respectively) and upon addition of MV there was little change in slope (W38 slope =0.0034 ΔA/μmol e^- m^{-2} s^{-2} and ssuR slope = 0.00353 ΔA/μmol e^- m^{-2} s^{-2}). However the slope of gapR was much higher (0.0062 ΔA/μmol e^- m^{-2} s^{-2}) and was reduced down to W38 levels with the addition of MV (0.00335 ΔA/μmol e^- m^{-2} s^{-2}). Error bars equal standard error n=3. For all lines of fit $P<0.02$.

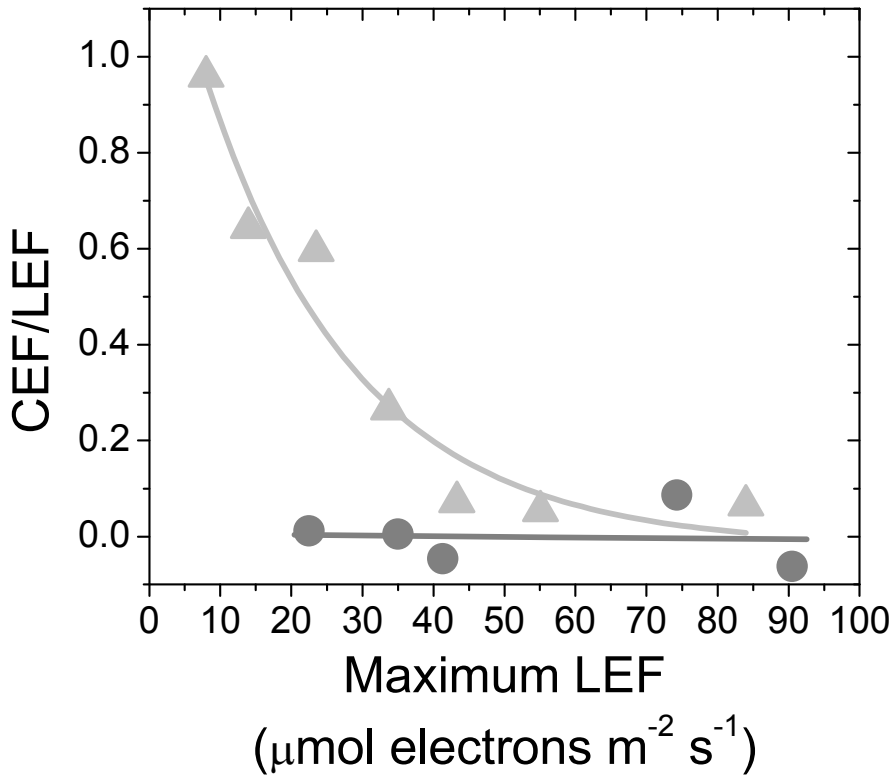

Figure 3. The fraction of CEF/LEF in the mutants, ssuR and gapR compared to maximum rate of LEF. The mutants ssuR (●) and gapR (▲) are compared over a variable range of inhibition which is inversely proportional to their maximum level of LEF.

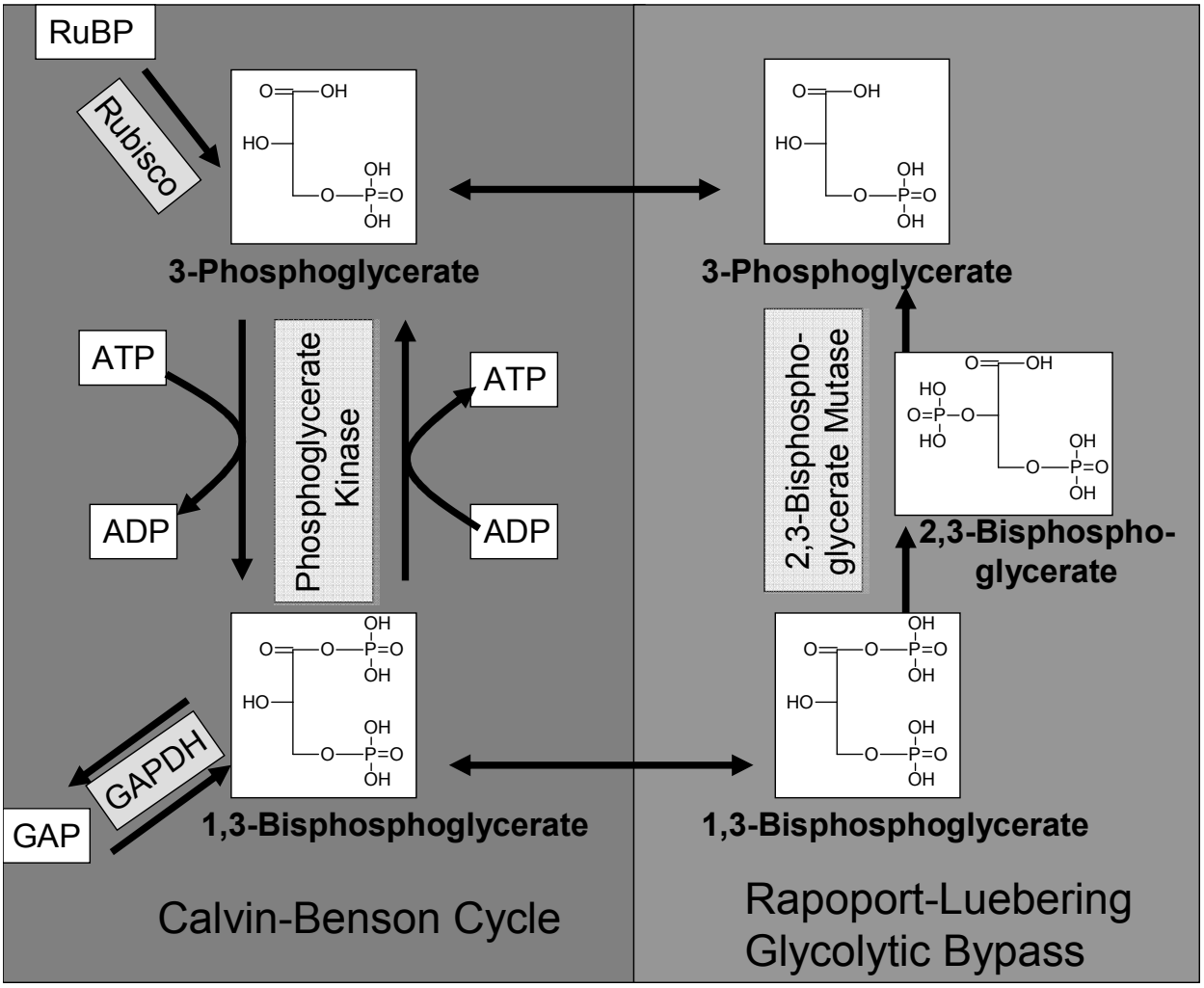

Figure 4. Possible ATP-consuming futile cycle in chloroplasts. Light grey boxes represent enzymes, and white boxes represent chemicals. The dark grey (left) side shows part of the Calvin-Benson Cycle, which is paired with the Rapoport-Luebering Glycolytic Bypass (light grey, right side). In this scheme, 3-phosphoglycerate (3-PGA) is converted to 1,3-bisphosphoglycerate (1,3-BPG) by phosphoglycerate kinase in an ATP consuming step. The 1,3-BPG is then converted to 2,3-bisphosphoglycerate and then back to 3-PGA by a single enzyme 2,3-Bisphosphoglycerate mutase.

References

Allen J.F. (2002) Photosynthesis of ATP- electrons, proton pumps, rotors, and poise. *Cell*, **110**, 273-276.

Asada K. (2000) The water-water cycle as alternative photon and electron sinks. *Philosophical Transactions of the Royal Society B: Biological Sciences*, **355**, 1419-1431.

Avenson T.J., Cruz J.A., Kanazawa A. & Kramer D.M. (2005a) Regulating the proton budget of higher plant photosynthesis. *Proceedings of the National Academy of Sciences*, **102**, 9709–9713.

Avenson T.J., Cruz J.A. & Kramer D.M. (2004) Modulation of energy dependent quenching of excitons (q_E) in antenna of higher plants. *Proceedings of the National Academy of Sciences*, **101**, 5530-5535.

Avenson T.J., Kanazawa A., Cruz J.A., Takizawa K., Ettinger W.E. & Kramer D.M. (2005b) Integrating the proton circuit into photosynthesis: progress and challenges. *Plant, Cell and the Environment*, **28**, 97-109.

Baker N.R., Harbinson J. & Kramer D.M. (2007) Determining the limitations and regulation of photosynthetic energy transduction in leaves. *Plant, Cell and the Environment*, **30**, 1107-1125.

Baker N.R. & Ort D.R. (1992) Light and crop photosynthetic performance. *In Crop Photosynthesis: Spatial and Temporal Determinants (eds N.R. Baker & H. Thomas)*, **Elsevier Science Publishers, Amsterdam, the Netherlands**, 289-312.

Breyton C., Nandha B., Johnson G., Joliot P. & Finazzi G. (2006) Redox modulation of cyclic electron flow around Photosystem I in C3 plants. *Biochemistry*, **45**, 13465-13475.

Carpentier R., Larue B. & Leblanc R.M. (1984) Photoacoustic spectroscopy of Anacystis nidulans : III. Detection of photosynthetic activities. *Archives of Biochemistry and Biophysics*, **228**, 534-543.

Cho J., King J.S., Qian X., Harwood A.J. & Shears S.B. (2008) Dephosphorylation of 2,3-bisphosphoglycerate by MIPP expands the regulatory capacity of the Rapoport-Luebering glycolytic shunt. *Proceedings of the National Academy of Sciences*, **105**, 5998-6003.

Cruz J.A., Avenson T.J., Kanazawa A., Takizawa K., Edwards G.E. & Kramer D.M. (2005) Plasticity in light reactions of photosynthesis for energy production and photoprotection. *Journal of Experimental Botany*, **56**, 395-406.

Cruz J.A., Emery C., Wüst M., Kramer D.M. & Lange B.M. (2008) Metabolite profiling of Calvin cycle intermediates by HPLC-MS using mixed-mode stationary phases. *The Plant Journal*, **55**, 1047-1060.

Cruz J.A., Sacksteder C.A., Kanazawa A. & Kramer D.M. (2001) Contribution of electric field ($\Delta\psi$) to steady-state transthylakoid proton motive force (*pmf*) *in vitro* and *in vivo*. Control of *pmf* parsing into $\Delta\psi$ and ΔpH by ionic strength. *Biochemistry*, **40**, 1226-1237.

Eberhard S., Finazzi G. & Wollman F.A. (2008) The dynamics of photosynthesis. *Annual Review of Genetics*, **42**, 463-515.

Edwards G.E. & Walker D.A. (1983) C_3, C_4:Mechanisms, and Cellular and Environmental Regulation of Photosynthesis. *Textbook on C3, C4 Photosynthesis*, **Blackwell Scientific**.

Finazzi G., Rappaport F., Furia A., Fleischmann M., Rochaix J.D., Zito F. & Forti G. (2002) Involvement of state transitions in the switch between linear and cyclic electron flow in *Chlamydomonas reinhardtii*. *European Molecular Biology Organization*, **3**, 280–285.

Fridlyand L.E., Backhausen J.E. & Scheibe R. (1998) Flux control of the Malate Valve in leaf cells. *Archives of Biochemistry and Biophysics*, **349**, 290-298.

Gambarova N.G. (2008) Activity of photochemical reactions and accumulation of hydrogen peroxide in chloroplasts under stress conditions. *Russian Agricultural Sciences*, **34**, 149-151.

Genty B., Briantais J.M. & Baker N.R. (1989) The relationship between the quantum yield of photosynthetic electron transport and quenching of chlorophyll fluorescence. *Biochimica et Biophysica Acta*, **990**, 87-92.

Harbinson J. & Foyer C.H. (1991) Relationships between the efficiencies of photosystems I and II and stromal redox state in CO_2-free air : Evidence for cyclic electron flow *in vivo*. *Plant Physiol*, **97**, 41-49.

Heber U. (2002) Irrungen, Wirrungen? The Mehler reaction in relation to cyclic electron transport in C3 plants. *Photosynthesis Research*, **73**, 23-231.

Heber U. & Walker D. (1992) Concerning a dual function of coupled cyclic electron transport in leaves. *Plant Physiology*, **100**, 1621-1626.

Hideg E., Spetea C. & Vass I. (1994) Singlet oxygen production in thylakoid membranes during photoinhibition as detected by EPR spectroscsopy. *Photosynthesis Research*, **39**, 191-199.

Hope A.B., Valente P. & Matthews D.B. (1994) Effects of pH on the kinetics of redox reactions in and around the cytochrome *bf* complex in an isolated system. *Photosynthesis Research*, **42**, 111-120.

Horton P., Ruban A. & Walters R. (1996) Regulation of light harvesting in green plants. *Annual Review of Plant Physiology and Plant Molecular Biology*, **47**, 655-684.

Hou D.Y., Xu H., Du G.Y., Lin J.T., Duan M. & Guo A.G. (2009) Proteome analysis of chloroplast proteins in stage albinism line of winter wheat (*triticum aestivum*) FA85. *Biochemistry and Molecular Biology Report*, **42**, 450-455.

Hudson G.S., Evans J.R., von Caemmerer S., Arvidsson Y.B.C. & Andrews T.J. (1992) Reduction of ribulose-1,5-bisphosphate carboxylase/oxygenase content by antisense RNA reduces photosynthesis in transgenic tobacco plants. *Plant Physiology*, **98**, 294-302.

Jia H., Oguchi R., Hope A.B., Barber J. & Chow W.S. (2008) Differential effects of severe water stress on linear and cyclic electron fluxes through Photosystem I in spinach leaf discs in CO_2-enriched air. *Planta*, **228**, 803-812.

Joët T., Cournac L., Peltier G. & Havaux M. (2002) Cyclic electron flow around photosystem I in C3 plants. *In vivo* control by the redox state of chloroplasts and involvement of the NADH-dehydrogenase complex. *Plant Physiology*, **128**, 760–769.

Johnson G.N. (2005) Cyclic Electron Transport in C_3 plants: facts or artefacts? *Journal of Experimental Botany*, **56**, 407-416.

Joliot P. & Joliot A. (2002) Cyclic electron transfer in plant leaf. *Proceedings of the National Academy of Sciences*, **99**, 10209–10214.

Junge W. & Witt H. (1968) On the ion transport system of photosynthesis--investigations on a molecular level. *Zeitschrift fuer Naturforschung, B*, **23**, 244-254.

Kanazawa A. & Kramer D.M. (2002) *In vivo* modulation of nonphotochemical exciton quenching (NPQ) by regulation of the chloroplast ATP synthase. *Proceedings of the National Academy of Sciences*, **99**, 12789-12794.

Kauffman K., Pajerowski J., Jamshidi N., Palsson B. & Edwards J. (2002) Description and analysis of metabolic connectivity and dynamics in the human red blood cell. *Journal of Biological Chemistry*, **83**, 646-662.

Klughammer C. & Schreiber U. (1993) An improved method, using saturating light pulses, for the determination of photosystem I quantum yield via $P700^{+}$-absorbance changes at 830 nm. *Planta*, **192**, 261-268.

Kohzuma K., Cruz J.A., Akashi K., Munekage Y., Yokota A. & Kramer D.M. (2008) The long-term responses of the photosynthetic proton circuit to drought. *Plant, Cell and the Environment*, **32**, 209-219.

Kramer D. & Crofts A. (1989) Activation of the chloroplast ATPase measured by the electrochromic change in leaves of intact plants. *Biochimica et Biophysica Acta*, **976**, 28-41.

Kramer D.M., Avenson T.J. & Edwards G.E. (2004) Dynamic flexibility in the light reactions of photosynthesis governed by both electron and proton transfer reactions. *Trends in Plant Science*, **9**, 349-357.

Kramer D.M. & Crofts A.R. (1996) Control of photosynthesis and measurement of photosynthetic reactions in intact plants. In: *Photosynthesis and the Environment* . *Advances in Photosynthesis* (ed N. Baker), pp. 25-66. Kluwer Academic Press, Dordrecht, The Netherlands.

Kubicki A., Funk E., Westhoff P. & Steinmüller K. (1996) Differential expression of plastome-encoded ndh genes in mesophyll and bundle-sheath chloroplasts of the C4 plant Sorghum bicolor indicates that the complex I-homologous NAD(P)H-plastoquinone oxidoreductase is involved in cyclic electron transport. *Planta*, **199**, 276-281.

Lascano H.R., Casano L.M., Martin M. & Sabater B. (2003) The activity of the chloroplastic Ndh complex is regulated by phosphorylation of the NDH-F subunit. *Plant Physiology*, **132**, 256-262.

Livingston A.K., Cruz J., Kohzuma K., Dhingra A. & Kramer D.M. (2010) An Arabidopsis mutant with high cyclic electron flow around photosystem I (*hcef*) involving the NDH complex. *Plant Cell*, **22**, 1-13.

Macpherson A.N., Telfer A., Barber J. & Truscott T.G. (1993) Direct detection of singlet oxygen from isolated photosystem II reaction centers. *Biochimica et Biophysica Acta*, **1143**, 301-309.

Miyake C. & Yokota A. (2000) Determination of the Rate of Photoreduction of O_2 in the Water-Water Cycle in Watermelon Leaves and Enhancement of the Rate by Limitation of Photosynthesis. *Plant Cell Physiology*, **41**, 335-343.

Nixon P.J. & Mullineaux C.W. (2001) Regulation of photosynthetic electron transport. In: *Advances in photosynthesis and respiration: regulation of photosynthesis* (eds E. Aro & B. Anderson). Kluwer Academic Publishers.

Noctor G. & Foyer C. (1998) A re-evaluation of the ATP:NADPH budger during C3 photosynthesis: a contribution form nitrate assimilation and its associated respiratory activity. *Journal of Experimental Botany*, **49**, 1895-1908.

Porra R.J., Thompson W.A. & Kriedemann P.E. (1989) Determination of accurate extinction coefficients and simultaneous equations for assaying chlorophylls a and b extracted with four different solvents: verification of the concentration of chlorophyll standards by atomic absorption spectroscopy. *Biochimica et Biophysica Acta*, **975**, 384-394.

Price G.D., Evans J.R., von Caemmerer S., Yu J.W. & Badger M.R. (1995) Specific reduction of chloroplast glyceraldehyde-3-phosphate dehydrogenase activity by antisense RNA reduces CO_2 assimilation via a reduction in ribulose bisphosphate regeneration in transgenic tobacco plants. *Planta*, **195**, 369-378.

Quick W.P., Schurr U., Scheibe R., Schulze E.D., Rodermel S.R., Bogorad L. & Stitt M. (1991) Decreased ribulose-1,5-bisphosphate carboxylase-oxygenase in transgenic tobacco transformed with "antisense" rbcS. *Planta*, **183**, 542-554.

Rapoport I., Berger H., Elsner R. & Rapoport S. (1977) pH-dependent changes of 2,3-bisphosphoglycerate in human red cells during transitional and steady states *in vitro*. *European Journal of Biochemistry*, **73**.

Ruuska S.A., Andrews T.J., Badger M.R., Price G.D. & von Caemmerer S. (2000) The role of chloroplast electron transport and metabolites in modulating rubisco activity in tobacco. Insights from transgenic plants with reduced amounts of cytochrome *b/f* complex or glyceraldehyde 3-phosphate dehydrogenase. *Plant Physiology*, **122**, 491–504.

Sacksteder C., Kanazawa A., Jacoby M.E. & Kramer D.M. (2000) The proton to electron stoichiometry of steady state photosynthesis in living plants: a proton-pumping Q-cycle is continuously engaged. *Proceedings of the National Academy of Sciences*, **97**, 14283-14288.

Sacksteder C. & Kramer D.M. (2000) Dark-interval relaxation kinetics (DIRK) of absorbance changes as a quantitative probe of steady-state electron transfer. *Photosynthesis Research*, **66**, 145-158.

Scandalios J.G. (1993) Oxygen stress and superoxide dismutases. *Plant Physiology*, **101**, 7-12.

Scheibe R. (2004) Malate valves to balance cellular energy supply : Redox regulation: from molecular responses to environmental adaptation. *Physiologia Plantarum*, **120**, 21-26.

Seelert H., Poetsch A., Dencher N.A., Engel A., Stahlberg H. & Müller D.J. (2000) Structural biology. Proton-powered turbine of a plant motor. *Nature*, **405**, 418-419.

Takizawa K., Cruz J.A., Kanazawa A. & Kramer D.M. (2007) The thylakoid proton motive force *in vivo*. Quantitative, non-invasive probes, energetics, and regulatory consequences of light-induced *pmf*. *Biochimica et Biophysica Acta*, **1767**, 1233-1244.

Takizawa K., Kanazawa A. & Kramer D.M. (2008) Depletion of stromal P_i induces high 'energy-dependent' antenna exciton quenching (q_E) by decreasing proton conductivity at CF_O-CF_1 ATP synthase. *Plant, Cell & Environment*, **31**, 235-243.

Chapter 3: A mutation in glyceraldehyde-3-phosphate dehydrogenase subunit B induces cyclic electron flow around photosystem I.

Aaron K. Livingston, Jeffrey A. Cruz, and David M. Kramer

Abstract

Cyclic electron flow around photosystem I (CEF1) is a mechanism to induce photoprotection and balance the chloroplast energy budget. We recently described an Arabidopsis mutant, *hcef1*, with a point mutation in fructose-1,6-bisphosphatase, in which CEF1 is highly activated. Here we introduce a second Arabidopsis high CEF1 mutant, *hcef2*, point mutant in the glyceraldehyde phosphatase dehydrogenase (GAPDH) subunit B (gapB). This *hcef2* mutant shows constitutively elevated CEF1, similar to a recently-reported tobacco mutant with antisense suppression of GAPDH expression. Crossing *hcef2* with *pgr5*, which is deficient in the antimycin A-sensitive plastoquinone reduction CEF1 pathway, resulted in a double mutant that maintained the high conductivity associated with PGR5 and high CEF1, implying that the PGR5-dependent pathway is not involved in the elevated CEF1 activity. On the other hand, crossing *hcef2* with *crr2-2*, deficient in thylakoid NADPH dehydrogenase (NDH) complex, produced a light-sensitive double mutant lacking elevated CEF1. These results suggest that, as in *hcef1,* the elevated CEF1 likely involves the NDH complex.

Keywords: *hcef,* Cyclic Electron Flow (CEF1), GAPDH, NADPH dehydrogenase

Introduction

Photosynthesis must balance its energy budget, so that production and consumption of ATP and NADPH precisely match (Edwards & Walker, 1983, Kramer, Avenson & Edwards, 2004). Linear electron flow (LEF) through both photosystem II (PSII) and photosystem I (PSI) produces a fixed ratio of ATP/NADPH of approximately 2.6 ATP/2 NADPH, whereas stromal metabolism requires ~2.9, or more under stressed conditions where ATP is needed for protein repair, transport etc (Edwards & Walker, 1983). Thus, it has been proposed that the chloroplast must possess mechanisms for either producing additional ATP or dissipating excess NADPH.

Three distinct ATP/NADPH balancing processes have been proposed, 1) the malate shunt (Scheibe, 2004), in which electrons from NADPH are shuttled to the mitochondrion; 2) the Mehler peroxidase reaction, or "water-water cycle "(Asada, 2000), in which electrons from PSI are shunted to O_2, forming superoxide which is detoxified in a process the consumes NADPH and produces ATP; and 3) cyclic electron flow around photosystem I (CEF1) (Heber & Walker, 1992, Livingston, Cruz, Kohzuma, Dhingra & Kramer, 2010a), a photochemical cycle that results in the production of ATP but no net reduction of NADPH.

In CEF1, photoactivation of PSI initiates electron transfer from plastocyanin to ferredoxin. The oxidized plastocyanin is reduced by oxidation of plastoquinol at the cytochrome b_6f complex, while reduced ferredoxin transfers its electron into the plastoquinone pool, via one or more plastoquinone reductase (PQR) pathways, completing the cycle. The reduction of plastoquinone at the PQR and its re-oxidation at the cytochrome b_6f complex results in the translocation of protons from the stroma to the lumen, producing an electrochemical gradient of protons, or proton motive force (*pmf*), across the thylakoid membrane that drives the synthesis of

ATP, increasing the ATP/NADPH output ratio and initiating the photoprotective q_E response (Heber & Walker, 1992, Kramer *et al.*, 2004).

Three major PQR pathways have been proposed: 1) the PGR5-dependent ferredoxin-PQ oxidoreductase (FQR) (Munekage, Hojo, Meurer, Endo, Tasaka & Shikanai, 2002); 2) the Qi site of the cytochrome b_6f complex, possibly involving ferredoxon:$NADP^+$ oxidoreductase (FNR) (Zhang, Whitelegge & Cramer, 2001); or 3) the thylakoid NADPH dehydrogenase complex (NDH) (Shikanai, Endo, Hashimoto, Yamada, Asada & Yokota, 1998, Lascano, Casano, Martin & Sabater, 2003).

Under non-stressed steady-state conditions in C_3 plants, most groups have found that CEF1 has a very small contribution to overall photosynthetic energy production, suggesting that the ATP/NADPH output of LEF is nearly sufficient to meet downstream needs (Harbinson & Foyer, 1991, Avenson, Cruz, Kanazawa & Kramer, 2005). However, substantial increases in CEF1 have been reported under high light (Baker & Ort, 1992), during induction of photosynthesis (Joët, Cournac, Peltier & Havaux, 2002, Joliot & Joliot, 2002), and under environmental stresses, such as drought (Jia, Oguchi, Hope, Barber & Chow, 2008, Kohzuma, Cruz, Akashi, Munekage, Yokota & Kramer, 2008). The increases in CEF1 likely reflect additional ATP demands imposed by stresses or altered metabolism (Kramer *et al.*, 2004).

Recently, we introduced a new class of mutants with highly elevated CEF1. The first of these, *hcef1*, was mapped to the Calvin-Benson Cycle enzyme, fructose-1,6-bisphosphatase (FBPase) (Livingston *et al.*, 2010a). It has also been shown that suppression of fructose 1,6-bisphosphate aldolase (Gotoh, Matsumoto, Ogawa, Kobayashi & Tsyama, 2009) increases CEF1. Most recently, high CEF1 was also found when the expression of glyceraldehyde-3-phosphate dehydrogenase, but not Rubisco, was suppressed in tobacco (Livingston, Kanazawa,

Cruz & Kramer, 2010b). We proposed that that mutation of FBPase or GAPDH suppression imposes an additional ATP demand, perhaps by activating an ATP consuming futile cycle involving synthesis and breakdown of 1,3-bisphosphoglycerate (Livingston *et al.*, 2010a, Livingston *et al.*, 2010b).

In this work, we describe a second high CEF1 mutant, *hcef2,* isolated from and EMS (ethyl methanesulfonate) mutagenized population, and mapped to chloroplast glyceraldehyde phosphatase dehydrogenase (GAPDH) subunit B (gapB), i.e. the same gene that, when suppressed in tobacco elevated CEF1 (Livingston *et al.*, 2010b). The availability of the *hcef2* mutant in Arabidopsis allows us to use genetics tools to further study the activation of CEF1 upon suppression of chloroplast metabolism, specifically testing for the involvement of proposed CEF1 pathways.

Material and Methods

Plant Material and Growth Conditions.

Arabidopsis thaliana (Columbia ecotype), wild and *hcef2* types, were grown photoautotrophic on soil under a 16:8 photoperiod at 85-90 μmol photons $m^{-2}s^{-1}$ at 23°C. Crosses of *pgr5 hcef2* and *crr2-2 hcef2* had to be grown at 40-45 μmol photons m^{-2} s^{-1} at 23°C with 16:8 photoperiod. The Arabidopsis mutants *pgr5* and *crr2-2* were a gift from Dr. T. Shikanai (Nara Institute of Science and Technology, Ikoma, Nara, Japan).

EMS mutagenization of Arabidopsis and screening of mutants.

Wild-type Columbia (Colell *et al.*) Arabidopsis mutagenized by EMS (ethylmethanesulfonate) described in (Kim, Schumaker & Zhu, 2006), was screened for high CEF1 by a three-stage screening process described in detail in (Livingston *et al.*, 2010a).

In Vivo Spectroscopic Assays.

Arabidopsis leaves were measured at 24 to 48 days old, when fully expanded, in an in-house constructed non-focusing optics spectrophtometer/fluorometer (NoFOSpec) (as described in (Livingston *et al.*, 2010a)) with continuously-flowing humidified air. The perimeters qE and photochemical yield of photosystem II (ϕ_{II}) was calculated by saturation-pulse chlorophyll fluorescence yield change (Genty *et al.*, 1989, Kanazawa & Kramer, 2002, Avenson *et al.*, 2004). Through the use of an Ulbricht integrating sphere (Knapp & Carter, 1998) the relative absortivities of Col and mutant *hcef2* where approximated at 0.5 and 0.46 respectively which allows us to estimate accurate rates of LEF (Ziyu, Maurice & Edwards, 2004).

After 15 minutes of actinic illumination, LEF was measured under steady state photosynthetic conditions. The perimeter qE was determined as described in (Kramer & Crofts, 1996, Kanazawa & Kramer, 2002) by collecting F_M" after 10 minutes of dark relaxation and taking F_M' at the end of actinic light activation. Light-induced, steady-state *pmf* was calculated from dark-interval relaxation kinetics (DIRK) change in absorbance at 520 nm, which is associated with the electrochromic shift (ECS) (Sacksteder & Kramer, 2000, Cruz *et al.*, 2005). The ECS_t measured over a 300 ms dark interval is equivalent to the amount of light-induced *pmf*. The inverse of the time constant of the ECS decay (τ_{ECS}) is proportional to g_H^+ (Sacksteder & Kramer, 2000, Kanazawa & Kramer, 2002, Cruz *et al.*, 2005). Using the initial slope of the perimeter of ECS the relative value of steady state proton flux across the thylakoid membrane

(v_H^+) was calculated (Avenson *et al.*, 2005, Takizawa *et al.*, 2008). ECS measurement were normalized, accounting for variations in leaf thickness and pigmentation, by the extent of rapid rise single-turnover flash induced ECS (Kramer & Crofts, 1989) and chlorophyll content (Porra, Thompson & Kriedemann, 1989) resulting in corrections of 49.9% and 51.5% respectively.

Introduction of methyl viologen into leaves.

When indicated, intact leaves (Arabidopsis) or 1 inch leaf disks (tobacco) where placed inside a Kimwipe (Kimberly-Clark, Mississauga, Ontario) saturated with either distilled water or 100 μM methyl viologen, and incubated for 60 minutes at low light (5~10 μmol photon m^{-2} s^{-1}). Before experimentation, leaf material was gently blotted with a fresh Kimwipe to remove excess liquid. Leaves infiltrated with MV are highly sensitive to photodamage and thus light intensity and assays times were minimized to 100 μmol photons m^{-2} s^{-1} and 25 min.

Map-based cloning.

The recessive mutant *hcef2* was mapped by derived from breeding homozygous *hcef2* (Columbia) and wild-type ecotype *Landsberg erecta* and using molecular markers created using cleaved amplified polymorphic sequence (Baumbusch, Sundal, Hughes, Galau & Jakobsen, 2001, Jander, Norris, Rounsley, Bush, Levin & Last, 2002) and single nucleotide polymorphisms (Drenkard, Richter, Rozen, Stutius, Angell, Mindrinos, Cho, Oefner, Davis & Ausubel, 2000). Genomic DNA was isolated from homozygous F2 plants for Col and *hcef2 hcef2* and the gene AT1G42970 was PCR amplified in both, using AmpliTAQ Gold PCR Master Mix (Applied Biosystems, Branchburg, New Jersey). All sequencing was accomplished using Big Dye Reagent

and ran at the Molecular Biology Core, Pullman, Washington on a ABI Prism 377 (reagent and machine from AME Bioscience, Toroed, Norway).

GAPDH enzyme activity.

The enzyme activity was GAPDH was found spectroscophically by measuring the initial rate of the consumption of NADPH as described in (Stitt, Lilley, Gerhardt & Heldt, 1989) following the modifications in (Ruuska *et al.*, 1998). The reagent DTT was removed from the extraction buffer and 4.5 mM was used only where indicated in the assay mixture.

***Hcef2* crosses.**

The crosses of *pgr5 hcef2* and *crr2-2 hcef2* were verified for the presence the mutations by genomic screening using the *pgr5* and *crr2-2* primers described in (Livingston *et al.*, 2010a). The double mutants were sequenced for the presence of the *hcef2* mutation.

Results

The mutant describe in this work, *hcef2*, was selected using the same procedure as described in Livingston et al. (2010a), which identified *hcef1*. Briefly, starting with EMS-mutagenized plants, we initially screen for mutants with high levels of q_E compared to Columbia wild-type. A secondary screen was performed to select which high q_E mutants displayed elevated *pmf* that could not be explained by down-regulation of the ATP synthase. A final screen was accomplished to distinguish those mutants with elevated CEF1, estimated by comparing light-driven proton flux (v_H^+) with LEF. Specific data demonstrating the high CEF1 phenotype are described below.

Growth of *hcef2*

The *hcef2* mutant grew photoautotrophically in soil, but at an impaired growth rate. When Columbia wild-type (or Col) achieved maturity (24-28 days), *hcef2* of the same age had a rosette diameter ~30% that of Col, but reached equal rosette diameter size in about 49-56 days. Bolting was slightly delayed in *hcef2* (32-38 days compared to Col 24-28 days).

Map-based cloning and complementation of *hcef2*.

Using the procedure described in Livingston et al. (2010a), the mutation of *hcef2* was mapped to chloroplast GAPDH subunit B (AT1G42970), as a G:C to T:A transversion, in a known branching point (Begerow, John & Oberwinkler, 2004) of the fifth intron of AT1G42970.

When next attempted to complement the mutation using the wild type sequence. Surprisingly, we found that every successful *E. coli* transformant (>30 separate lines) containing the wild-type GAPDH construct was found to have the inverted orientation (data not shown). We conclude that the GAPDH gene is lethal for *E. coli*. In addition, previous work (Chuang, Hough & Senatorov, 2005, Colell, Green & Ricci, 2009), showing that expression of GAPDH leads to apoptosis in mammalian cells. Given the likelihood of failure, we took two alternative approaches to confirming the locus of the *hcef2* mutant. In the first approach, we demonstrated that antisense suppression of GADPH in tobacco (Ruuska, Andrews, Badger, Hudson, Laisk & von Caemmerer, 1998, Ruuska, Andrews, Badger, Price & von Caemmerer, 2000) also show elevated CEF1 (Livingston *et al.*, 2010b), as discussed below.

In a second approach, we crossed *hcef2* against a transposon insertion mutant of chloroplast GAPDH subunit B (line CS814250). The homozygous transposon insert mutant has a

seedling lethal phenotype, so we started with heterozygous lines. If, as implied by our mapping, the *hcef2* mutant occurred in the GAPDH gene, we would expect 50% of the F1 generation to be deficient in GAPDH activity and show elevated CEF1. The remaining 50% would be at least partly complemented by wild type GAPDH and show wild-type characteristics. On the other hand, if the *hcef2* mutation was located on a different gene, crossing against the heterozygous GAPDH knockout would result in all F1 plants with near wild-type phenotype. Three separate crosses where made from *hcef2* into heterozygous CS814250, which due to low levels of seed production in both mutants, resulted in 10 individuals. Of the 10 individuals, 4 had growth and photosynthetic phenotypes resembling heterozygous CS814250 (increased photosynthesis compared to *hcef2*, low CEF1) and 6 individuals were highly light sensitive, which photobleached and died when subjected to only 15 μmol photons m^{-2} s^{-1} of light. Genotyping of the plants which showed the heterozygous CS814250 phenotype where found to be heterozygous for the *hcef2* mutation and a copy of the T-DNA insert.

Comparison of GAPDH activity between *hcef2* and Col.

Our mapping and complementation results indicate that *hcef2* is mutated in the B-subunit of GAPDH. To confirm a lesion at this biochemical step, we assayed GAPDH activity. Figure 4 shows the rate of GAP-dependent NADPH oxidation in chloroplast extracts. Non-chloroplast or non-enzymatic GAPDH activity was accounted for by comparing rates in the presence of dithiothreitol (DTT), where the chloroplast GADPH is active, and in the absence of DTT, where chloroplast GADPH is inactive (Ruuska *et al.*, 2000). Col reached an activity of ~8 μmol NADPH min^{-1} per mg chlorophyll which is similar to previous findings (Strand, Hurry, Henkes, Huner, Gustafssön, Gardestrom & Stitt, 1999). Col showed an approximate 7 fold increase in

activity with the addition of DTT, which is similar to previous findings (Howard, Metodiev, Lloyd & Raines, 2008). The mutant *hcef2* showed 45% less GAPDH activity than Col, indicating a decrease in overall GAPDH activity, consistent with our assignment of *hcef2*.

Photosynthetic properties of *hcef2* compared to Col

Responses of photosynthetic electron transport. Compared to Col, *hcef2* showed a ~5-fold decrease in LEF, after making absorptivity corrections, at saturating light (500 μmol photons m^{-2} s^{-1}) (Fig. 1A). The light intensity at the half saturation point for LEF in *hcef2* (~70 μmol photons m^{-2} s^{-1}) was about half that of Col (~140 μmol photons m^{-2} s^{-1}).

The response of 'energy-dependent' photoprotection (q_E) to light intensity was far more sensitive in *hcef2* than Col. A q_E value of 0.5 was reached at only ~75 μmol photons m^{-2} s^{-1} in *hcef2* where this point was not reached until ~280 μmol photons m^{-2} s^{-1} in Col (Fig. 1B). The light intensity at half-saturation for the q_E response was reached was ~75 and ~200 μmol photons m^{-2} s^{-1} for *hcef2* and Col, respectively. Under saturating light, *hcef2* achieved a higher extent of q_E (~1.05) than Col (~0.7). These relative q_E responses were similar to those seen previously with Col and *hcef1* (Livingston *et al.*, 2010a). The most pronounced difference in q_E extents were seen at ~150 μmol photons m^{-2} s^{-1}, where the response in *hcef2* was ~5 fold greater than that in Col.

Responses of the photosynthetic proton circuit of hcef2. The transthylakoid electric field measured by analysis of the electrochromic shift signal (ECS) allows for an estimation of the *pmf* (using the ECS_t parameter) the extent of light-driven proton flux (v_H^+), and the activation state of the ATP synthase (by g_H+) (Sacksteder & Kramer, 2000, Cruz, Sacksteder, Kanazawa & Kramer, 2001, Baker, Harbinson & Kramer, 2007) Despite the fact that *hcef2* had

suppressed LEF compared to Col, it showed substantially higher light-driven *pmf*, as indicated by increased ECS_t values. The amplitude of ECS_t at the highest light intensity used, 500 μmol photons m^{-2} s^{-1}, was about 2-fold higher in *hcef2* than in Col (Fig. 2A).

The extent of thylakoid *pmf* is controlled by the rate of light-driven proton translocation as well as the activity of the ATP synthase, which controls the conductivity of the membrane to proton efflux, g_H^+. For a given proton flux, a decrease in g_H^+ should result in a proportional increase in *pmf* (Kanazawa & Kramer, 2002). While the ATP synthase is known to regulate the *pmf* under a large range of conditions (Cruz, Avenson, Kanazawa, Takizawa, Edwards & Kramer, 2005), the *hcef2* mutant showed only small (20-30%) decreases in g_H^+ compared to Col (Fig. 2B). This small decrease in g_H^+ was insufficient to account for the 2-fold increase in *pmf*, suggesting that CEF1 was highly activated in *hcef2*.

Estimates of CEF1 in *hcef2*

We used several complimentary approaches to estimate rates of CEF1 in Col and *hcef2*. In the first, we compared estimated of light-induced *pmf* with that expected for LEF alone (Avenson *et al.*, 2005, Baker *et al.*, 2007). The flux of protons through the ATP synthase is proportional to the *pmf* and the conductivity of the ATP synthase to protons (g_H^+) (Sacksteder, Kanazawa, Jacoby & Kramer, 2000). We can estimate g_H^+ using the first-order decay constant for the ECS decay (Kanazawa & Kramer, 2002, Cruz *et al.*, 2005). Proton flux driven by LEF alone should be proportional to LEF, and can be estimated by measuring fluorescence yield changes (Genty, Briantais & Baker, 1989, Kanazawa & Kramer, 2002, Avenson, Cruz & Kramer, 2004). We can then estimate *pmf* generated by LEF alone (pmf_{LEF}) (Avenson *et al.*, 2005) as

pmf_{LEF}=LEF/ g_H^+ (1)

If LEF is operating alone, with no contributions from CEF1, the relationship between pmf_{LEF} and ECS_t (estimated total *pmf*) should be a linear, with a slope proportional to the proton-to-electron stoichiometry for LEF. An increase in this slope would imply proton transfer rates above that supported by LEF alone, and would be consistent with activation of CEF1. Figure 4A shows the slope of ECS_t against pmf_{LEF} was 5-fold higher in *hcef2* than Col, suggesting up-regulation of CEF1.

In another approach, we compared estimates of proton flux , v_H^+, estimated by the initial rate of ECS decay, with LEF (Takizawa, Kanazawa & Kramer, 2008). As shown in Fig. 3B, the slope of the relationship between v_H^+ and LEF, over a range of light intensities between 0 and ~150 μmol photon m^{-2} s^{-1} was ~2 fold higher in *hcef2* than in Col, again indicating the engagement of CEF1. To test this assignment, we repeated these experiments after infiltration with 100 μM methyl viologen (MV), which inhibits CEF1 by shunting electrons from PSI to O_2, and away from PQR. MV completely abolished the observed elevated proton flux, supporting a substantially higher proton translocation in *hcef2*, consistent with activation of CEF1.

Characterization of double mutants *hcef2 pgr5* and *hcef2 crr2-2*.

The *hcef2* mutant was crossed with *pgr5*, which is deficient in the AA-sensitive CEF1 pathway (Munekage *et al.*, 2002), resulting in the double mutant, *hcef2 pgr*5. Interestingly, *hcef2 pgr*5 was photosyntheticaly very similar to *hcef2*, with elevated *pmf* (ECSt, not shown), high ATP synthase activity (g_H^+, Fig. 5A, inset) and most importantly, an elevated v_H^+ compared

to LEF (Fig. 5A). As with *hcef2*, the elevated v_H^+ observed in the *hcef2 pgr*5 double mutant was abolished by infiltration with MV (Fig. 5A) implying that it is generated by increased CEF1.

We also crossed *hcef2* with the NDH knockout mutant *crr2-2*. The *hcef2 crr2-2* double mutant grew photoautotrophically, but was severely slowed in growth, and photobleached when grown at light intensities above 50 μmol photons m^{-2} s^{-1}. Importantly, the *hcef2 crr2-2* double mutant lost the elevated CEF1 as indicated by the loss of MV-sensitive elevated v_H^+ vs. LEF(Fig. 5B). All assays done in Figure 5, *pgr5, hcef2, crr2-2*, Col, *hcef2 pgr5* and *hcef2 crr2-2,* where accomplished on plants grown at ~45 μmol photons m^{-2} s^{-1}.

Discussion

The new high CEF1 (*hcef*) mutant: hindering GAPDH induces CEF1.

Recently, we demonstrated that *hcef1*, a lesion in chloroplast FBPase, led to a dramatic increase in CEF1(Livingston *et al.*, 2010a). Here, we show that *hcef2*, a mutant with a point mutation in GAPDH, uncovered by a screen of EMS-treated Arabidopsis, also shows elevated CEF1. While the increase in CEF1 is similar to that seen the GAPR tobacco lines, with antisense-suppression of GAPDH (Livingston *et al.*, 2010b), the availability of *hcef2* allows us to use powerful genetics tools available in Arabidopsis.

The phenotypes of *hcef,* GAPR, and *hcef2* showed both similarities and differences. GAPR (Livingston *et al.*, 2010b), *hcef1* (Livingston *et al.*, 2010a) and *hcef2* (Fig. 1A) showed sharply reduced LEF, compared to Col, probably induced by restrictions in CO_2 assimilation. Like *hcef1* (Livingston *et al.*, 2010a), *hcef2* and GAPR (Livingston *et al.*, 2010b) also showed substantially higher light-driven *pmf* (Fig. 2A) and subsequent q_E responses (Fig. 1B), despite the dramatic decreases in LEF (and associated proton translocation). The *hcef2* mutant grew more

rapidly and to a larger size than *hcef1*, despite the fact that maximal photosynthesis was inhibited to similar extents, indicating that *hcef1* has strong secondary effects not directly related to assimilation rates.

Typically, slowing photosynthesis e.g. by lowering CO_2 (Kanazawa & Kramer, 2002) or imposition of feedback-limitations (Kiirats, Cruz, Edwards & Kramer, 2009), results in down-regulation of the ATP synthase, allowing thylakoid *pmf* to build up even though light-driven proton flux decreases (Cruz *et al.*, 2005). This response was observed in *hcef1*, partly but not completely accounting for the increase in *pmf* and q_E responses (Livingston *et al.*, 2010a). In the case of *hcef2*, the ATP synthase activity was only decreased by about ~30% compared to Col (Fig. 2B), similar to that seen in GAPR (Livingston *et al.*, 2010b), indicating that the large increases in *pmf* could not be attributed to deactivation of ATP synthase. Instead, the observation of dramatic increases in MV-sensitive proton translocation in *hcef2* compared to Col (Fig. 3B) indicated strong activation of CEF1. The increased CEF1 resulted in an increase in *pmf* (Fig. 2A) and subsequently higher q_E responses (Fig. 1B), as also seen in the GAPR mutants (Livingston *et al.*, 2010b).

PGR5 does not catalyze elevated CEF1 in *hcef2*, but does alter the activity of the ATP synthase

It has been proposed that the PGR5 protein is essential for the major pathway for CEF1 (Munekage *et al.*, 2002). However, we found that the *hcef2 pgr5* double mutant retained the high CEF1 seen in *hcef2* alone (Fig. 5A). These results were very similar to those obtained by crossing *hcef1* with *pgr5* (Livingston *et al.*, 2010a). We thus conclude that PGR5 is not involved in the elevated CEF1 observed in mutants that disrupt certain steps in the Calvin-Benson cycle,

although we cannot rule out its participation under different conditions. This conclusion is consistent the results of Avenson et al (2005), who showed that *pgr5* shows at most a ~14% decrease in steady-state photosynthetic proton translocation compared to Col under non-stressed conditions. The large effect of *pgr5* on lowering the q_E response was attributed instead to a combination of decreased LEF and a large increase in the activity of the ATP synthase, resulting in a low steady-state *pmf*.

We confirm these results here, showing that *pgr5* has a high ATP synthase activity (Fig. 5A insert), decreased LEF (Avenson *et al.*, 2005) and little change in proton translocation compared to Col (Fig. 5) (Avenson *et al.*, 2005). Interestingly, the *hcef2 pgr5* double mutant retained the high ATP synthase activity (g_H^+) of *pgr5* (Fig. 5A insert), while also showing the high proton translocation rates (v_H^+) attributed to increased CEF1 of *hcef2* (Fig. 5). In the *hcef2 pgr5* double mutant, the increased ATP synthase activity resulted in a decreased *pmf* compared to *hcef2*, resulting in a lowered q_E response (data not shown), as seen previously in *pgr5* (Avenson *et al.*, 2005). These results raise the possibility, previously proposed by Avenson et al (2005), that a major effect of *pgr5* is an increased ATP synthase activity, rather than on CEF1, and that this phenotype persists even when CEF1 is increased by mutation of GAPDH.

Elevated CEF1 in *hcef2* involves the NDH complex.

Crossing *hcef2* with *crr2-2*, a knockout of NDH, resulted in a double mutant *hcef2 crr2-2* that was light-sensitive, and exhibited strong suppression of LEF (Data not shown). We also observed complete loss of increased proton translocation attributable to elevated CEF1 (Fig. 5B), implying that CEF1 in *hcef2,* as in *hcef1* (Livingston *et al.*, 2010a), is dependent on NDH. Given its similarity to the proton-translocating ubiquinone reductase (complex I) in mitochondria and

bacteria (Zickermann, Kerscher, Zwicker, Tocilescu, Radermacher & Brandt, 2009), it seems likely that NDH acts as the PQ reductase in elevated CEF1 observed in *hcef1* (Livingston *et al.*, 2010a) and *hcef2*. However, we cannot rule out a regulatory role for NDH.

***hcef2* is possibly triggered by increased ATP demand.**

There is now strong evidence that suppression of three Calvin-Benson cycles enzyme (FBPase (Livingston, 2010 #332), fructose 1,6-bisphosphate aldolase (Gotoh *et al.*, 2009) and GAPDH (Livingston *et al.*, 2010b)) upregulates CEF1, whereas suppression of Rubisco (Livingston *et al.*, 2010b) or lowering CO_2 does not. One possibility is that lesions at certain steps in assimilation impose a greater demand for ATP/NADPH, in turn triggering CEF1 (Kramer *et al.*, 2004, Livingston *et al.*, 2010a). For example, *hcef2* leads to a 3-fold reduction in GAPDH activity compared to Col (Fig. 4), which may lead to the build-up of 1,3-bisphosphoglycerate (1,3-BPG). Because 1,3BPG is unstable, it should break down relatively rapidly, re-forming PGA and releasing P_i. The resulting futile cycle (Livingston *et al.*, 2010b) should deplete the chloroplast of ATP and triggering NDH dependent CEF1. In contrast, suppression of the Rubisco Small Subunit should deplete 1,3BPG, preventing the futile cycle (Livingston *et al.*, 2010b), leading to lower assimilation but no increase in CEF1.

CEF1 may also be triggered by the buildup of reduced electron carriers. When FBPase is inhibited (Tanaka, Mitsuhashi, Kondo & Sugahara, 1982), or GADPH activity decreased (Hald, Nandha, Patrick & Johnson, 2008), like in *hcef1* and *hcef2*/GAPDH respectively, the amount of NADPH increases slightly. This increase in NADPH or the consequence of a highly reduced PSI electron acceptor pool, reactive oxygen species production, i.e. H_2O_2, could trigger CEF1 (Casano, Martin & Sabater, 2001, Lascano *et al.*, 2003).

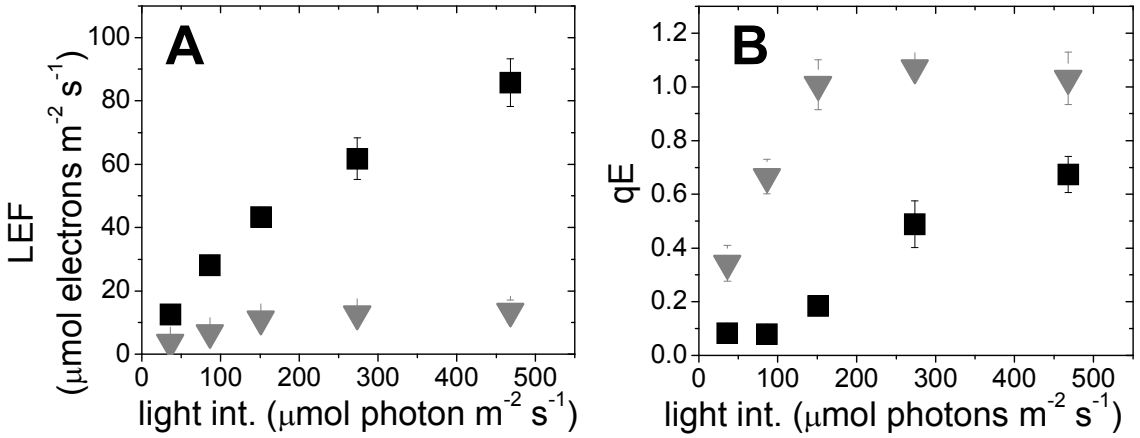

Figure 1. Comparison of photosynthetic responses to electron transport *hcef2* and Col. (A-B) Columbia (■) and *hcef2* (▼) are compared for differences in LEF (A), q_E (B), versus light intensity. Error bars equal standard error n=3.

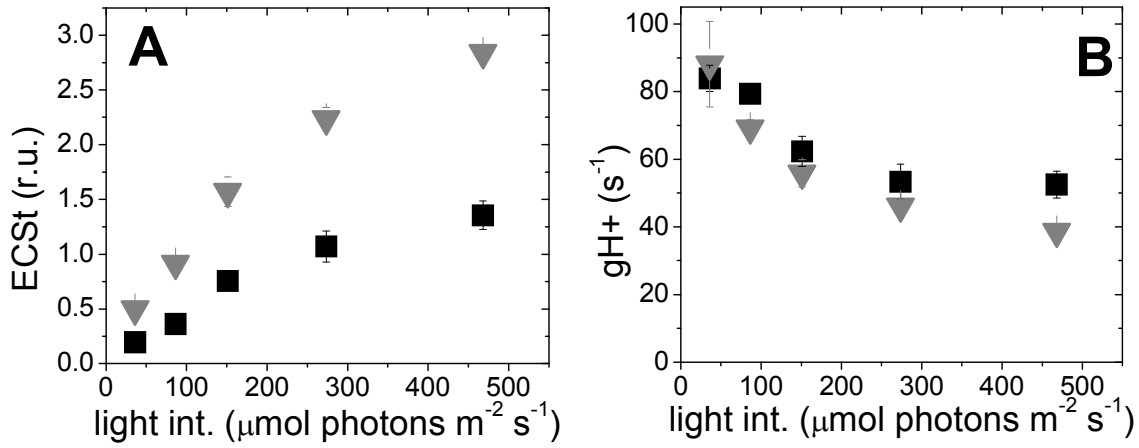

Figure 2. The photosynthetic proton circuit of *hcef2* and Col. (A-B) Columbia (■) and *hcef2* (▼) are compared for differences in ECS_t (A) and g_{H^+} (B) versus light intensity. Error bars equal standard error n=3.

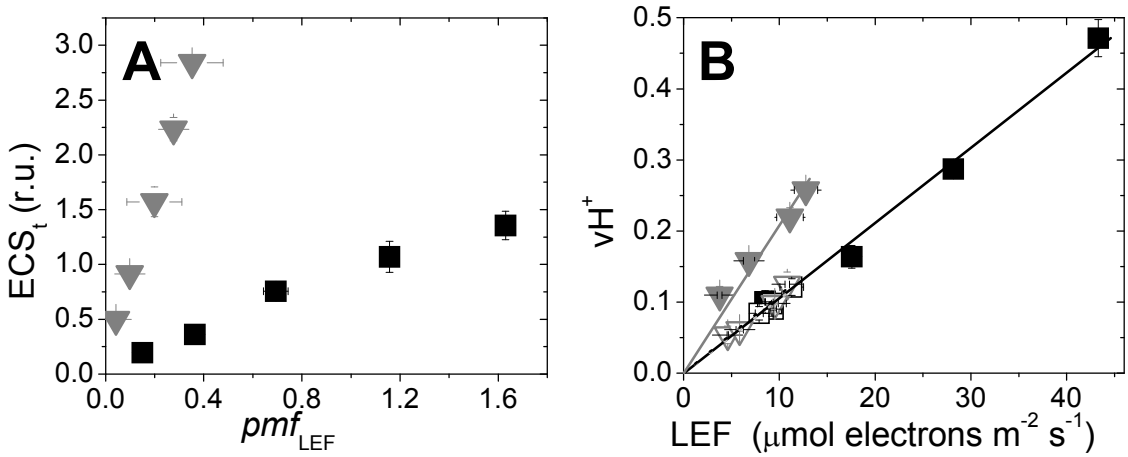

Figure 3. Comparison of additional proton pumping in *hcef2* and Col . (A) Columbia (■) and *hcef2* (▼) are compared for differences in the light-driven *pmf* and the *pmf* expected from LEF alone. (B) Columbia (■) and *hcef2* (▼) without methyl viologen (MV) and with 100 μM MV Columbia (□) and *hcef2* (▽). The slope of Col was 0.01057 ΔA/μmol e^- m^{-2} s^{-2} and *hcef2* was 0.0208 ΔA/μmol e^- m^{-2} s^{-2}. Where as under the presence of MV Col was 0.01043 ΔA/μmol e^- m^{-2} s^{-2} and *hcef2* was 0.01099 ΔA/μmol e^- m^{-2} s^{-2}. Error bars equal standard error n=3.

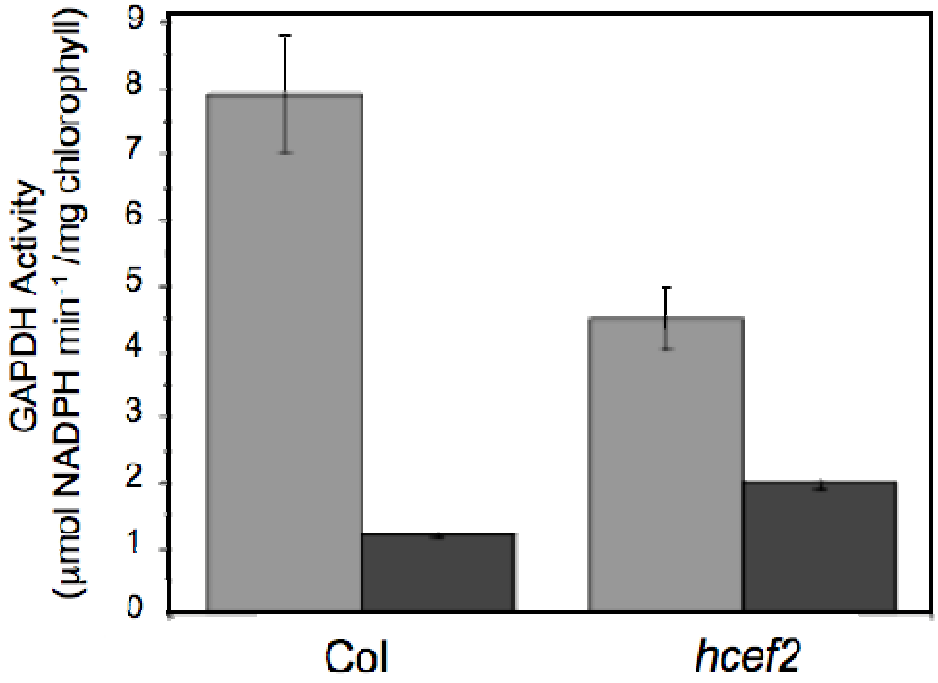

Figure 4. Activity levels of GAPDH in Col and *hcef2.* The light grey represents the presence of 4.5 mmol DTT, and the dark grey represent the absence of DTT. Values were corrected to chlorophyll content; *hcef2* contained approximately 90% the chlorophyll content of Col. Standard deviation. n=3.

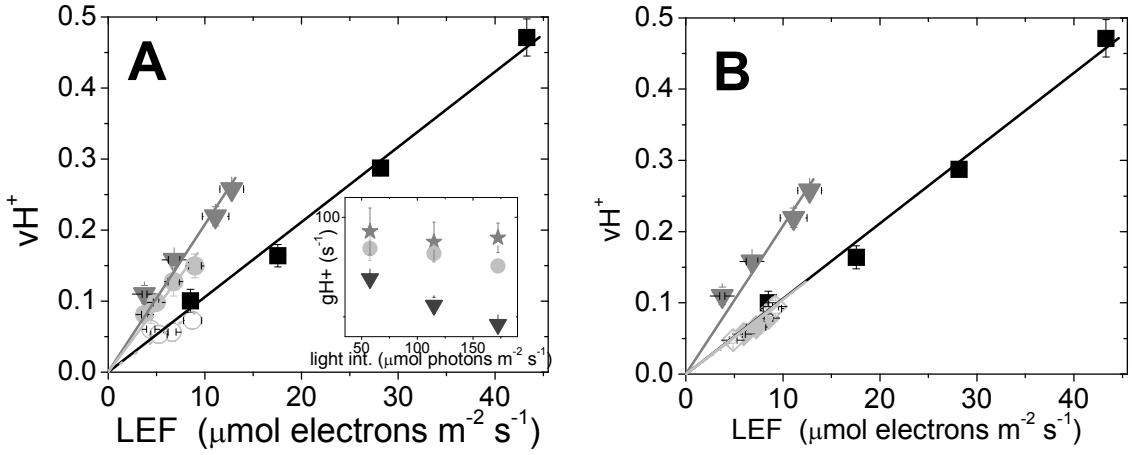

Figure 5. Analysis of the pathway of CEF1 in *hcef2*. The amount of CEF1 was compared in various ecotypes using LEF versus steady-state proton flux into the lumen (v_H^+). (A, B) use the Columbia (■) and *hcef2* (▼) data from figure 3. The slope of Col was 0.01057 ΔA/μmol e^- m^{-2} s^{-2} and *hcef2* was 0.0208 ΔA/μmol e^- m^{-2} s^{-2}. Where as under the presence of MV Col was 0.01043 ΔA/μmol e^- m^{-2} s^{-2} and *hcef2* was 0.01099 ΔA/μmol e^- m^{-2} s^{-2}. In (A) the double mutant *hcef2 pgr5* (●) was found to have a similar slope as normal *hcef2* (0.01815 ΔA/μmol e^- m^{-2} s^{-2}), however as seen in the (4A) insert it maintained *pgr5* (H) high levels of gH+. Upon the addition of MV the *hcef2 pgr5* (○) slope (0.00931 ΔA/μmol e^- m^{-2} s^{-2}) dropped to Col levels. In (B) the double mutant of *hcef2 crr2-2* (◆) had a slope (0.00922 ΔA/μmol e^- m^{-2} s^{-2}) that was similar to that of Col, and did not change upon the addition of MV (◇) (Slope=0.01021 ΔA/μmol e^- m^{-2} s^{-2}). For all points standard error was used n=3. For all lines P< 0.03).

References

Asada K. (2000) The water-water cycle as alternative photon and electron sinks. *Philosophical Transactions of the Royal Society B: Biological Sciences*, **355**, 1419-1431.

Avenson T.J., Cruz J.A., Kanazawa A. & Kramer D.M. (2005) Regulating the proton budget of higher plant photosynthesis. *Proceedings of the National Academy of Sciences*, **102**, 9709–9713.

Avenson T.J., Cruz J.A. & Kramer D.M. (2004) Modulation of energy dependent quenching of excitons (q_E) in antenna of higher plants. *Proceedings of the National Academy of Sciences*, **101**, 5530-5535.

Baker N.R., Harbinson J. & Kramer D.M. (2007) Determining the limitations and regulation of photosynthetic energy transduction in leaves. *Plant, Cell & Environment*, **30**, 1107-1125.

Baker N.R. & Ort D.R. (1992) Light and crop photosynthetic performance. *In Crop Photosynthesis: Spatial and Temporal Determinants (eds N.R. Baker & H. Thomas)*, **Elsevier Science Publishers, Amsterdam, the Netherlands**, 289-312.

Baumbusch L.O., Sundal I.K., Hughes D.W., Galau G.A. & Jakobsen K.S. (2001) Efficient Protocols for CAPS-Based Mapping in Arabidopsis. *Plant Molecular Biology Reporter*, **19**, 137-149.

Begerow D., John B. & Oberwinkler F. (2004) Evolutionary relationships among B-tubulin gene sequences of basidiomycetous fungi. *Mycological Review*, **108**, 1257-1263.

Casano L.M., Martin M. & Sabater B. (2001) Hydrogen peroxide mediates the induction of chloroplastic Ndh complex under photooxidative stress in barley. *Plant Physiology*, **125**, 1450-1458.

Chuang D.M., Hough C. & Senatorov V.V. (2005) Glyceraldehyde-3-phosphate dehydrogenase, apoptosis, and neurodegenerative diseases. *Annual Review of Pharmacological Toxicology*, **45**, 269-290.

Colell A., Green D.R. & Ricci J.E. (2009) Novel roles for GAPDH in cell death and carcinogenesis. *Cell Death and Differentiation*, **16**, 1573-1581.

Cruz J.A., Avenson T.J., Kanazawa A., Takizawa K., Edwards G.E. & Kramer D.M. (2005) Plasticity in light reactions of photosynthesis for energy production and photoprotection. *Journal of Experimental Botany*, **56**, 395-406.

Cruz J.A., Sacksteder C.A., Kanazawa A. & Kramer D.M. (2001) Contribution of electric field ($\Delta\psi$) to steady-state transthylakoid proton motive force (*pmf*) *in vitro* and *in vivo*. Control of *pmf* parsing into $\Delta\psi$ and ΔpH by ionic strength. *Biochemistry*, **40**, 1226-1237.

Drenkard E., Richter B.G., Rozen S., Stutius L.M., Angell N.A., Mindrinos M., Cho R.J., Oefner P.J., Davis R.W. & Ausubel F.M. (2000) A Simple Procedure for the Analysis of Single Nucleotide Polymorphisms Facilitates Map-Based Cloning in Arabidopsis. *Plant Physiology*, **124**, 1483-1492.

Edwards G.E. & Walker D.A. (1983) *C_3, C_4:Mechanisms, and Cellular and Environmental Regulation of Photosynthesis.* Blackwell Scientific, Oxford.

Genty B., Briantais J.M. & Baker N.R. (1989) The relationship between the quantum yield of photosynthetic electron transport and quenching of chlorophyll fluorescence. *Biochimica et Biophysica Acta*, **990**, 87-92.

Gotoh E., Matsumoto M., Ogawa K., Kobayashi Y. & Tsyama M. (2009) A qualitative analysis of the regulation of cyclic electron flow around photosystem I form the post-illumination

chlorophyll flyorescence transient in Arabidopsis: a new platform for th in vivo invesigation of the chloroplast redox state. *Photosynthesis Research*, **103**, 111-123.

Hald S., Nandha B., Patrick G. & Johnson G.N. (2008) Feedback regulation of photosynthetic electro transport by NADP(H) redox poise. *Biochimica et Biophysica Acta*, **1777**, 433-440.

Harbinson J. & Foyer C.H. (1991) Relationships between the efficiencies of photosystems I and II and stromal redox state in CO_2-free air : Evidence for cyclic electron flow *in vivo*. *Plant Physiology*, **97**, 41-49.

Heber U. & Walker D. (1992) Concerning a dual function of coupled cyclic electron transport in leaves. *Plant Physiology*, **100**, 1621-1626.

Howard T.P., Metodiev M., Lloyd J.C. & Raines C.A. (2008) Thioredoxin-mediated reversible dissociation of a stromal multiprotein complex in response to changes in light availability. *Proceedings of the National Academy of Sciences*, **105**, 4056-4061.

Jander G., Norris S.R., Rounsley S.D., Bush D.F., Levin I.M. & Last R.L. (2002) Arabidopsis Map-Based Cloning in the Post-Genome Era. *Plant Physiology*, **129**, 440-450.

Jia H., Oguchi R., Hope A.B., Barber J. & Chow W.S. (2008) Differential effects of severe water stress on linear and cyclic electron fluxes through Photosystem I in spinach leaf discs in CO_2-enriched air. *Planta*, **228**, 803-812.

Joët T., Cournac L., Peltier G. & Havaux M. (2002) Cyclic electron flow around photosystem I in C3 plants. *In vivo* control by the redox state of chloroplasts and involvement of the NADH-dehydrogenase complex. *Plant Physiology*, **128**, 760–769.

Joliot P. & Joliot A. (2002) Cyclic electron transfer in plant leaf. *Proceedings of the National Academy of Sciences*, **99**, 10209–10214.

Kanazawa A. & Kramer D.M. (2002) *In vivo* modulation of nonphotochemical exciton quenching (NPQ) by regulation of the chloroplast ATP synthase. *Proceedings of the National Academy of Sciences*, **99**, 12789-12794.

Kiirats O., Cruz J.A., Edwards G.E. & Kramer D.M. (2009) Feedback limitation of phtosynthesis at high CO_2 acts by modulating the activity of the chloroplast ATP synthase. *Functional Plant Biology*, **36**, 893-901.

Kim Y., Schumaker K.S. & Zhu J.-K. (2006) EMS Mutagenesis of Arabidopsis. *Methods in Molecular Biology*, **323**, 101-103.

Knapp A.K. & Carter G.A. (1998) Variability in leaf optical properties amoung 26 species from a broad range of habitats. *American Journal of Botany*, **85**, 940-946.

Kohzuma K., Cruz J.A., Akashi K., Munekage Y., Yokota A. & Kramer D.M. (2008) The long-term responses of the photosynthetic proton circuit to drought. *Plant Cell and the Environment*, **32**, 209-219.

Kramer D.M., Avenson T.J. & Edwards G.E. (2004) Dynamic flexibility in the light reactions of photosynthesis governed by both electron and proton transfer reactions. *Trends in Plant Science*, **9**, 349-357.

Kramer D.M. & Crofts A.R. (1989) Activation of the chloroplast ATPase measured by the electrochromic change in leaves of intact plants. *Biochim Biophys Acta*, **976**, 28-41.

Kramer D.M. & Crofts A.R. (1996) Control of photosynthesis and measurement of photosynthetic reactions in intact plants. In: *Photosynthesis and the Environment* . *Advances in Photosynthesis* (ed N. Baker), pp. 25-66. Kluwer Academic Press, Dordrecht, The Netherlands.

Lascano H.R., Casano L.M., Martin M. & Sabater B. (2003) The activity of the chloroplastic Ndh complex is regulated by phosphorylation of the NDH-F subunit. *Plant Physiology*, **132**, 256-262.

Livingston A.K., Cruz J.A., Kohzuma K., Dhingra A. & Kramer D.M. (2010a) An Arabidopsis mutant with high cyclic electron flow around photosystem I (*hcef*) involving the NDH complex. *Plant Cell*, **22**, 1-13.

Livingston A.K., Kanazawa A., Cruz J.A. & Kramer D.M. (2010b) Regulation of Cyclic Electron Flow in C3 Plants: Differential effects of limiting photosynthesis at Rubisco and Glyceraldehyde-3-phosphate Dehydrogenase. *Plant Cell and the Environment*.

Munekage Y., Hojo M., Meurer J., Endo T., Tasaka M. & Shikanai T. (2002) PGR5 is involved in cyclic electron flow around photosystem I and is essential for photoprotection in Arabidopsis. *Cell*, **110**, 361-371.

Porra R.J., Thompson W.A. & Kriedemann P.E. (1989) Determination of accurate extinction coefficients and simultaneous equations for assaying chlorophylls a and b extracted with four different solvents: verification of the concentration of chlorophyll standards by atomic absorption spectroscopy. *Biochimica et Biophysica Acta*, **975**, 384-394.

Ruuska S., Andrews T., Badger M., Hudson G., Laisk A. & von Caemmerer S. (1998) The interplay between limiting processes in C3 photosynthesis studied by rapid-response gas exchange using transgenic tobacco impaired in photosynthesis. *Australian Journal of Plant Physiology*, **25**, 859-870.

Ruuska S.A., Andrews T.J., Badger M.R., Price G.D. & von Caemmerer S. (2000) The role of chloroplast electron transport and metabolites in modulating rubisco activity in tobacco.

Insights from transgenic plants with reduced amounts of cytochrome *b/f* complex or glyceraldehyde 3-phosphate dehydrogenase. *Plant Physiology*, **122**, 491–504.

Sacksteder C., Kanazawa A., Jacoby M.E. & Kramer D.M. (2000) The proton to electron stoichiometry of steady state photosynthesis in living plants: a proton-pumping Q-cycle is continuously engaged. *Proceedings of the National Academy of Sciences*, **97**, 14283-14288.

Sacksteder C. & Kramer D.M. (2000) Dark-interval relaxation kinetics (DIRK) of absorbance changes as a quantitative probe of steady-state electron transfer. *Photosynthesis Research*, **66**, 145-158.

Scheibe R. (2004) Malate valves to balance cellular energy supply: Redox regulation: from molecular responses to environmental adaptation. *Physiologia Plantarum*, **120**, 21-26.

Shikanai T., Endo T., Hashimoto T., Yamada Y., Asada K. & Yokota A. (1998) Directed disruption of the tobacco ndhB gene impairs cyclic electron flow around photosystem I. *Proceedings of the National Academy of Sciences*, **95**, 9705-9709.

Stitt M., Lilley R., Gerhardt R. & Heldt H. (1989) Metabolite levels in specific cells and subcellular compartments of plant leaves. *Methods Enzymol*, **174**, 518-522.

Strand A., Hurry V., Henkes S., Huner N., Gustafssön P., Gardestrom P. & Stitt M. (1999) Acclimation of Arabidopsis leaves developing at low temperatures. Increasing cytoplasmic volume accompanies increased activities of enzymes in the Calvin Cycle and in sucrose-biosunthesis pathway. *Plant Physiology*, **119**, 1387-1398.

Takizawa K., Kanazawa A. & Kramer D.M. (2008) Depletion of stromal P_i induces high 'energy-dependent' antenna exciton quenching (q_E) by decreasing proton conductivity at CF_O-CF_1 ATP synthase. *Plant, Cell & Environment*, **31**, 235-243.

Tanaka K., Mitsuhashi H., Kondo N. & Sugahara K. (1982) Further evidence for inactivation of fructose-1,6-bisphosphatase at the beginning of SO_2 fumigation. Increase in fructose-1,6-bisphosphate and decrease in fructose-6-phosphate in SO_2-fumigated spinach leaves. *Plant and Cell Physiology*, **23**, 1467-1470.

Zhang H., Whitelegge J.P. & Cramer W.A. (2001) Ferredoxin:NADP+ oxidoreductase is a subunit of the chloroplast cytochrome b_6f complex. *Journal of Biological Chemistry*, **276**, 38159-38165.

Zickermann V., Kerscher S., Zwicker K., Tocilescu M., Radermacher M. & Brandt U. (2009) Architecture of complex I and its implications for electron transfer and proton pumping. *Biochemia Biophysica Acta*, **1787**, 574-583.

Ziyu D., Maurice S.B.K. & Edwards G.E. (2004) Oxygen sensitivity of photosynthesis and photorespiration in different photosynthetic types in the genus Flaveria. *Planta*, **198**, 563-571.

Chapter 4: Regulation of Cyclic Electron Flow around Photosystem I *in vivo* by Hydrogen Peroxide.

Aaron K. Livingston and David M. Kramer

Abstract

Several models have been proposed to account for the regulation of cyclic electron transfer around photosystem I (CEF1), including imbalances in ATP/ADP, NADPH/NADPH, redox state of ferredoxin, phosphorylation of the NAD(P)H:plastoquinone oxidoreductase (NDH) and the reactive oxygen species H_2O_2. Analysis of the *hcef1* mutant of Arabidopsis, which shows high rates of CEF1, also showed highly elevated H_2O_2 levels, supporting the possibility of H_2O_2 in activating CEF1.

In this work we tested the possibility of H_2O_2 regulating CEF1 and determined the relative roles of different CEF1 pathways in H_2O_2-related CEF1. Chloroplast H_2O_2 was increased *in vivo* either by infiltration or by introduction of glycolate oxidase in the chloroplast i.e. the GO mutants introduced by Dr. Maurino (Fahnenstich, Scarpeci, Valle, Flügge & Maurino, 2008). In each case, CEF1 was found to increase substantially. Co-infiltration of lincomycin with H_2O_2 prevented the increase in CEF1, likely indicating that CEF1 induction required chloroplast protein translation. Induction of CEF1 upon infiltration of H_2O_2 occurred after a 60 min lag period and reached full activation in ~105 min. These results imply that *de novo* synthesis of CEF1 complexes is required for full activation of CEF1. Infiltration of H_2O_2 in the *pgr5* mutant resulted in essentially the same extent of CEF1 as in the wild type, indicating that the PGR5 pathway is not involved in H_2O_2-induced CEF1. By contrast, CEF1 was not induced when H_2O_2 was introduced to *crr2-2*, deficient in thylakoid NADPH dehydrogenase

(NDH) complex, suggesting that H_2O_2 induced CEF1 involves the NDH complex. Additionally, the *hcef1*, which was demonstrated to have elevated CEF1, also shows increased H_2O_2 production compared to Columbia wild type. When dark adapted *hcef1* and GO5 plants where illuminated under low oxygen concentrations, CEF1 activity was lost, but was quickly re-activated under 21% O_2, suggesting that pre-synthesized NDH also requires activation by a reactive O_2 species. Consistent with previous *in vitro* work (Casano, Martin & Sabater, 2001), we propose that the formation of the NDH complex is induced by H_2O_2; 2) once formed the NDH complex is activated by H_2O_2; 3) the amount of CEF1 is regulated by the concentration of H_2O_2.

Introduction

Photosynthetic electron transfer in cyanobacteria and chloroplasts follows two distinct pathways, linear electron flow (LEF) and cyclic electron flow around photosystem I (CEF1). The LEF pathway (Mitchell, 1976, Cruz, Sacksteder, Kanazawa & Kramer, 2001) involves two photochemical reaction centers, photosystem I (PSI) and photosystem II (PSII). Electrons are extracted from water at photosystem II (PSII), releasing molecular oxygen, and transferred through an electron transfer chain comprised of a pool of plastoquinone (PQ), the cytochrome b_6f complex (b_6f), plastocyanin and photosystem I (PSI), to NADPH. In addition to storing energy in the $NADPH/NADP^+$ and $H_2O/(O_2 + H^+)$ couples, LEF generates an electrochemical gradient of protons or proton motive force, *pmf*, via the release of protons into the lumen from water oxidation and the transfer of protons during plastoquinone reduction and oxidation. The *pmf* drives the synthesis of ATP at the chloroplast ATP synthase via chemiosmotic coupling (Cruz *et al.*, 2001, Allen, 2002).

Because proton and electron transfer reactions are tightly coupled in LEF, this process produces a fixed output ratio of ATP/NADPH of approximately ~2.6 ATP per 2 NADPH (Sacksteder, Kanazawa, Jacoby & Kramer, 2000, Seelert, Poetsch, Dencher, Engel, Stahlberg & Müller, 2000, Kramer, Avenson & Edwards, 2004). In contrast, the Calvin-Benson Cycle consumes 3 ATP/ 2 NADPH, and even accounting for nitrate assimilation, and photorespiration, the overall consumption ratio should be >2.9 ATP/ 2 NADPH (Noctor & Foyer, 1998, Kramer *et al.*, 2004, Avenson, Kanazawa, Cruz, Takizawa, Ettinger & Kramer, 2005b). In addition, even higher ATP demands may be expected under biotic or abiotic stresses (Kramer *et al.*, 2004). If the rate of ATP/NADPH consumption deviates even by a small amount, reduced electron transfer intermediates will accumulate leading to the generation of toxic reactive oxygen species (Edwards & Walker, 1983, Nixon & Mullineaux, 2001, Avenson *et al.*, 2005b).

Cyclic electron flow around photosystem I (CEF1) has been proposed to account for the expected shortfall in ATP production (Heber & Walker, 1992, Kramer *et al.*, 2004, Livingston, Cruz, Kohzuma, Dhingra & Kramer, 2010a). In CEF1 electrons are transferred from the reducing side of PSI back into the plastoquinone (PQ) pool (Heber & Walker, 1992). The reduced PQ, plastoquinol (PQH_2), transfers its electrons back to PSI through the cytochrome b_6f complex resulting in the translocation of protons into the thylakoid lumen. The CEF1 proton translocation increases *pmf*, which drives the chloroplast ATP synthase producing additional ATP with no net increase in the production of NADPH (reviewed in (Kramer *et al.*, 2004, Eberhard, Finazzi & Wollman, 2008)). The increased *pmf* generated by CEF1 can also enhance photoprotection and down regulation of LEF through acidification of the thylakoid lumen (Heber & Walker, 1992, Kramer *et al.*, 2004, Livingston *et al.*, 2010a).

CEF1 has been found to increase under conditions where additional ATP demand is expected. The increased ATP is necessary to run CO_2 concentrating mechanisms in C_4 plants (Kubicki, Funk, Westhoff & Steinmüller, 1996), green algae (Finazzi, Rappaport, Furia, Fleischmann, Rochaix, Zito & Forti, 2002) and cyanobacteria (Carpentier, Larue & Leblanc, 1984). CEF1 also occurs under stress conditions such as drought (Jia, Oguchi, Hope, Barber & Chow, 2008, Kohzuma, Cruz, Akashi, Munekage, Yokota & Kramer, 2008), high light (Baker & Ort, 1992) or during induction of photosynthesis in dark-adapted plants (Joët, Cournac, Peltier & Havaux, 2002, Joliot & Joliot, 2002). In contrast, CEF1 appears to be minimally engaged in unstressed C_3 plants, possibly because little extra ATP/NADPH is required (Harbinson & Foyer, 1991, Avenson, Cruz, Kanazawa & Kramer, 2005a). Recently, three high CEF1 mutants have been reported, *hcef1*, a point mutation in chloroplast fructose-1,6-bisphosphatase (Livingston *et al.*, 2010a), a chloroplast fructose bisphosphate aldolase mutant (Gotoh, Matsumoto, Ogawa, Kobayashi & Tsyama, 2009) and a GAPDH antisense tobacco mutant, gapR (Livingston, Kanazawa, Cruz & Kramer, 2010b). It was hypothesized that these mutants have either elevated ATP demand or "inadvertent" activation of the CEF1 pathway (Livingston *et al.*, 2010a, Livingston *et al.*, 2010b).

Three major pathways have been proposed for a key step in CEF1, the transfer of electrons back into the PQ pool: 1) via an antimycin A (AA)-sensitive ferredoxin-PQ oxidoreductase (FQR) (Bendall & Manasse, 1995) inhibited in the *pgr5* mutant (Munekage, Hojo, Meurer, Endo, Tasaka & Shikanai, 2002); 2) via the Q_i site of the cytochrome b_6f complex (Bendall & Manasse, 1995); and 3) through a thylakoid NADPH dehydrogenase complex (NDH) (Endo, Shikanai, Sato & Asada, 1998). Recent work on the high CEF1 mutant, *hcef1,* supports the participation of the NDH pathway in Arabidopsis (Livingston *et al.*, 2010a). The *hcef1*

mutant showed a dramatic increase in NDH protein levels, but a decrease in PGR5 expression, compared to wild-type (Livingston *et al.*, 2010a). When *hcef1* (Livingston *et al.*, 2010a), and another high cyclic mutant, fructose bisphosphate aldolase (Gotoh *et al.*, 2009), where crossed with a NDH knockout, *crr2-2,* both showed almost a complete loss of CEF1 function and strong suppression of photosynthesis. In addition, C_4 plants show strong correlation between the amount of CEF1 and the expression level of NDH, but not the expression level of PGR5 (Sazanov, Burrows & Nixon, 1996, Quiles, 2005).

If, as expected, CEF1 acts to balance ATP/NADPH output ratios, it must be very well regulated to prevent ATP excess or deficit (Kramer *et al.*, 2004, Avenson *et al.*, 2005a). Several CEF1 regulatory processes have been proposed, including sensing of ATP/ADP ratios (Joliot & Joliot, 2002), regulation via the redox status of NAD(P)H or ferredoxin (Fd) (Breyton, Nandha, Johnson, Joliot & Finazzi, 2006), various Calvin-Benson cycle intermediates (Fan, Nie, Hope, Hillier, Pogson & Chow), and the reactive oxygen species H_2O_2 (Lascano, Casano, Martin & Sabater, 2003, Gambarova, 2008). Metabolic analyses of *Arabidopsis* and tobacco high CEF1 mutants argued against ATP/ADP, NADPH/$NADP^+$ or major Calvin Cycle intermediate pools as major regulators of CEF1 (Livingston *et al.*, 2010b). In this work we use *in vivo* spectroscopy to assay the initiation of CEF1 in the presence of elevated H_2O_2 to test whether this reactive oxygen species could be the regulator of CEF1.

Materials and Methods

Plant Material and Growth Conditions.

Arabidopsis mutants expressing varying levels of glycolate oxidase in the chloroplast, termed GO mutants (Fahnenstich *et al.*, 2008), were obtained from Dr. Verónica Maurino (Botanisches Institut Universität zu Köln). All plants, Columbia wild-type (col), the GO mutants,

pgr5, crr2-2 and *hcef1* were grown on soil under growth chamber conditions with 16 hr light (~80 μmol m^{-2} sec^{-1} intensity): 8 hr dark photoperiod, and 22°C/18°C (day/night) cycle.

In vivo Spectroscopic Assays.

All measurements were made using intact ~25-30 day old *Arabidopsis,* dark adapted for 10 hours, and was measured using actinic lights between 50-180 μmol photon m^{-2} s^{-1}. We measured chlorophyll *a* fluorescence yield changes and light induced absorbance changes on a non-focusing optics spectrophotometer/fluorimeter (NoFOSpec), described in (Livingston *et al.*, 2010a). Chlorophyll *a* fluorescence yield was collected under saturating light levels ($F_{M'}$) and photosynthetic steady state conditions (F_s) (Kanazawa & Kramer, 2002, Avenson, Cruz & Kramer, 2004), from which photochemical yield of photosystem II (ϕ_{II}) and LEF are calculated (Genty, Briantais & Baker, 1989).

Dark interval relaxation kinetics (Hannah, Wiese, Freund, Fiehn, Heyer & Hincha) of absorbance changes at 520 nm, which is attributable to the electrochromic shift (ECS) and proportional to the transthylakoid electric field, was used to estimate the light-induced, steady-state *pmf* (Sacksteder & Kramer, 2000, Cruz, Avenson, Kanazawa, Takizawa, Edwards & Kramer, 2005). To account for the appearance of interfering signals, key experiments were repeated using ECS signals deconvoluted using absorption kinetics taken at three wavelengths (505, 520 and 535 nm) as described in (Sacksteder *et al.*, 2000, Sacksteder & Kramer, 2000), with similar results. As described in detail previously (Kramer & Crofts, 1996, Sacksteder & Kramer, 2000, Cruz *et al.*, 2005), the total amplitude of the ECS signal, ECS_t, was taken to be proportional to the relative extent of light-induced *pmf* and conductivity proton flux through the thylakoid membrane, g_H^+, was taken to be proportional to the inverse of the time constant of ECS decay (τ_{ECS}). Relative steady state proton fluxes across the thylakoid membrane (v_H^+) were

estimated from the initial slopes of the ECS decay (Avenson *et al.*, 2005a, Takizawa, Kanazawa & Kramer, 2008). The ECS measurements were normalized for variations in leaf thickness and pigmentation by the extent of the rapid rise single-turnover flash induced ECS (Avenson *et al.*, 2005b).

LEF, with no contributions from CEF1, should produce a constant ratio of proton flux to electron transfer through PSII of 3 H^+/e^- (Sacksteder *et al.*, 2000), which in our measurements should be reflected as a constant slope of v_H^+ plotted against LEF. We use as a standard leaves infiltrated with methyl viologen (MV), which should prevent CEF1 by diverting electrons from the PQ reductase to O_2, leading to pure LEF (Livingston *et al.*, 2010a). Activation of CEF1 can be estimated by the increase in v_H^+ above that which can be attributed to LEF alone. Estimates of CEF/LEF were obtained as described in (Livingston *et al.*, 2010b), by comparing the rates of LEF through PSII by chlorophyll fluorescence analysis, with light-driven proton flux estimated by the initial rate of decay of the electrochromic shift (ECS) signal. The ratio of CEF/LEF was calculated by:

$$CEF/LEF = ((v_H^+/LEF) - (v_H^+{}_{MV}/LEF_{MV}))/ (v_H^+{}_{MV}/LEF_{MV}) \quad (1)$$

where v_H^+ and $v_H^+{}_{MV}$ were the relative measured proton fluxes in the absence and presence of MV and LEF and LEF_{MV} were the measured LEF values in the absence and presence of MV (no CEF1).

Infiltration of methyl viologen and hydrogen peroxide into leaves.

Where indicated, leaves were incubated for 60 minutes at low light (5~15 μmol photon m^{-2} s^{-1}) between two layers of tissue paper (Kimwipe, Kimberly-Clark, Mississauga, Ontario) and saturated with either distilled water or a solution of 100 μM methyl viologen (Livingston *et al.*, 2010a). Excess liquid was removed from the leaf material, before experimentation by gently blotting with a fresh Kimwipe.

Where indicated Columbia wild-type leaves were detached and placed between two layers of tissue paper and saturated with distilled water or a percentage of hydrogen peroxide for 120 minutes. Where indicated leaves were also saturated with 100 μg/ml of lincomycin, along with water or a set hydrogen peroxide concentration.

Measurement of hydrogen peroxide production in leaves

Hydrogen peroxide was detected by 3,3' diaminobenzidine (DAB) staining, as described in (Fahnenstich *et al.*, 2008). Full leaves were wrapped in a Kimwipe tissue paper, soaked with 1 mg mL^{-1} DAB in distilled water, and left 1 hour in the dark to facilitate uptake. The leaves were placed on top of the DAB soaked Kimwipes and either illuminated with ~90 μmol m^{-2} sec^{-1} of light for 50 minutes or subjected to varying concentrations of H_2O_2 with ~15 μmol m^{-2} sec^{-1} of light for 2 hours. Pigments where then removed from the leaf by boiling in 95% ethanol.

Results

Hydrogen peroxide concentration of high CEF1 mutant, hcef1.

Relative extents of H_2O_2 accumulation in the perviously described high CEF1 mutant was *hcef1* (Livingston *et al.*, 2010a) was tested by DAB staining. Compared to Columbia wild-type (Fig. 1A), the mutant *hcef1* (Fig. 1B) showed a high total leaf increase in H_2O_2.

H_2O_2 concentration induction and regulation of CEF1

Figure 2 shows that infiltration of leaves with a range of concentrations of H_2O_2 induced varying levels of CEF1. In the absence of H_2O_2, there was little to no CEF1. However, infiltration of Col infiltrated with 0.001%, 0.01% and 0.1% H_2O_2 induced CEF/LEF of 21%, 42% and 68% of the water-infiltrated control. The increases in CEF/LEF were inhibited when leaves were co-infiltrated with H_2O_2 and lincomycin, which inhibits protein synthesis. In fact a small apparent decrease in CEF/LEF of about 10% of proton flux compared to LEF was measured perhaps reflecting a inhibition of CEF1, similar to that reported for the *pgr5* mutant using the same assays (Avenson *et al.*, 2005a). Parallel DAB staining assays were performed to confirm that H_2O_2 levels in leaves were altered by addition of H_2O_2 and that addition of lincomycin did not alter these levels (data not shown).

H_2O_2 increases in the chloroplast induces CEF1

Addition of H_2O_2 to whole leaves will probably preferentially affect processes outside of the chloroplast. We thus aimed to test our results by adjusting H_2O_2 production in the chloroplast, taking advantage of a series of mutants produced in the Maurino laboratory that express peroxisomal glycolate oxidase (GO) in the chloroplast (GO5, GO16, and GO20) and consequently accumulate varying amounts of H_2O_2 (Fahnenstich *et al.*, 2008).

The GO5 mutant, which shows approximately 35% of the peroxisomal GO activity in the chloroplast (Fahnenstich *et al.*, 2008), displayed an ~90% increase in the slope between v_H^+ and LEF compared to Col (Fig. 3A), indicating a large induction of proton flux that could not be attributable to LEF. Infiltration of MV into GO5 leaves (Fig. 2A) resulted in a v_H^+ versus LEF

slope that was indistinguishable from Col (ANCOVA P>0.05), indicating that the observed increase in v_H^+ could be attributed to induction of CEF1.

The mutants GO16 (Fig. 3B) and GO20 (Fig. 3C) mutants, which show 20% and 30% of peroxisomal GO expressed in chloroplasts (Fahnenstich *et al.*, 2008), displayed 39% and 46% increases in proton translocation compared to Col. As with GO5, infiltration of MV inhibited the observed increase in v_H^+ (Figs. 1B and 1C, ANCOVA P>0.05).

Hydrogen peroxide concentrations.

Relative extents of H_2O_2 accumulation in the GO mutants were assayed using DAB staining. As expected, staining was nearly undetectable with Col (Fig. 4A), but consistent with (Fahnenstich *et al.*, 2008), the GO mutants showed obvious, but variable staining (Fig. 4B, 4C and 4D). GO5, showing the highest GO expression (Fahnenstich *et al.*, 2008), was stained uniformly (Fig. 4B), whereas the mutants GO16 (Fig. 4C) and GO20 (Fig. 4D) showed patchy staining, consistent with their previously reported phenotypes (Fahnenstich *et al.*, 2008).

Additionally the pervious described high CEF1 mutants was tested for increased H_2O_2, *hcef1* (Livingston *et al.*, 2010a). The mutant *hcef1* (Fig. 3E) showed a high total leaf increase in H_2O_2, similar to that seen in GO5 (Fig. 2B).

The effect of CO_2 and O_2 levels on CEF1.

We next explored the effects of altered O_2 and CO_2 on induction of CEF1. Lowering the O_2 concentration from 20% to 1% should reduce the rate of H_2O_2 production, but also lower photorespiration. To distinguish between these effects, we also assayed the effects of increased the CO_2 level to 2000 ppm at 21% O_2, which should decrease photorespiration but not directly

affect H_2O_2 production. Col (Fig. 5A) showed no proton translocation attributable to CEF1, under ambient air, high CO_2 or 1% O_2, in agreement with previous results (Avenson *et al.*, 2005a). In contrast, *hcef1* (Fig. 5A) showed a large (~2.5 fold) excess of v_H^+/LEF compared to Col under ambient air, indicating a large induction of CEF1, as previously seen for this mutant (Livingston *et al.*, 2010a). Increasing CO_2 concentration to 2000 ppm did not substantially alter the relationship between v_H^+ versus LEF (Fig. 5A), indicating that CEF1 was not sensitive to changes in photorespiration. Placing *hcef1* under low O_2 it resulted in a decrease of v_H^+ versus LEF, essentially blocking the excess proton flux attributed to CEF1, indicating that CEF1 is sensitive to O_2 levels.

These experiments were repeated with the GO5 mutant, which also shows a large increase in CEF1 as evidenced by excess v_H^+ compared to LEF (Fig. 3A). As with *hcef1*, increasing CO_2 levels to 2000 ppm did not significantly decrease CEF1 in GO5 (Fig. 5B). Lowering O_2 to 1% resulted in a partial (~60%) reduction in v_H^+ versus LEF in GO5 compared to ambient air, resulting in a slope about 30% higher than that seen in Col. We conclude that CEF1 in GO5 was also sensitive to O_2 levels, as seen *hcef1*.

Kinetics of CEF1 induction by H_2O_2.

Figure 6 shows that upon infiltration of Col leaves with 0.1% H_2O_2, CEF1 induction started after a lag of ~60 minutes. A maximum CEF/LEF, of ~67%, was reached after ~105 minutes. The increase in CEF/LEF over the time course was not seen when the leaves where soaked in water or in 0.1% H_2O_2 + lincomycin.

The effect of H_2O_2 on CEF1 knockout mutants.

When the *pgr5* mutant, deficient in the antimycin A-sensitive (PGR5-dependent) CEF1 pathway, was infiltrated with 0.1% H_2O_2 for 2 hours, CEF/LEF was induced to ~65% of control levels, similar to that seen in Col (Fig. 7), indicating that loss of PGR5 did not hinder induction of CEF1. On the other hand, infiltration with 0.1% H_2O_2 of *crr2-2*, which is deficient in NDH activity (Hashimoto, Endo, Peltier, Tasaka & Shikanai, 2003), failed to induce increased CEF/LEF (Fig. 7), indicating that CEF1 induction by H_2O_2 requires NDH.

Discussion

CEF1 is induced by hydrogen peroxide.

There is increasing evidence that reactive oxygen species play an important role in intracellular signaling, particularly in response to biotic and abiotic stress (Bowler & Fluhr, 2000, Foreman, Demidchik, Bothwell, Mylona, Miedema, Torres, Linstead, Costa, Brownlee & Jones, 2003, Laloi, Apel & Danon, 2004), controlling transcription (Quinn, Findlay, Dawson, Jones, Morgan & Toone, 2002) and enzyme activation (Casano *et al.*, 2001). Several lines of evidence suggest that H_2O_2 may play a role in activation of CEF1. Micro array data shows that incubation with H_2O_2 causes a strong induction of nuclear genes encoding NDH subunits in *Arabidopsis* (Vandenbroucke, Robbens, Vandepoele, Inzé, Van de Peer & Van Breusegem, 2008). Treatment with H_2O_2 also induces the formation of the NDH complex (Casano *et al.*, 2001) and activates the NDH complex *in vitro* (Lascano *et al.*, 2003).

Using a series of new spectroscopic and genetics tools, we aimed to test whether CEF1 is activated by H_2O_2 *in vivo* and if so, by which pathway. We first showed that our recently reported *hcef1* mutant (Livingston *et al.*, 2010a) also shows elevated H_2O_2 production (Fig. 1B), consistent with a role for the ROS in triggering CEF1.

We next tested whether H_2O_2 infiltration itself would trigger CEF1. Infiltration of leaves with varying concentration of H_2O_2 does indeed induce CEF1 as measured by our proton flux assays (Fig. 2). To test whether similar effects were observed when H_2O_2 was produced in the chloroplast, we used as series of mutants produced by Dr. Maurino with glycolate oxidase expressed in the chloroplast, producing varying amounts of H_2O_2 (Fahnenstich *et al.*, 2008). We demonstrated that the increased levels of H_2O_2 in the GO mutants (Fig. 4) were accompanied by elevated and proton pumping associated with CEF1 (Fig. 3).

Is the extent of CEF1 controlled by the concentration hydrogen peroxide?

The extent of CEF1 induction in wild type Arabidopsis leaves depended strongly on the concentration of H_2O_2 infiltrated in the leaf (Fig. 2). Soaking wild-type plants with a high concentration of H_2O_2 (0.1%) induced a high increase in CEF1 activity (~68%), whereas lesser concentrations (0.01% and 0.001%) produced lower levels of CEF1 induction (~42% and 21% respectively) (Figure 2). It was not possible to ascertain the local chloroplast H_2O_2 concentrations under these conditions due to the high activities of H_2O_2 detoxifying systems in the leaf. We thus repeated this type of analysis using a series of GO mutants with varying H_2O_2 production levels. The GO mutants also showed a strong relationship between GO activity (Fahnenstich *et al.*, 2008), H_2O_2 production (Fig. 4), and induction of CEF1 (Fig. 3). Overall, these data are consistent with incremental activation of CEF1 by H_2O_2.However, the DAB staining for the GO mutants showed varying levels of patchiness (Figs. 4 B, C D), suggesting that there are sectors of higher and lower local H_2O_2 concentrations. Since ECS assays and LEF assays average data over an approximately 0.5 cm^2 leaf area, the effects of this patchiness would also be averaged, perhaps leading to apparent rather than real incremental control. In other

words, the presence of H_2O_2 could lead to an all-or-none induction of CEF1. On the other hand, the DAB staining, indicating CO_2 concentration, and the related level of increased in CEF1 were correlated in the H_2O_2 infiltration studies (Fig. 2), the GO mutants (Fig. 3, 4) and the *hcef1* mutant (Fig. 1, 5A). This leads us to propose that the observed regulation of CEF1 by the concentration of H_2O_2 is probably physiologically relevant, at least in the mutants and conditions explored here.

O_2 is involved in CEF1 activation.

To further test if H_2O_2 is the trigger for CEF1, we determined whether O_2, the substrate for H_2O_2 production, was required. When dark-adapted *hcef1* (Fig. 5A) and GO5 (Fig. 5B) were subjected to ambient air with 21% O_2, CEF1 was quickly activated. Neither *hcef1* (Fig. 5A) or GO5 (Fig. 5B) showed a significant change in the rate of CEF1 when CO_2 was increased to 2000 ppm with 21% O_2 which should decrease photorespiration but leave H_2O_2 production unchanged.

Furthermore, when dark-adapted *hcef1* (Fig. 5A) and GO5 (Fig. 5B) plants where illuminated under low oxygen concentrations there was almost a complete loss of CEF1 activity. In GO5 (Fig. 5B), there was only a loss of ~60% of the activity of CEF1 under 1% oxygen, but this is most likely because glycolate oxidase has a low Km (200 μm) for oxygen (Macheroux, Kleweg, Massey, Söderlind, Stenberg & Lindqvist, 1993) and so GO5 is able to maintain some activity. Wild-type Columbia showed no change in proton flux associated with CEF1 under any condition, high CO_2, ambient air, or low O_2. Overall this suggests that CEF1 can be quickly activated based on the production of H_2O_2, if the CEF1 mechanism is in place.

Activation of CEF1 proceeds after a distinct time lag and requires de novo protein synthesis.

In Figure 2, a wild-type leaf subjected to 0.1% hydrogen peroxide and lincomycin, which inhibits protein synthesis, showed no increase in CEF1. This suggests that H_2O_2 causes formation of a protein or protein complex necessary for CEF1 activity.

Additionally, when we plot a time course of CEF1 induction under 0.1% hydrogen peroxide, we found that it takes ~60 minutes to begin CEF1 induction and 105 minutes to achieve maximum activity (Fig. 6). When we plot the time course with just water or with H_2O_2 plus the protein translation inhibitor lincomycin, there is no induction of CEF1 (Fig. 6). This suggests that hydrogen peroxide induced CEF1 requires both *de novo* protein synthesis and a distinct time lag.

H_2O_2-induced CEF1 involves the NDH complex but does not require the PGR5 protein

When *pgr5*, a mutant deficient in the antimycin A sensitive ferredoxin quinone reductase (AA-FQR) pathway of CEF1, was subject to H_2O_2, CEF1 increased to a level similar to wild-type under H_2O_2 (Figure 7). Suggesting that H_2O_2 does not induce AA-FQR mediated CEF1. However, when a knockout of the NDH complex, *crr2-2*, was subject to H_2O_2, CEF1 was not induced (Fig. 7). This data suggests that H_2O_2 induces NDH dependent CEF1. Overall our findings are inline with previous studies which suggest that the NDH complex is both induced and activated by H_2O_2 (Casano *et al.*, 2001, Lascano *et al.*, 2003) and the NDH complex is the main pathway for CEF1 (Livingston *et al.*, 2010a).

Conclusion

In these experiments, we show that hydrogen peroxide likely induces the formation of the NDH complex for CEF1 in *Arabidopsis*. CEF1 activity is proposed to be activated and regulated

by the concentration of hydrogen peroxide. This discovery now gives a method to study plants with an inducible increase in CEF1 and an up-regulation of NDH complex. Overall this research brings us closer to understanding the role and regulation of CEF1.

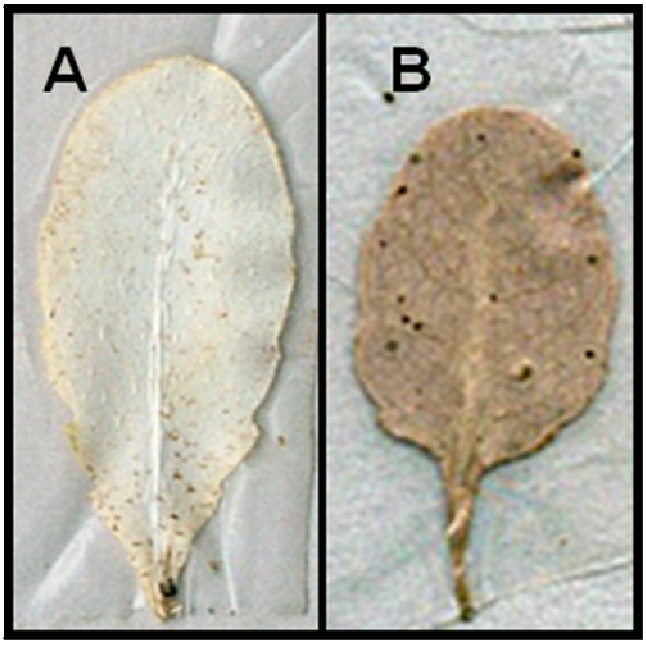

Figure 1. Hydrogen Peroxide production in Columbia wild-type and *hcef1*.

DAB staining was accomplished on **(A)** Columbia wild-type, **(B)** *hcef1*.

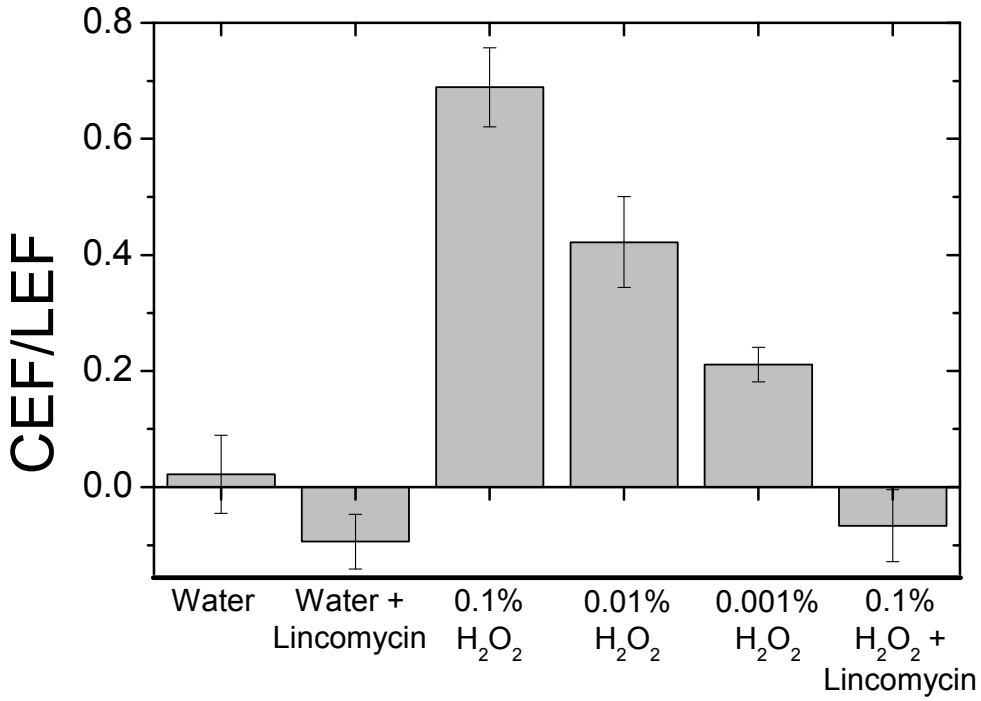

Figure 2. Hydrogen peroxide concentration on CEF/LEF Levels.

Calculated CEF/LEF for Columbia Wild-type under a variety of H_2O_2 concentrations and +/- lincomycin. Each data point represents calculated CEF/LEF from three separate experimental sets for each condition. Error bars represent standard deviation of the average of the three fits.

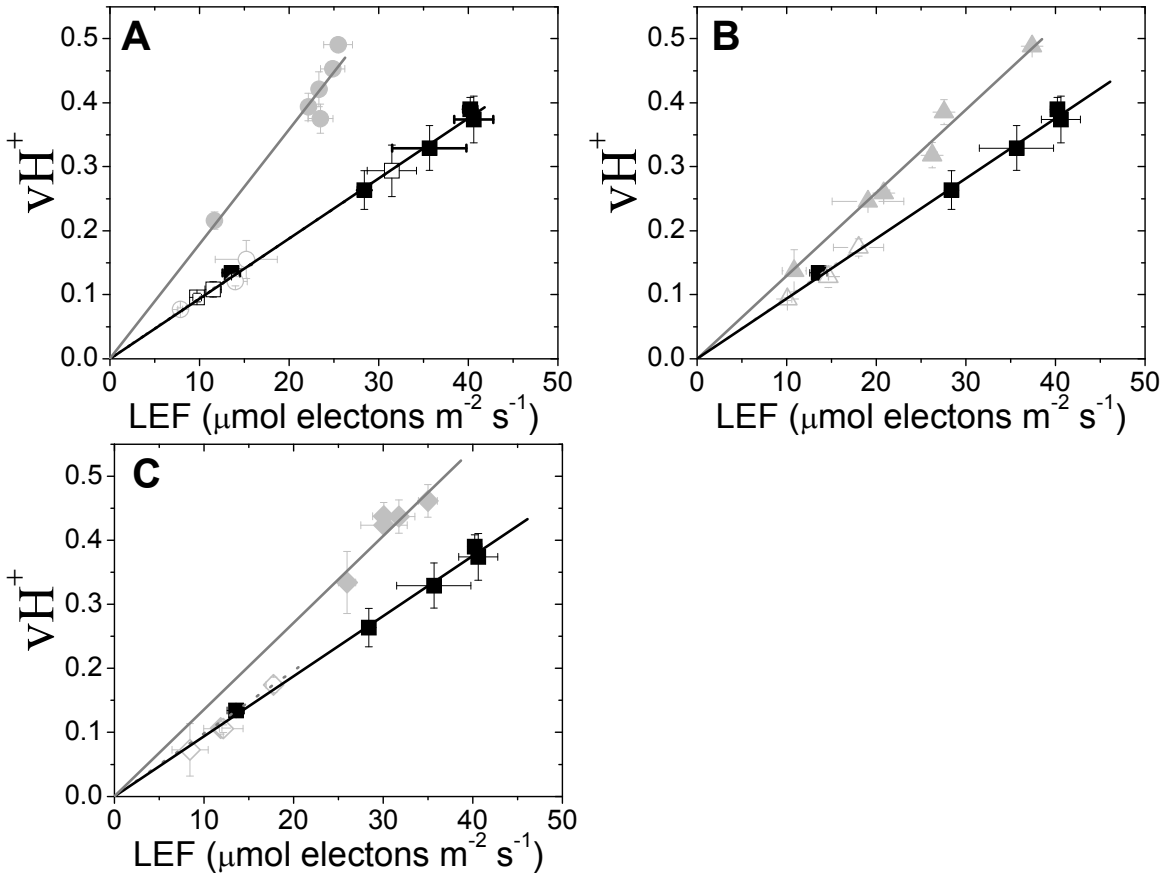

Figure 3. The GO mutants and CEF1. The relationships between light-driven proton translocation across the thylakoid (v_H^+) and linear electron flow (LEF) were assessed in leaves of Col (■□) and the GO mutants. All data indicated by the filled symbols was obtained on leaves infiltrated with distilled water, open symbols represent methyl violgen. The data for Col is reproduced in all panels. **(A)** GO5 (●○); **(B)** *GO16* (▲△); and (**C)** GO20 (◆◇). For all linear fits $P < 0.05$. Error bars represent standard deviation, with n=3.

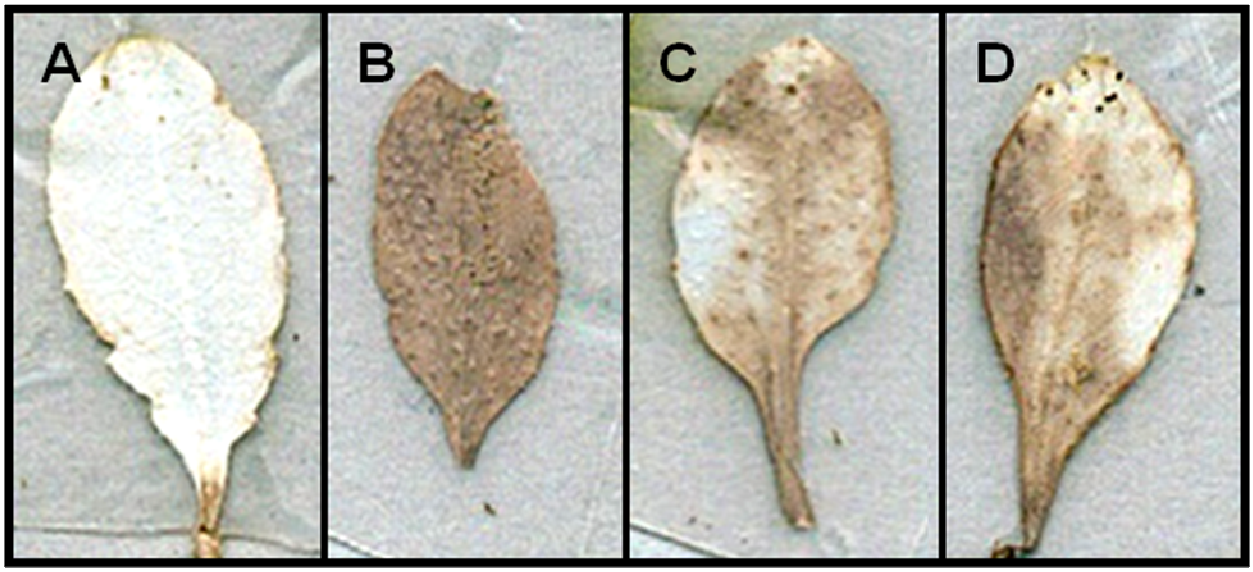

Figure 4. Hydrogen Peroxide production in GO5, GO16, and GO20.

DAB staining was accomplished on **(A)** Columbia wild-type, **(B)** GO5, **(C)** GO16, and **(D)** GO20.

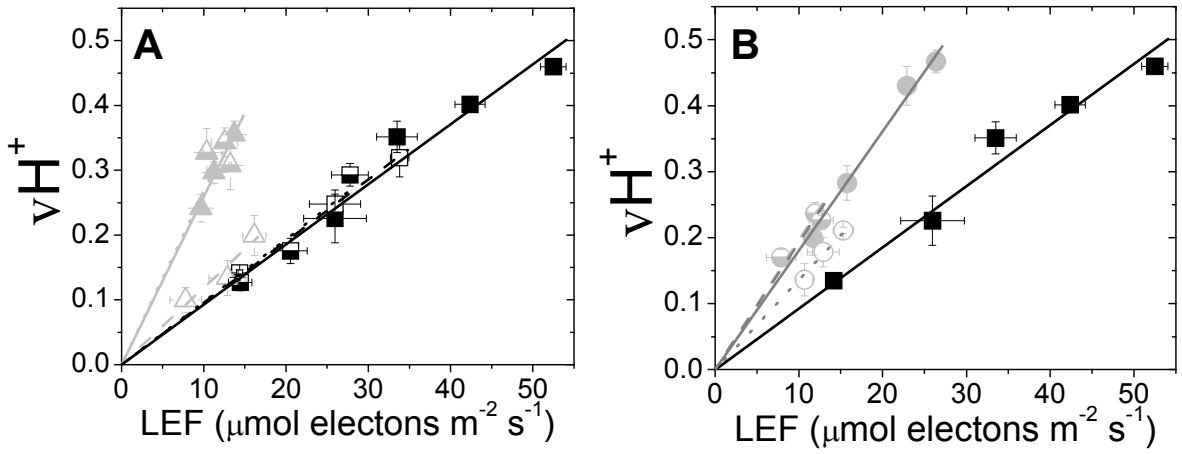

Figure 5. Gas concentration studies on *hcef1* and GO5.

The relationship between light-driven proton translocation across the thylakoid (v_{H^+}) and linear electron flow (LEF) under various gas conditions was probed. All data indicated by the filled symbols was obtained under ambient air, the half-filled symbols represents 2000 ppm CO_2 and the open symbols represent 1% oxygen. Col (■) is the same in **(A)** and **(B). (A)** *hcef1* (▲); **(B)** GO5 (●). For all linear fits $P < 0.05$. Error bars represent standard deviation, with *n*=3.

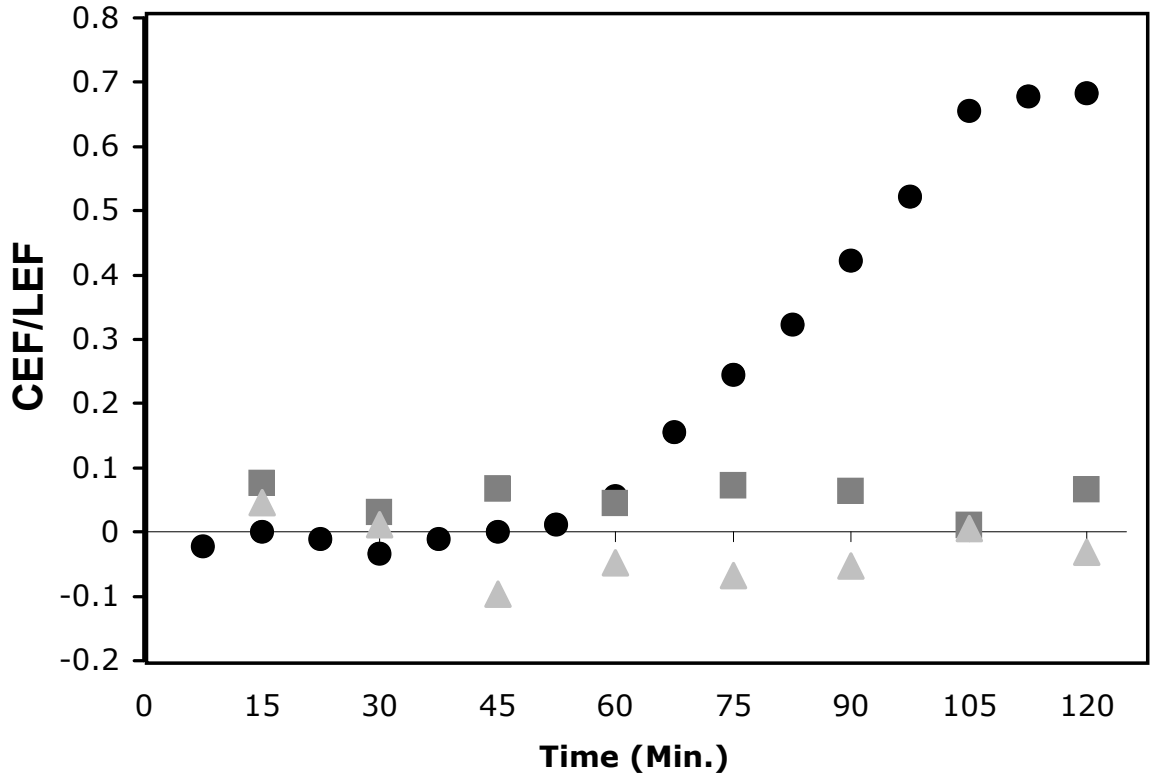

Figure 6. Time course of CEF/LEF for Columbia leaves exposed to 0.1% H_2O_2.

Each data point represents CEF/LEF Col with H_2O(■) , Col with 0.1 % H_2O_2 (●), or Col with 0.1 % H_2O_2 + lincomyocin (▲).

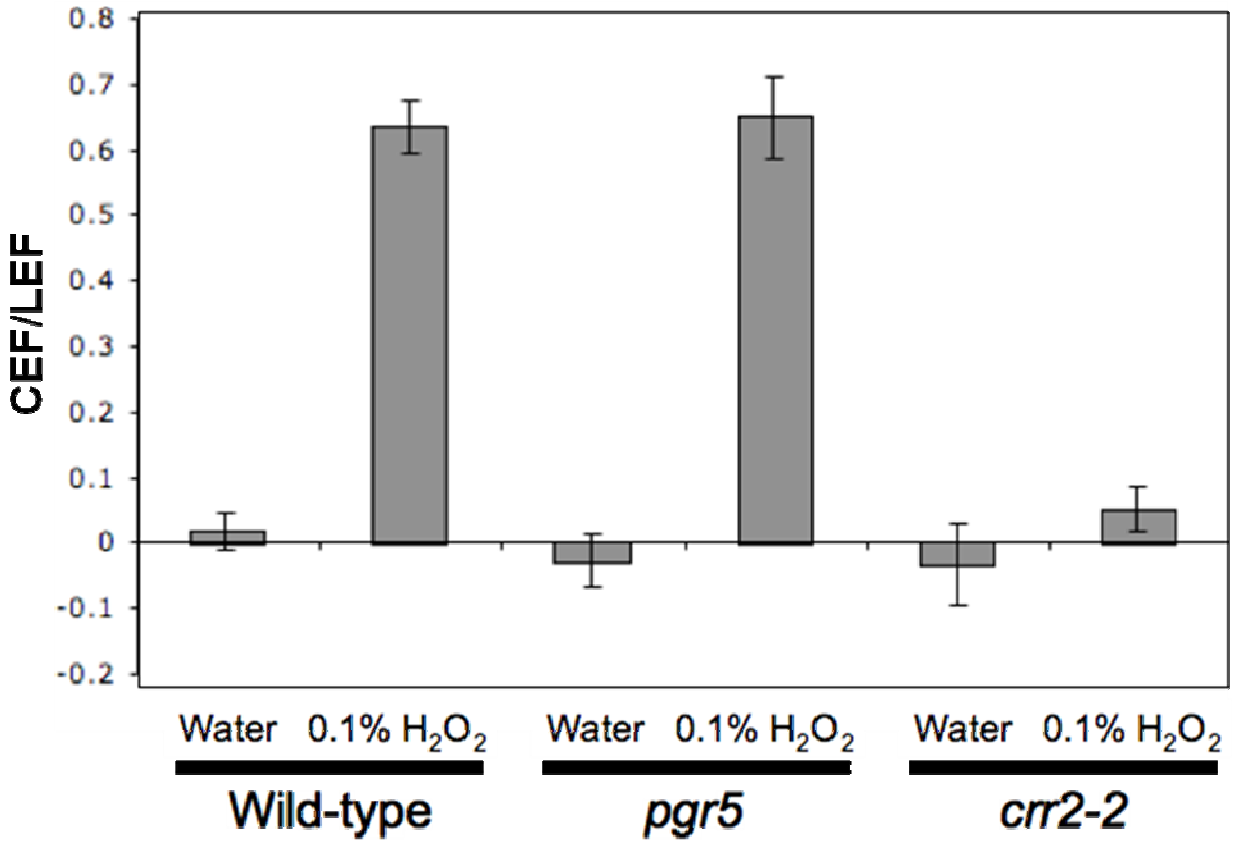

Figure 7. Cyclic mutants *pgr5* and *crr2-2* exposure to H_2O_2.

Each data point represents calculated CEF/LEF from three separate experimental sets for each condition. Error bars represent standard deviation.

References

Allen J.F. (2002) Photosynthesis of ATP- electrons, proton pumps, rotors, and poise. *Cell*, **110**, 273-276.

Avenson T.J., Cruz J.A., Kanazawa A. & Kramer D.M. (2005a) Regulating the proton budget of higher plant photosynthesis. *Proceedings of the National Academy of Sciences*, **102**, 9709–9713.

Avenson T.J., Cruz J.A. & Kramer D.M. (2004) Modulation of energy dependent quenching of excitons (q_E) in antenna of higher plants. *Proceedings of the National Academy of Sciences*, **101**, 5530-5535.

Avenson T.J., Kanazawa A., Cruz J.A., Takizawa K., Ettinger W.E. & Kramer D.M. (2005b) Integrating the proton circuit into photosynthesis: progress and challenges. *Plant, Cell and the Environment*, **28**, 97-109.

Baker N.R. & Ort D.R. (1992) Light and crop photosynthetic performance. *In Crop Photosynthesis: Spatial and Temporal Determinants (eds N.R. Baker & H. Thomas)*, **Elsevier Science Publishers, Amsterdam, the Netherlands**, 289-312.

Bendall D.S. & Manasse R.S. (1995) Cyclic photophosphorylation and electron transport. *Biochemia Biophysica Acta*, **1229**, 23-38.

Bowler C. & Fluhr B. (2000) The role of calcium and activated oxygens as signals for controlling cross-tolerance. *Trends in Plant Science*, **5**, 241-246.

Breyton C., Nandha B., Johnson G., Joliot P. & Finazzi G. (2006) Redox modulation of cyclic electron flow around Photosystem I in C3 plants. *Biochemistry*, **45**, 13465-13475.

Carpentier R., Larue B. & Leblanc R.M. (1984) Photoacoustic spectroscopy of Anacystis nidulans : III. Detection of photosynthetic activities. *Archives of Biochemistry and Biophysics*, **228**, 534-543.

Casano L.M., Martin M. & Sabater B. (2001) Hydrogen peroxide mediates the induction of chloroplastic Ndh complex under photooxidative stress in barley. *Plant Physiology*, **125**, 1450-1458.

Cruz J.A., Avenson T.J., Kanazawa A., Takizawa K., Edwards G.E. & Kramer D.M. (2005) Plasticity in light reactions of photosynthesis for energy production and photoprotection. *Journal of Experimental Botany*, **56**, 395-406.

Cruz J.A., Sacksteder C.A., Kanazawa A. & Kramer D.M. (2001) Contribution of electric field ($\Delta\psi$) to steady-state transthylakoid proton motive force (*pmf*) *in vitro* and *in vivo*. Control of *pmf* parsing into $\Delta\psi$ and ΔpH by ionic strength. *Biochemistry*, **40**, 1226-1237.

Eberhard S., Finazzi G. & Wollman F.-A. (2008) The Dynamics of Photosynthesis. *Annual Review of Genetics*, **42**, 463-515.

Edwards G.E. & Walker D.A. (1983) *C_3, C_4:Mechanisms, and Cellular and Environmental Regulation of Photosynthesis.* Blackwell Scientific, Oxford.

Endo T., Shikanai T., Sato F. & Asada K. (1998) NAD(P)H dehydrogenase dependet, antimycin A-sensitive electron donation to plastoquinone in tobacco chloroplasts. *Plant and Cell Physiology*, **39**, 1226-1231.

Fahnenstich H., Scarpeci T.E., Valle E.M., Flügge U.-I. & Maurino V.G. (2008) Generation of hydrogen peroxide in chloroplasts of Arabidopsis overexpressing glycolate oxidase as an inducible system to study oxidative stress. *Plant Physiology*, **148**, 719-729.

Fan D.-Y., Nie Q., Hope A.B., Hillier W., Pogson B.J. & Chow W.S. (2007) Quantification of cyclic electron flow around Photosystem I in spinach leaves during photosynthetic induction. *Photosynthesis Research*, **94**, 347-357.

Finazzi G., Rappaport F., Furia A., Fleischmann M., Rochaix J.D., Zito F. & Forti G. (2002) Involvement of state transitions in the switch between linear and cyclic electron flow in *Chlamydomonas reinhardtii*. *European Molecular Biology Organization*, **3**, 280–285.

Foreman J., Demidchik V., Bothwell J.H., Mylona P., Miedema H., Torres M.A., Linstead P., Costa S., Brownlee C. & Jones J.D. (2003) Reactive oxygen speceis produced by NADPH oxidase regulate plant cell growth. *Nature*, **422**, 442-446.

Gambarova N.G. (2008) Activity of photochemical reactions and accumulation of hydrogen peroxide in chloroplasts under stress conditions. *Russian Agricultural Sciences*, **34**, 149-151.

Genty B., Briantais J.M. & Baker N.R. (1989) The relationship between the quantum yield of photosynthetic electron transport and quenching of chlorophyll fluorescence. *Biochimica et Biophysica Acta*, **990**, 87-92.

Gotoh E., Matsumoto M., Ogawa K., Kobayashi Y. & Tsyama M. (2009) A qualitative analysis of the regulation of cyclic electron flow around photosystem I form the post-illumination chlorophyll flyorescence transient in Arabidopsis: a new platform for th in vivo invesigation of the chloroplast redox state. *Photosynthesis Research*, **103**, 111-123.

Hannah M.A., Wiese D., Freund S., Fiehn O., Heyer A.G. & Hincha D. (2006) Natural Genetic Variation of Freezing Tolerance in Arabidopsis. *Plant Physiology*, **142**, 98-112.

Harbinson J. & Foyer C.H. (1991) Relationships between the efficiencies of photosystems I and II and stromal redox state in CO_2-free air : Evidence for cyclic electron flow *in vivo*. *Plant Physiology*, **97**, 41-49.

Hashimoto M., Endo T., Peltier G., Tasaka M. & Shikanai T. (2003) A nucleus-encoded factor, CRR2, is essential for the expression of chloroplast ndhB in *Arabidopsis. Plant Journal*, **36**, 541-549.

Heber U. & Walker D. (1992) Concerning a dual function of coupled cyclic electron transport in leaves. *Plant Physiology*, **100**, 1621-1626.

Jia H., Oguchi R., Hope A.B., Barber J. & Chow W.S. (2008) Differential effects of severe water stress on linear and cyclic electron fluxes through Photosystem I in spinach leaf discs in CO_2-enriched air. *Planta*, **228**, 803-812.

Joët T., Cournac L., Peltier G. & Havaux M. (2002) Cyclic electron flow around photosystem I in C3 plants. *In vivo* control by the redox state of chloroplasts and involvement of the NADH-dehydrogenase complex. *Plant Physiology*, **128**, 760–769.

Joliot P. & Joliot A. (2002) Cyclic electron transfer in plant leaf. *Proceedings of the National Academy of Sciences*, **99**, 10209–10214.

Kanazawa A. & Kramer D.M. (2002) *In vivo* modulation of nonphotochemical exciton quenching (NPQ) by regulation of the chloroplast ATP synthase. *Proceedings of the National Academy of Sciences*, **99**, 12789-12794.

Kohzuma K., Cruz J.A., Akashi K., Munekage Y., Yokota A. & Kramer D.M. (2008) The long-term responses of the photosynthetic proton circuit to drought. *Plant Cell and the Environment*, **32**, 209-219.

Kramer D.M., Avenson T.J. & Edwards G.E. (2004) Dynamic flexibility in the light reactions of photosynthesis governed by both electron and proton transfer reactions. *Trends in Plant Science*, **9**, 349-357.

Kramer D.M. & Crofts A.R. (1996) Control of photosynthesis and measurement of photosynthetic reactions in intact plants. In: *Photosynthesis and the Environment* . *Advances in Photosynthesis* (ed N. Baker), pp. 25-66. Kluwer Academic Press, Dordrecht, The Netherlands.

Kubicki A., Funk E., Westhoff P. & Steinmüller K. (1996) Differential expression of plastome-encoded ndh genes in mesophyll and bundle-sheath chloroplasts of the C4 plant Sorghum bicolor indicates that the complex I-homologous NAD(P)H-plastoquinone oxidoreductase is involved in cyclic electron transport. *Planta*, **199**, 276-281.

Laloi C., Apel K. & Danon A. (2004) Reactive oxygen signaling: the latest news. *Current Opinion in Plant Biology*, **7**, 323-328.

Lascano H.R., Casano L.M., Martin M. & Sabater B. (2003) The activity of the chloroplastic Ndh complex is regulated by phosphorylation of the NDH-F subunit. *Plant Physiology*, **132**, 256-262.

Livingston A.K., Cruz J.A., Kohzuma K., Dhingra A. & Kramer D.M. (2010a) An Arabidopsis mutant with high cyclic electron flow around photosystem I (*hcef*) involving the NDH complex. *Plant Cell*, **22**, 1-13.

Livingston A.K., Kanazawa A., Cruz J.A. & Kramer D.M. (2010b) Regulation of Cyclic Electron Flow in C3 Plants: Differential effects of limiting photosynthesis at Rubisco and Glyceraldehyde-3-phosphate Dehydrogenase. *Plant Cell and the Environment*.

Macheroux P., Kleweg V., Massey V., Söderlind E., Stenberg K. & Lindqvist Y. (1993) Role of tyrosine 129 in the active site of spinach glycolate oxidase. *European Journal of Biochemistry*, **213**, 1047-1054.

Mitchell P. (1976) Possible molecular mechanisms of the protonmotive function of cytochrome systems. *Journal of Theorthical Biology*, **62**, 327-367.

Munekage Y., Hojo M., Meurer J., Endo T., Tasaka M. & Shikanai T. (2002) PGR5 is involved in cyclic electron flow around photosystem I and is essential for photoprotection in Arabidopsis. *Cell*, **110**, 361-371.

Nixon P.J. & Mullineaux C.W. (2001) Regulation of photosynthetic electron transport. In: *Advances in photosynthesis and respiration: regulation of photosynthesis* (eds E. Aro & B. Anderson). Kluwer Academic Publishers.

Noctor G. & Foyer C. (1998) A re-evaluation of the ATP:NADPH budger during C3 photosynthesis: a contribution form nitrate assimilation and its associated respiratory activity. *Journal of Experimental Botany*, **49**, 1895-1908.

Quiles M.J. (2005) Regulation of the expression of chloroplast *ndh* genes by light intensity applied during oat plant growth. *Plant Science*, **168**, 1561-1569.

Quinn J., Findlay V.J., Dawson K., Jones N., Morgan B.A. & Toone W.M. (2002) Distinct regulatory proteins control the adaptive and acute response to H_2O_2 in *Schizosaccharomyces pombe. Molecular Biology of the Cell*, **13**, 805-816.

Sacksteder C., Kanazawa A., Jacoby M.E. & Kramer D.M. (2000) The proton to electron stoichiometry of steady state photosynthesis in living plants: a proton-pumping Q-cycle is continuously engaged. *Proceedings of the National Academy of Sciences*, **97**, 14283-14288.

Sacksteder C. & Kramer D.M. (2000) Dark-interval relaxation kinetics (DIRK) of absorbance changes as a quantitative probe of steady-state electron transfer. *Photosynthesis Research*, **66**, 145-158.

Sazanov L.A., Burrows P.A. & Nixon P.J. (1996) Detection and characterization of a complex I-like NADH-specific dehydrogenase from pea thylakoids. *Biochemical Society Transactions*, **24**, 739-743.

Seelert H., Poetsch A., Dencher N.A., Engel A., Stahlberg H. & Müller D.J. (2000) Structural biology. Proton-powered turbine of a plant motor. *Nature*, **405**, 418-419.

Takizawa K., Kanazawa A. & Kramer D.M. (2008) Depletion of stromal P_i induces high 'energy-dependent' antenna exciton quenching (q_E) by decreasing proton conductivity at CF_O-CF_1 ATP synthase. *Plant, Cell and the Environment*, **31**, 235-243.

Vandenbroucke K., Robbens S., Vandepoele K., Inzé D., Van de Peer Y. & Van Breusegem F. (2008) Hydrogen Peroxide-Induced gene expression across kingdoms: A comparative analysis. *Molecular Biology and Evolution*, **25**, 507-516.